Zootaxa 4461 (3): 301–349
http://www.mapress.com/j/zt/

Article

ISSN 1175-5326 (print edition)
ZOOTAXA
ISSN 1175-5334 (online edition)

https://doi.org/10.11646/zootaxa.4461.3.1
http://zoobank.org/urn:lsid:zoobank.org:pub:B646DF09-BADE-43F1-9CE5-39EF1E2971A8

Description of five new rheophilic *Orthochromis* species (Teleostei: Cichlidae) from the Upper Congo drainage in Zambia and the Democratic Republic of the Congo

FREDERIC DIETER BENEDIKT SCHEDEL[1], EMMANUEL J.W.M.N. VREVEN[2,3], BAUCHET KATEMO MANDA[2,3,4], EMMANUEL ABWE[2,3,4], AUGUSTE CHOCHA MANDA[4] & ULRICH KURT SCHLIEWEN[1,5]

[1]*SNSB-Bavarian State Collection Zoology (ZSM), Department of Ichthyology, Münchhausenstraße 21, München, Germany,*
[2]*Vertebrate Section, Royal Museum for Central Africa (RMCA), Leuvensesteenweg 13, B-3080 Tervuren, Belgium*
[3]*KU Leuven, Laboratory of Biodiversity and Evolutionary Genomics, Charles Deberiotstraat 32, B-3000 Leuven, Belgium*
[4]*Unité de Recherche en Biodiversité et Exploitation durable des Zones Humides (BEZHU), Faculté des Sciences Agronomiques, Université de Lubumbashi, Route Kasapa, Lubumbashi, R.D Congo*
[5]*Corresponding author. E-mail: schliewen@snsb.de*

Table of contents

Abstract

Five new rheophilic haplochromine cichlid species are described from the Upper Congo drainage of Zambia and the Democratic Republic of the Congo: *Orthochromis mporokoso* **sp. nov.** and *O. katumbii* **sp. nov.** from the Bangwelu-Mweru ecoregion, *O. kimpala* **sp. nov.** and *O. gecki* **sp. nov.** from the Upper Lualaba ecoregion, and *O. indermauri* **sp. nov.** from the Lufubu River of the Lake Tanganyika ecoregion. *Orthochromis kimpala* sp. nov, *O. gecki* **sp. nov.**, and *O. indermauri* **sp. nov.** are distinguished from all currently valid species of the genus *Orthochromis* Greenwood 1954, except for *O. torrenticola* (Thys van den Audenaerde 1963), by the presence of eggspots or eggspot-like maculae on the anal fin (vs. no eggspots). The three species can be easily distinguished from *O. torrenticola* by having three anal spines (vs. four anal spines). Moreover, all five new species can be individually distinguished from all currently known rheophilic taxa placed in the genera *Orthochromis*, *Schwetzochromis* Poll 1948 and the rheophilic species of the genus *Haplochromis* Hilgendorf 1888 (e.g. *H. bakongo* Thys van den Audenaerde 1964, *H. snoeksi* Wamuini Lunkayilako & Vreven 2010, *H. vanheusdeni* Schedel *et al.* 2014) either based on meristic values, morphometric distances and colouration patterns, or on a combination of them.

Key words: Upper Congo basin, Lualaba, Luapula, Lufubu, *Orthochromis*, *Schwetzochromis*, rheophilic cichlids

Accepted by J. Armbruster: 27 Jun. 2018; published: 22 Aug. 2018

Introduction

While literally hundreds of endemic species are described from each Lake Tanganyika, Lake Malawi and Lake Victoria, strikingly few haplochromine taxa are known to inhabit exclusively rivers (Greenwood 1979) and the number of species considered to be rheophilic is even less with currently 19 valid species. Ecomorphologically, bentho-rheophilic cichlids are vaguely characterized by morphological adaptations such as reduced squamation on head, nape, and chest, rounded pelvic fins, and a comparatively slender body presumably facilitating a bottom-oriented life in the strong, current (Roberts & Stewart 1976). Taxonomically, rheophilic haplochromine taxa are currently classified in different genera, i.e. *Orthochromis* Greenwood 1954 and the single member of the genus *Schwetzochromis* Poll 1948, *S. neodon* Poll 1948. In addition, several rheophilic taxa are placed in the catch-all genus *Haplochromis* Hilgendorf 1888, but a consensus about a phylogenetically consistent classification has not yet been reached (Schedel *et al.* 2014). Currently eight species endemic to the Malagarasi and Luiche drainages are classified as *Orthochromis* ("Malagarasi-*Orthochromis*" sensu Weiss *et al.* 2015) including the type species of the genus, *O. malagaraziensis* (David 1937), originally described as *Haplochromis malagaraziensis*. These Malagarasi-*Orthochromis* appear to form a monophyletic group (Koblmüller *et al.* 2008, Schwarzer *et al.* 2012, Dunz & Schliewen 2013, Weiss *et al.* 2015, Matschiner *et al.* 2016). An additional five *Orthochromis* have been described from the Luapula-Mweru system, i.e. *O. kalungwishiensis* (Greenwood & Kullander 1994), *O. luongoensis* (Greenwood & Kullander 1994), *O. polyacanthus* (Boulenger 1899), and *O. torrenticola* (Thys van den Audenaerde 1963) from the Lufira River and *O. stormsi* (Boulenger 1902) from the Congo-Lualaba mainstream including Lake Mweru (Greenwood & Kullander 1994). Finally, *Orthochromis machadoi* (Poll 1967) is known only from the Cunene River in Namibia and Angola. These latter six *Orthochromis* species from outside of the Malagarasi and Luiche drainage systems are not closely related to the Malagarasi-*Orthochromis* based on molecular phylogenetic results (Salzburger *et al.* 2002, Koblmüller *et al.* 2008, Schwarzer *et al.* 2012, Dunz & Schliewen 2013, Weiss *et al.* 2015, Matschiner *et al.* 2016). This is equally true for the few rheophilic haplochromines currently classified in *Haplochromis*, i.e. *H. bakongo* Thys van den Audenaerde 1964, *H. snoeksi* Wamuini Lunkayilakio & Vreven 2010 from the Lower Congo basin, and *H. vanheusdeni* Schedel, Friel & Schliewen 2014 from the Great Ruaha River drainage in Tanzania, which represent different lineages of their own (Schwarzer *et al.* 2012, unpublished data). The greater Congo drainage, i.e., including Lake Tanganyika and its affluents, is home to almost all of these taxa except for *H. vanheusdeni* and *O. machadoi* (Poll 1967).

Recently, three apparently undescribed rheophilic haplochromine cichlids have been collected in Upper Congo affluents of Zambia including the Lufubu River, a southern affluent of Lake Tanganyika (Schedel *et al.* 2014, Indermaur 2014), and two additional ones, from the Lubudi River and from Kalule North River in the Upper Lualaba (Congo) basin respectively (Fig. 1). Further, preliminary observations revealed that the new species differ in several diagnostic characters from *Orthochromis* or *Schwetzochromis* sensu De Vos & Seegers (1998). For instance, the two new species from southeastern DRC (rivers Lubudi and Kalule Nord; Upper Lualaba ecoregion) as well as the new species from the Lufubu River have eggspots or eggspot-like maculae on the anal fin, a situation that contrasts with that found in *Orthochromis,* which either have no eggspots, or, in the case of *O. torrenticola*, only eggspot-like maculae on the anterior lower margin of the anal fin (De Vos & Seegers 1998). The two species from the Luapula affluents fit with most diagnostic characteristics for the genus *Orthochromis,* but they both exhibit a well-developed cheek squamation vs. absence or extensive reduction in cheek squamation according to De Vos & Seegers (1998). Finally, genomic data suggest that all new species are not closely related to the Malagarasi-*Orthochromis* (Schedel *et al.*, unpublished). In addition, all five new species possess a lachrymal stripe which is lacking in *Schwetzochromis*. As a generic revision of haplochromine genera is still pending, all new species are described in the phenotypically overall similar genus *Orthochromis* until a phylogenetic sound generic revision of haplochromine cichlids becomes available. This approach has become common practice for haplochromine cichlids (e.g. Wamuini Lunkayilakio & Vreven 2010, De Zeeuw *et al.* 2013, Schedel *et al.* 2014) following the logic of Van Oijen *et al.* (1991) and Van Oijen (1996), with the difference, however, that the new rheophilic taxa are placed in the current catch-all genus for rheophilic haplochromine cichlids *Orthochromis* and not in *Haplochromis*. This because the genus *Haplochromis* should be rather restricted to taxa closely related to the type species of *Haplochromis* from the Lake Victoria Region superflock, i.e. *Haplochromis obliquidens* Hilgendorf, 1888.

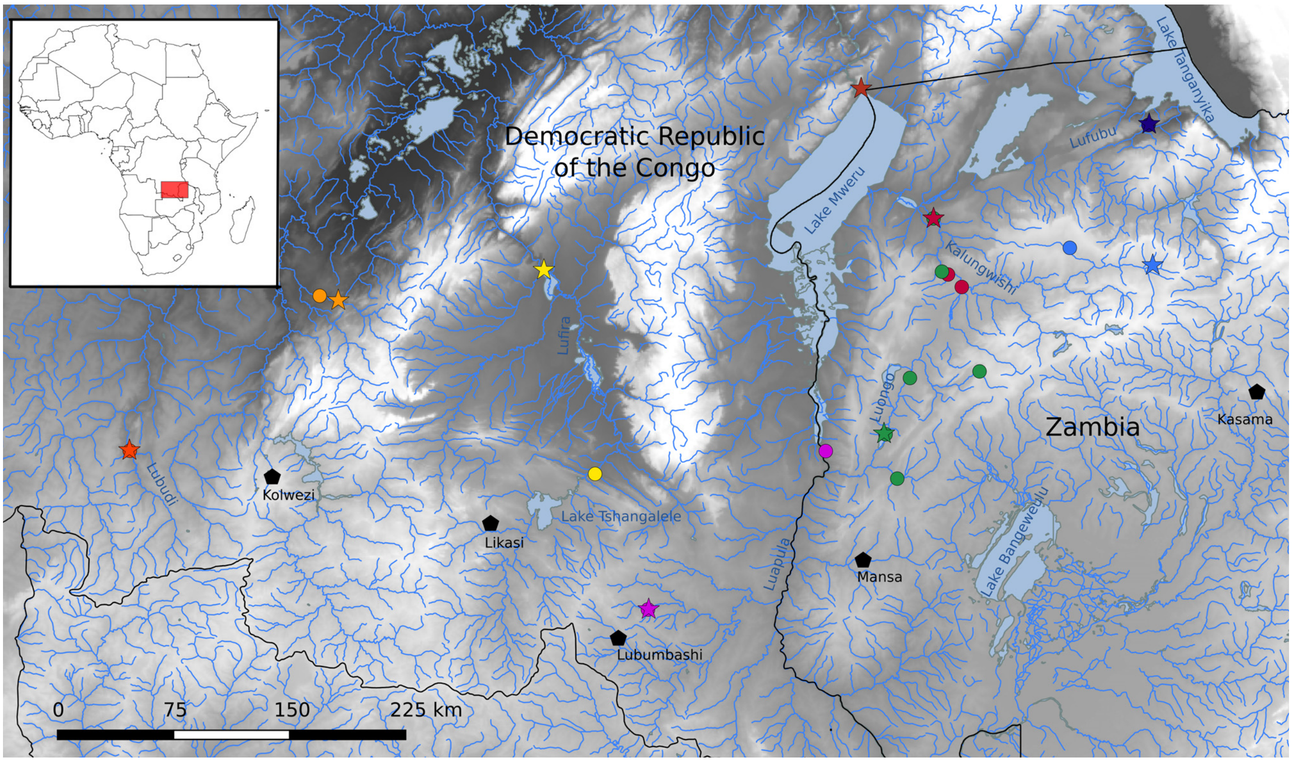

FIGURE 1. Map of south-eastern DRC and Northern Zambia, with indications of the type localities of the known *Orthochromis* species of the Upper Congo drainage system and new *Orthochromis* species. Star = type locality, circle = either paratype locality or sample locality of comparative specimens. Species indicated by colour: *O. mporokoso* **sp. nov.** (light blue); *O. katumbii* **sp. nov.** (purple); *O. kimpala* **sp. nov. (**orange); *O. gecki* **sp. nov.** (deep orange); *O. indermauri* **sp. nov.** (deep blue); *O. kalungwishiensis* (dark red); *O. luongoensis* (green). *O polyacanthus* (brown) and *O. torrenticola* (yellow). Major citys are depicted in black. Map is based on shapefiles obtained from DIVA-GIS (http://www.diva-gis.org/Data).

Materials and methods

A total of 344 specimens of rheophilic haplochromine cichlids were examined for morphological comparison (see Appendix). These are deposited in CUMV (Cornell University Museum of Vertebrates, Ithaca); NHM (Natural History Museum London); MRAC (Royal Museum for Central Africa, Tervuren); Tanganjikasee-Buntbarsch-Sammlung (collection of the University of Basel); ZSM (Bavarian State Collection of Zoology, Munich); and at the personal collection of O. Seehausen (EAWAG - Swiss Federal Institute of Aquatic Sciences and Technology, Dübendorf). All five new species described herein share morphological characters typical of rheophilic haplochromines. Therefore, the new putative species were compared with all haplochromine cichlid species currently placed in the rheophilic genera *Orthochromis* and *Schwetzochromis* as recognized in the revision of De Vos & Seegers (1998), and, in addition, with all rheophilic representatives of the genus *Haplochromis* Hilgendorf 1888 sharing *Orthochromis*-like body shape, i.e. rounded pelvic fins and a slender body. Furthermore, one yet undescribed *Orthochromis* species from the Malagarasi drainage was included in the comparisons as well.

Overall, 28 meristic characters were recorded for almost all examined specimens of the five new species, which were either based on stereomicroscope observations (18 characters) or on digital x-rays (10 characters using a Faxitron UltraFocus LLC x-ray unit) following previous publications (Barel *et al.* 1977, Dunz & Schliewen 2010, Schedel *et al.* 2014, Schedel & Schliewen 2017). In addition, four morphological character states as defined in Schedel & Schliewen 2017 were examined: (1) position of the pterygiophore supporting the last dorsal-fin spine [used for Principal Components Analyses (PCA)]; (2) position of the pterygiophore supporting the last anal-fin spine (used for PCA); (3) state of hypurals 1 and 2; and (4) state of hypurals 2 and 3. Live colour notes were based on photographs of fresh wild caught specimens (adults) as well as on live specimens kept in aquaria (if available). In addition, we took colour notes of preserved specimens with a focus on head stripes and bars (commonly referred as "head mask") that appear to be of diagnostic value for the different species of *Orthochromis* (De Vos & Seegers 1998). For the PCA, a subsample of 20 meristic characters (eight squamation characters and twelve skeletal characters) of most examined specimens (N=327) was used. Twenty-nine morphometric distance measurements were used for species descriptions, i.e. they were only measured in the types and additional specimens of the new species, but not in the specimens for the comparison study except for a number of selected species in which there was overlap in meristic counts with the new species, e.g. *O. machadoi*, *O. luongoensis,* and *H. vanheusdeni*. All measurements were recorded as defined in Schedel & Schliewen (2017), a compilation of distance measurement definitions largely but not completely based on previous cichlid studies (Barel *et al.* 1977, Dunz & Schliewen 2010, Schedel *et al.* 2014). Measurements were taken point-to-point on the left side of specimens using digital callipers (accuracy of the calliper 0.1 mm). Head measurements are given as percentage of the head length (HL), all remaining measurements as percentage of the standard length (SL). Measurements of the lower pharyngeal jaw were taken from digital microscope images of dissected lower pharyngeal jaws and are given in percentage of the head length (HL).

To test for morphological discreteness of putative new species and to identify diagnostic character states or combinations, a first PCA using a correlation matrix was performed for 20 meristic characters (see above) of the total data set. The monophyletic Malagarasi-*Orthochromis* were grouped together in our analysis due to their phenotypic similarity and to simplify subsequent interpretation. After identifying clearly separate clusters in the total dataset, five subsequent species-specific PCAs with reduced taxon sets were performed, each composed of one of the five new species and those described species with overlapping PC values in bivariate plots of PC I vs. PC II of the total dataset. For three of these species-specific PCAs nonvariant meristic counts were excluded. For example, in the species-specific PCA targeting the diagnostic differentiation of *O. kimpala* **sp. nov.** counts for scales between the upper lateral line and last dorsal-fin spine were nonvariant for the used data subsets while for the two species-specific PCAs targeting the diagnostic differentiation of *O. gecki* **sp. nov.** and *O. indermauri* **sp. nov.** counts for the anal-fin spines were excluded due to nonvariance. This exercise was done to reduce the total variance in each dataset to test for increased separation of each of the new species with the morphologically closest taxa. The software PAST 3.07 (Hammer *et al.* 2001) was used to calculate PCs. Scores of most informative principal components (PC I, PC II and in some cases for PC III) were visualized using bivariate plots, and variables contributing most to PC variation were identified using their loadings as tabulated. The PCA focused on meristic characters only because these characters appear to be unambiguous and are available for all included species and specimens.

Results

In the first PCA on the meristic values (all specimens included, N = 327, Fig. 2, Table 1), PC I explained 32.18 %, PC II 12.81 %, and PC III 10.16% of the total variance. Differences in the total number of vertebrae, scales in a horizontal line, and the number of scales in the upper lateral line contributed most to the factor loadings of PC I; PC II is mainly influenced by different counts for scales on the cheek and in the lower lateral line, and by the number of upper procurrent caudal-fin rays. The PC I and PC II scores of *Orthochromis mporokoso* **sp. nov.** overlap with *O. machadoi*, *Haplochromis snoeksi*, *O. katumbii* **sp. nov.**, *O. kimpala* **sp. nov.**, *O. gecki* **sp. nov.**, and *Schwetzochromis neodon*. *Orthochromis katumbii* **sp. nov.** is grouped with *O. mporokoso* **sp. nov.**, *O. gecki* **sp. nov.**, *O. kimpala* **sp. nov.**, *O. luongoensis*, *O. torrenticola, S. neodon,* and with the Malagarasi-*Orthochromis* based on the PC scores I and II. Scores of PC I and PC II of *Orthochromis kimpala* **sp. nov.** overlap with those of *H. bakongo*, *H. snoeksi*, *H. vanheusdeni*, *O. machadoi*, *O. stormsi, O. katumbii* **sp. nov.**, *O. mporokoso* **sp. nov.**, and *O. gecki* **sp. nov.** while the PC I and PC II scores of *O. gecki* **sp. nov.** overlap with those of *O. mporokoso* **sp. nov.**, *O. kimpala* **sp. nov.**, *O. katumbii* **sp. nov.**, *O. indermauri* **sp. nov.**, *O. polyacanthus, S. neodon*, and Malagarasi-*Orthochromis*. Finally, the PC I and PC II scores of *O. indermauri* **sp. nov.** overlap with those of *O. stormsi, H. vanheusdeni, O. gecki* **sp. nov.** and with the Malagarasi-*Orthochromis.*

The first species-specific PCA with a reduced taxon set (106 specimens included, Table 1; Appendix: Fig. S1) targets the diagnostic differentiation of *O. mporokoso* **sp. nov.** from the six species which overlap with their PC I and PC II scores of the total dataset (see above). In this PCA PC I explains 27.87 %, PC II 15.43 %, and PC III 10.77 % of the total variance. PC I mainly integrates the variance of the total number of vertebrae, caudal-fin rays, and of scales in the upper lateral line, and PC II mainly the variance of the number of dorsal-fin spines, dorsal-fin rays, and position of the pterygiophore supporting the last dorsal-fin spine. PC III mainly integrates the variance of the number of caudal and abdominal vertebrae and the position of the pterygiophore supporting the last anal-fin spine. The PCA plots separate *O. mporokoso* **sp. nov.** from *H. snoeksi* based on low PC II scores and from S. *neodon* based on high PC I scores, while a combination of low PC II scores and low PC III further separates it from *O. gecki* **sp. nov.**

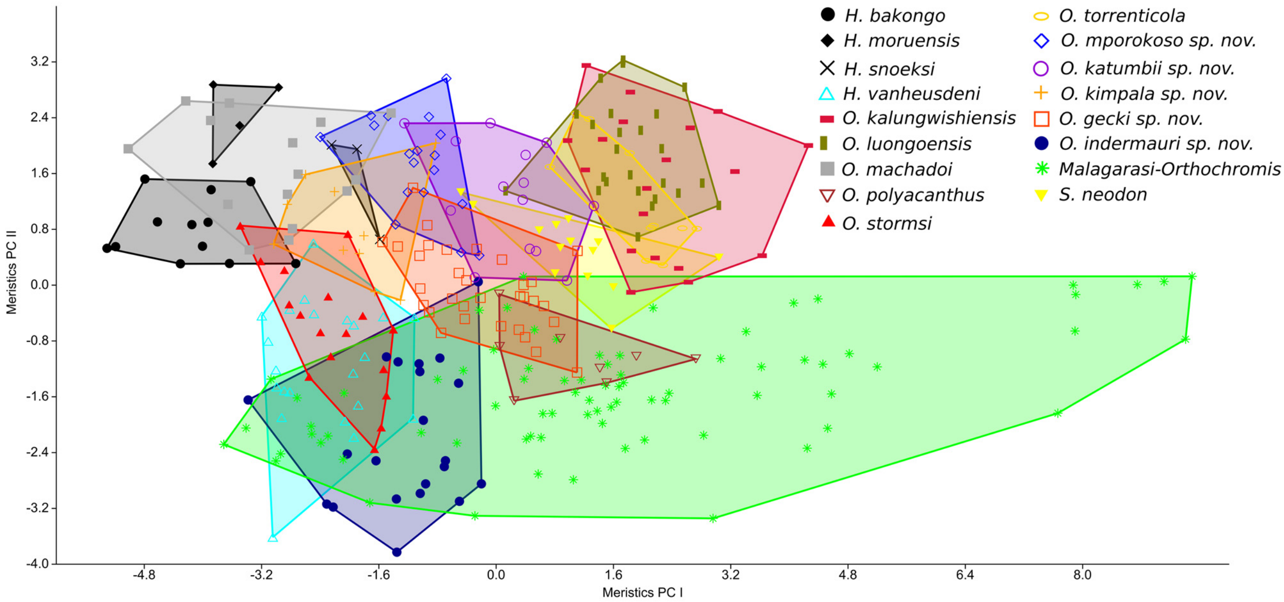

FIGURE 2. PCA scatter plots based on 20 meristic values; species score limits visualized as convex hulls. PC I vs PC II for all examined specimens (N = 327). PC I explain 32.18 % of the variance and PC II explains 12.81 %.

The second species-specific PCA (225 specimens included, Table 1; Appendix: Fig. S2) targets the diagnostic differentiation of *O. katumbii* **sp. nov.** from the six species and the Malagarasi-*Orthochromis* which overlap with their PC I and PC II scores of the total dataset (see above). In this PCA PC I explains 30.76 %, PC II 14.68 %, and PC III 9.89 % of the total variance. PC I mainly integrates the variance of the total number of vertebrae, scales in a horizontal line, and of the position of the pterygiophore supporting the last dorsal-fin spine, and PC II mainly the variance of the number of scales on cheek and in the lower lateral line, and number of anal-fin rays. The species-specific PCA separates *O. katumbii* **sp. nov.** from *O. kimpala* **sp. nov.** mainly based on low PC I scores. Values of PC II and PC III for *O. katumbii* **sp. nov.** overlapped with all remaining species.

The third species-specific PCA (143 specimens included, Table 1, Appendix: Fig. S3) targets the diagnostic differentiation of *O. kimpala* **sp. nov.** from the eight species overlapping with their PCI and PCII scores in the total dataset (see above). PC I explains 23.09 %, PC II 14.63 % and PC III 12.34 % of the total variance. The variance of the number of scales along the horizontal line, total number of vertebrae, and caudal vertebrae contributed most to PC I whereas the variance of the number of upper and lower procurrent caudal-fin rays and total number of caudal-fin rays contributed most to PC II. PC III is mainly composed of the variance of the number of abdominal vertebrae, the number of dorsal-fin spines, and the position of the pterygiophore supporting the last dorsal-fin spine. The species-specific PCA separates *O. kimpala* **sp. nov.** from *H. snoeksi* based on low PC III scores.

The fourth species-specific PCA (196 specimens included, Table 1, Appendix: Fig. S4) targets the diagnostic differentiation of *O. gecki* **sp. nov.** from the six species and the Malagarasi-*Orthochromis* which overlap with their PCI and PCII scores of the total dataset (see above). PC I explains 33.42 %, PC II 14.91 % and PC III 11.95 % of the total variance. Differences in the number of scales along the horizontal line, total number of vertebrae, and dorsal-fin spines contribute most to PC I whereas differences in the number of scales on the cheek, number of upper procurrent caudal-fin rays, and total number of caudal-fin rays mainly contribute to PC II. PC III mainly integrates variance of the number of circumpeduncular scales and in the number of dorsal- and anal-fin rays. The

TABLE 1. Factor loadings of PCI-III for all examined specimens (Fig. 2) plus for each species-specific PCA (see Fig. S1-5). Highest loadings for each principal component indicated in boldface.

	PCA with all specimens (N=327)			*Orthochromis mporokoso* **sp. nov.** (N=106)			*Orthochromis katumbii* **sp. Nov**. (N=225)		
	PC I	PC II	PC III	PC I	PC II	PC III	PC I	PC II	PC III
Series of scales on cheek	-0,0538	**0,5058**	-0,0066	-0,2745	0,0904	0,2475	-0,0504	**0,4975**	0,1096
Scales on operculum	-0,0512	0,3297	0,1617	-0,2495	0,1200	0,1003	-0,0210	0,3706	0,1952
Scales (horizontal line)	**0,3385**	0,2389	-0,0506	0,2777	0,2315	-0,1634	**0,3503**	0,1770	-0,0869
Upper lateral line scale	**0,3293**	-0,0039	-0,0612	**0,3115**	0,0203	-0,1542	0,3179	-0,0803	-0,1693
Lower lateral line scales	0,1232	**0,3751**	-0,0158	0,2074	0,1374	0,2064	0,1244	**0,3912**	0,0475
Circumpeduncular scales	-0,0487	0,0250	**0,3931**	-0,2595	0,1491	-0,3037	0,0064	0,1138	0,2233
Scales between lateral line and dorsal fin origin	0,0120	-0,1232	0,2786	0,0362	-0,2740	-0,1456	0,0791	-0,0410	-0,1569
Scales between upper lateral line and last dorsal fin spine	0,0364	0,2251	-0,1445	-0,0926	0,0188	-0,2220	0,0092	0,0580	0,0476
Abdominal vertebrae	0,2956	0,0819	0,1977	0,1889	0,1736	**0,4192**	0,3362	0,0736	-0,1027
Caudal vertebrae	0,3022	0,1597	-0,2102	0,2548	0,1006	**-0,4350**	0,2920	0,0802	0,0155
Total number of vertebrae	**0,3662**	0,1545	-0,0565	**0,3497**	0,1965	-0,1388	**0,3803**	0,0930	-0,0539
Anal-fin spines	0,0420	0,0907	0,0814	-0,0792	-0,0647	0,0934	0,0390	0,1020	0,0558
Anal-fin rays	0,1752	-0,2181	-0,2514	0,1547	-0,1911	0,1162	0,0531	**-0,4779**	-0,1426
Dorsal-fin spines	0,3166	-0,1378	**0,3135**	0,0459	**0,5130**	-0,0837	0,3416	-0,1154	-0,0114
Dorsal-fin rays	0,0864	0,1461	**-0,4678**	0,2332	**-0,3591**	0,1904	-0,0539	0,0103	-0,2847
Upper procurrent caudal-fin rays	0,1696	**-0,3438**	-0,1644	0,2835	-0,1002	-0,0781	0,0996	-0,2696	**0,4046**
Lower procurrent caudal-fin rays	0,1972	-0,0791	-0,1397	0,2361	-0,0673	0,1228	0,1546	-0,0255	**0,4757**
Caudal-fin rays	0,2162	-0,2712	-0,1874	**0,3123**	-0,1026	0,0036	0,1584	-0,1969	**0,5519**
Position of the pterygiophore supporting the last dorsal fin spine	0,3219	-0,1234	0,3043	0,0171	**0,4787**	0,0770	**0,3421**	-0,1165	-0,0314
Position of pterygiophore supporting the last anal fin spine	0,2855	0,0753	0,2581	0,1564	0,2022	**0,4429**	0,3296	0,0893	-0,1442

……*continued on the next page*

TABLE 1. (Continued)

	Orthochromis kimpala **sp. nov.** (N=143)			*Orthochromis gecki* **sp. nov.** (N=196)			*Orthochromis indermauri* **sp. nov.** (N=171)		
	PC I	PC II	PC III	PC I	PC II	PC III	PC I	PC II	PC III
Series of scales on cheek	0,0248	-0,3120	0,0227	-0,1689	**0,3667**	0,0915	-0,1157	0,1830	0,1384
Scales on operculum	-0,0008	-0,2372	0,0908	-0,1033	0,1429	0,2516	-0,0530	0,1433	-0,1954
Scales (horizontal line)	**0,3956**	-0,1295	-0,0580	**0,3326**	0,2514	-0,0233	**0,3421**	0,1076	0,1817
Upper lateral line scale	0,3787	0,0555	-0,1323	0,3300	0,0651	-0,0609	0,3284	0,0757	0,0975
Lower lateral line scales	0,0644	0,0383	0,1245	0,0721	0,3279	0,0232	0,0511	0,2736	0,0604
Circumpeduncular scales	0,0887	-0,1313	-0,0077	-0,0452	-0,1550	**0,3695**	-0,0584	0,1207	0,0094
Scales between lateral line and dorsal fin origin	0,0072	0,1803	0,0508	0,0559	-0,0845	0,2242	-0,0453	**0,4258**	-0,1205
Scales between upper lateral line and last dorsal fin spine	excluded from PCA			0,0683	0,2038	-0,2198	0,0563	-0,0059	**0,3406**
Abdominal vertebrae	0,0391	0,1583	**0,3919**	0,3196	0,1261	0,1910	0,2995	0,2229	-0,2027
Caudal vertebrae	**0,4111**	-0,1008	-0,1867	0,2644	0,1628	-0,2447	0,2940	-0,0699	**0,3180**
Total number of vertebrae	**0,4402**	-0,0336	-0,0346	**0,3632**	0,1820	-0,0498	**0,3627**	0,0695	0,1133
Anal-fin spines	-0,0330	-0,0565	-0,0302	excluded from PCA			excluded from PCA		
Anal-fin rays	0,2794	-0,1319	-0,1872	0,1725	-0,1549	**-0,3444**	0,2492	-0,2348	0,2526
Dorsal-fin spines	0,2593	0,1741	**0,4253**	**0,3313**	-0,1227	0,2700	0,3294	0,0784	-0,2793
Dorsal-fin rays	0,2374	-0,1346	-0,3119	0,0010	0,2911	**-0,4298**	0,0960	0,0526	**0,5315**
Upper procurrent caudal-fin rays	0,0876	**0,5017**	-0,1843	0,1337	**-0,3879**	-0,1702	0,1089	**-0,3981**	-0,1837
Lower procurrent caudal-fin rays	-0,0074	**0,3556**	-0,2083	0,1582	-0,2408	-0,1464	0,1597	-0,3228	-0,1216
Caudal-fin rays	0,0613	**0,5232**	-0,2258	0,1806	**-0,3928**	-0,1968	0,1658	**-0,4443**	-0,1880
Position of the pterygiophore supporting the last dorsal fin spine	0,2775	0,1206	**0,4299**	0,3342	-0,1101	0,2696	**0,3323**	0,0885	-0,2583
Position of pterygiophore supporting the last anal fin spine	0,1786	0,0598	0,3680	0,3092	0,1524	0,2273	0,2913	0,2581	-0,1893

species-specific PCA separates *O. gecki* **sp. nov.** from *O. indermauri* **sp. nov.** based on low PC II scores and from *H. snoeksi* based on high PC II scores and from *O. polyacanthus* by high PC III scores.

Finally, the fifth species-specific PCA (171 specimens included, Table 1, Appendix: Fig. S5) targets the diagnostic differentiation of *O. indermauri* **sp. nov.** from the three species and the Malagarasi-*Orthochromis* which overlap with their PCI and PCII scores of the total dataset (see above). PC I explains 36.45 %, PC II 13.84 % and 10.65 % of the total variance. Differences in the number of scales along the horizontal line, total number of vertebrae, and the position of the pterygiophore supporting the last dorsal-fin spine contribute most to PC I while differences in the number of scales between the upper lateral line and dorsal-fin origin, number of upper procurrent caudal-fin rays, and total number of caudal-fin rays mainly contribute to PC II. The species-specific PCA separates *O. indermauri* **sp. nov.** from *O. gecki* **sp. nov.** based on high PC II scores. Values of PC III for *O. indermauri* **sp. nov.** overlap for all remaining species.

In summary, meristic values alone allow to diagnostically separate each of the new species from almost all analysed rheophilic haplochromine species with the exception of a few taxa; these are, however, well diagnosable using morphometric measurements and colour patterns. Differential diagnoses for the new species were therefore based on a combination of meristic characters, which are supplemented by additional characters.

Orthochromis mporokoso **sp. nov.**

Orthochromis sp. "Kasinsha"—Schedel *et al.* 2014

Holotype. ZSM 46840 (59.04 mm SL, ex ZSM 41443), Zambia, Kasinsha stream north of Luwinga affluent to Lake Mweru (-9.4894/30.5769).

Paratypes. ZSM 41429 (9, 34.0–74.48 mm SL), Zambia, Mutoloshi stream above Kapuma Falls at Mporokoso on road Mukunsa-Luwinga (-9.3889/30.0956).—ZSM 41443 (4, 40.9–63.2 mm SL), collected with holotype.—MRAC 2018-006-P-0009-0011 (3, 48.7–51.9 mm SL) Zambia, Mutoloshi stream above Kapuma Falls at Mporokoso on road Mukunsa-Luwinga (-9.3889/30.0956).

Additional material. ZSM 46841 (1, ex 41429, 54.28 mm SL; specimen with deformed jaws), Zambia, Mutoloshi stream above Kapuma Falls at Mporokoso on road Mukunsa-Luwinga (-9.3889/30.0956).

Differential diagnosis. *Orthochromis mporokoso* can be readily distinguished from all species currently placed in *Orthochromis* species of the genus *Orthochromis* and *O*. sp. "Igamba" from the Malagarasi drainage system by having more scale rows on cheek (2–4 vs. 0–1). Furthermore, *O. mporokoso* can be distinguished from *O. kasuluensis*, *O. mosoensis,* and *O. rugufensis* by having more scales on operculum (3–4 vs. 0–2); from *O. kasuluensis* by having fewer total vertebrae (30 vs. 31–32); from *O. rugufuensis* by fewer dorsal-fin spines (16–17 vs. 19); from *O. mazimeroensis* by more horizontal line scales (29–30 vs. 26–28), more abdominal vertebrae (14 vs. 12–13) and more total vertebrae (30 vs. 28–29); from *O. rubrolabialis* and *O. uvinzae* by fewer dorsal-fin spines (16–17 vs. 18–20); it has more total gill rakers than *O. rubrolabialis* (10–12 vs. 8–9) and differs in position of pterygiophore supporting last dorsal-fin spine (vertebral count: 16 vs. 17–18). It differs from *O. uvinzae* additionally by having fewer scales between upper lateral line and dorsal-fin origin (4–5 vs. 6–8), fewer abdominal vertebrae (14 vs. 15–16), fewer total vertebrae (30 vs. 31–33), position of pterygiophore supporting last dorsal-fin spine (vertebral count: 16 vs. 18–19), position of pterygiophore supporting last anal-fin spine (vertebral count: 14-15 vs. 16–17); from *O. luongoensis* and *O. torrenticola* by having fewer caudal vertebrae (16 vs. 17–18) and total vertebrae (30 vs. 31–33); from *O. kalungwishiensis* by having fewer total vertebrae (30 vs. 31–33) and fewer horizontal line scales (29–30 vs. 31–32); from *O. torrenticola* additionally by having fewer anal-fin spines (3 vs. 4) and position of pterygiophore supporting last anal-fin spine (vertebral count: 14–15 vs. 16–17). It can be distinguished from *O. stormsi* and *O. polyacanthus* by having fewer scales between upper lateral line and dorsal-fin origin (4–5 vs. 6–9). In addition, it is distinguished from *O. stormsi* by having more horizontal line scales (29–30 vs. 26–28), more total vertebrae (30 vs. 28–29) and fewer total gill rakers (10–12 vs. 13–15); from *O. polyacanthus* by having more series of scales on cheek (2–4 vs. 0), fewer dorsal-fin spines (16–17 vs. 18–20) and in position of pterygiophore supporting last dorsal-fin spine (vertebral count: 16 vs. 17–18) as in position of pterygiophore supporting last anal-fin spine (vertebral count: 14–15 vs. 16–17). Meristic values of *O. mporokoso* overlap with those of *O. machadoi*, but it can be readily distinguished by having more vertical bars on flanks (13–15 vs. 9–10), which moreover extend mainly ventrally; those of *O. machadoi* extend mainly dorsally. In addition, it is distinguished in head mask pattern, i.e. *V*-shape nostril stripe in *O. mporokoso* vs. straight nostril stripe in *O. machadoi*; cheek stripe present vs. absent in *O. machadoi*. It differs from *Schwetzochromis neodon* by having more circumpeduncular scales (16 vs. 12), fewer inner series of teeth (1–3 vs. 4–6) and fewer dorsal-fin rays (9–10 vs. 11–12). It differs from *H. bakongo* and *H. moeruensis* by having more horizontal line scales (29–30 vs. 26–28), more caudal vertebrae (16 vs. 12–15) and more total vertebrae (30 vs. 26–29). Additionally, it is distinguished from *H. moeruensis* by having more upper lateral line scales (21–23 vs. 19–20); from *H. bakongo* by having more dorsal-fin spines (16–17 vs. 14–15) and in position of pterygiophore supporting last dorsal-fin spine (vertebral count: 16 vs. 13–14); and from *H. snoeksi* it is distinguished by having more abdominal vertebrae (14 vs. 13), fewer caudal vertebrae (16 vs. 17), more anal-fin rays (7–9 vs. 5–6), more total gill rakers (10–12 vs. 9), and in position of pterygiophore supporting last dorsal-fin spine (vertebral count: 16 vs. 15) and position pterygiophore supporting last anal-fin spine (vertebral count: 14–15 vs. 13). Meristic values of *O. mporokoso* overlap with those of *H. vanheusdeni,* but it lacks eggspots, has a nostril stripe (vs. absent in *H. vanheusdeni*), exhibits a cheek stripe (vs. absent in *H. vanheusdeni*), and has higher number of vertical bars on flank (13–15 vs. 6–7). It differs from herein newly described species *O. kimpala* by having fewer scales between upper lateral line and dorsal-fin origin (4–5 vs. 6–7); from *O. indermauri* by having more series of scales on the cheek (2–4 vs. 0–1), more caudal vertebrae (16 vs. 14–15), and more total vertebrae (30 vs. 28–29). Meristic values of *O. mporokoso* overlap with those of *O. katumbii* but former differs by having more vertical bars on flank (13–15 vs. 7–9) and by head mask pattern (i.e.: cheek stripe present vs. absent in *O. katumbii*). Meristic values of *O. mporokoso* overlap with those of *O. gecki* but former is distinguished by having much wider interorbital (15.3–19.5 vs. 9.6–12.9 % HL) and by lacking eggspots on anal fin vs. present in *O. gecki*.

Description. Morphometric measurements and meristic characters are based on 17 type specimens and one additional deformed specimen. Values and their ranges are presented in Table 2. For general appearance see figure 3. Maximum length of wild caught specimens 74.5 mm SL. Moderately slender species with maximum body depth (24.7–29.3 % SL) at level of dorsal-fin origin, slowly decreasing towards caudal peduncle. Caudal peduncle rather elongated and moderately deep (ratio of caudal-peduncle length to depth: 1.5–2.3). Head length almost one third of standard length. Dorsal head profile slightly curved without prominent nuchal gibbosity. Eye diameter larger than interorbital width. Jaws isognathous or slightly retrognathous. Posterior tip of maxilla not reaching anterior margin of orbit but ending slightly before. Lips not noticeably enlarged or thickened. Two separate lateral lines.

Squamation. Flank above and below lateral lines covered with comparatively large ctenoid to cycloid scales, especially in large specimens only few scales of ctenoid appearance. Anterior dorsal and ventral flank area covered by cycloid scales. Belly with comparatively small cycloid scales. Chest covered with even smaller cycloid scales compared to belly squamation; chest to flank transition with larger cycloid scales. Snout scaleless up to anterior margin of orbit. Interorbital, nape, and occipital region with medium sized cycloid scales. Cheeks covered by small cycloid scales; 2–4 scale rows on cheek. Cycloid scales on operculum of variable size (small to medium sized) and shape (ovoid to circular); opercular blotch partially covered by medium sized scales, but posterior margin scaleless. 3–4 scales on horizontal line starting from edge of postero-dorsal angle of operculum to anterior edge of operculum.

Upper lateral line scales 21–23 and lower lateral line 9–11. Horizontal line scales 29–30. Caudal fin with 0–2 pored scales. Upper and lower lateral lines separated by two scales. 3–5 scales between upper lateral line and dorsal-fin origin. Anterior part of caudal fin covered with 4–5 vertical columns of small cycloid scales with median scales slightly larger; scaled area of caudal fin extended posteriorly especially at upper and lower area with minute, interradial scales (approximately up to one third of caudal fin). Sixteen scales around caudal peduncle.

Jaws and dentition. Anterior bicuspid teeth of outer row in both upper and lower jaw large and closely set; posterior teeth becoming almost subequally bicuspid; towards corner of mouth teeth smaller and less closely set, may become unicuspid or weakly bicuspid especially in upper jaw. Individual bicuspid teeth with minimally expanded brownish crown, cusps (major cusp with almost horizontal edge) uncompressed and moderately widely set, and neck moderately slender to stout. Outer row upper jaw with 31–44 teeth and outer row lower jaw with 23–33 teeth (specimens: 34.0–59.0 mm SL). Larger specimens generally with more teeth. Two to three (rarely one) inner upper and lower jaw tooth rows with small tricuspid teeth. Lower pharyngeal bone (Fig. 3) of single dissected paratype (ZSM 41429, 59.8 mm SL) about 1.3 times wider than long with short anterior keel about 0.4 times length dentigerous area. Dentigerous area of lower pharyngeal bone about 1.5 times wider than long, with 10+10 teeth along posterior margin and 7–8 teeth along midline. Anterior pharyngeal teeth (towards keel) bevelled and slender; those of posterior row larger than anterior ones, bevelled (bicuspid; well-developed major and minor cusp). Largest teeth medially situated in posterior row. Teeth along midline slightly larger than more lateral ones.

Gill rakers. Total gill raker count 10–12, with two epibranchial, one angle, and 7–9 ceratobranchial gill rakers. Most anterior ceratobranchial gill rakers very small, increasing in size towards cartilaginous plug (angle). Gill raker in angle slightly shorter than longest ceratobranchial raker and epibranchial gill rakers further decreasing in size.

Fins. Dorsal fin with 16–17 spines and with 9–10 rays. First dorsal-fin spine always shortest. Dorsal-fin base length between 50.2–55.6 % SL. Posterior end of dorsal-fin rays ending slightly before or at caudal fin base; posterior tip of anal fin ending slightly before caudal-fin base. Caudal-fin outline subtruncate and fin composed of 26–29 rays (16 principal caudal-fin rays and 10–13 procurrent caudal-fin rays). Anal fin with three spines (third spine longest) and 7–9 rays. Anal-fin base length between 15.2–20.1 % SL. Pectoral fin with 15–16 rays. Pectoral-fin length between 21.6–25.7 % SL, longest pectoral ray not reaching level of anus. First upper and lower pectoral-fin rays very short to short. Pelvic fin with first spine thickly covered with skin and five rays. Pelvic-fin base slightly posterior of pectoral-fin base. Pelvic fin slightly longer than pectoral fin; longest pelvic-fin ray almost reaching anus (ending approximately 0.5–2 flank scale widths before).

TABLE 2. Measurements and counts of the holotype, paratypes and one additional specimen (no proportions given due to deformed jaws) of *Orthochromis mporokoso* **sp. nov.**

Measurements	holotype	holotype + paratypes				ZSM 46841
		min	Max	SD	n	
Total length (mm)	72.7	42.0	90.0		17	62.2
Standard length SL (mm)	59.0	34.0	74.5		17	54.3
Head length HL (mm)	17.5	11.3	23.0		17	17.2
% HL						
Interorbital width	18.4	29.6	34.0	1.5	17	-
Preorbital width	31.4	24.5	32.0	2.4	17	-
Horizontal eye length	23.2	21.3	28.2	1.7	17	-
Snout length	36.2	26.9	38.1	2.8	17	-
Internostril distance	15.8	13.5	18.8	1.5	17	-
Cheek depth	23.9	19.6	25.5	1.7	17	-
Upper lip length	30.6	25.4	32.1	2.1	17	-
Lower lip length	26.1	19.2	30.0	2.9	17	-
Lower lip width	29.1	19.6	34.9	3.9	17	-
Lower jaw length	29.7	22.0	34.1	3.6	17	-
Lower pharyngeal jaw length	-	28.0		-	1	-
Lower pharyngeal jaw width	-	36.2		-	1	-
Width of dentigerous area of lower pharyngeal jaw	-	25.9		-	1	-
% SL						
Predorsal distance	32.8	32.1	37.9	1.6	17	-
Dorsal-fin base length	55.5	50.2	55.6	1.5	17	-
Last dorsal-fin spine length	11.1	10.7	13.9	0.9	17	-
Anal fin-base length	16.3	15.2	20.1	1.3	17	-
Third anal-fin spine length	15.1	11.4	16.4	1.3	17	-
Pelvic fin length	22.9	22.1	27.3	1.5	17	-
Pectoral fin length	23.2	21.6	25.7	1.2	17	-
Caudal peduncle depth	10.8	7.9	11.7	1.0	17	-

......*continued on the next page*

TABLE 2. (Continued)

Measurements	holotype	holotype + paratypes				ZSM 46841
		min	Max	SD	n	
Caudal peduncle length	20.7	16.5	20.7	1.2	17	-
Body depth (pelvic fin base)	15.2	24.7	29.3	1.2	17	-
Preanal length	59.7	46.1	64.5	4.1	17	-
Anus-anal fin base distance	3.8	2.0	3.8	0.5	17	-
Interpectoral width	15.1	9.0	15.8	1.6	17	-
Counts						
Dorsal-fin spines	17	16 (2); 17 (15)			17	17
Dorsal-fin rays	10	9 (4); 10 (13)			17	10
Anal-fin spines	3	3 (17)			17	3
Anal-fin rays	8	7 (4); 8 (12); 9 (1)			17	8
Pelvic-fin spines	1	1 (17)			17	1
Pelvic-fin rays	5	5 (17)			17	5
Pectoral-fin rays	16	15 (8); 16 (9)			17	16
Upper procurrent caudal-fin rays	6	5 (1); 6 (14); 7 (2)			17	7
Lower procurrent caudal-fin rays	6	5 (3); 6 (14)			17	6
Caudal-fin rays	28	26 (1); 27 (2); 28 (12); 29 (2)			17	29
Scales (horizontal line)	30	29 (9); 30 (8)			17	29
Upper lateral line	21	21 (8); 22 (8); 23 (1)			17	22
Lower lateral line	11	9 (8); 10 (2); 11 (7)			17	11
Circumpeducular	16	16 (17)			17	16
Series of scales on cheek	3	2 (3); 3 (9); 4 (5)			17	3
Scales (horizontal line) on operculum	4	3 (13); 4 (4)			17	3
Scales between lateral line and dorsal fin origin	3	3 (1); 4 (15); 5(1)			17	5
Scales between upper lateral line and last dorsal fin spine	2	2 (17)			17	2
Abdominal vertebrae	14	14 (17)			17	14
Caudal vertebrae	16	16 (17)			17	16
Total number of vertebrae	30	30 (17)			17	30
Teeth in upper outer row	44	31 (1); 33 (1); 35 (2); 39 (1); 40 (3); 41 (1); 42 (2); 43 (3); 44 (2)			17	-
Teeth in lower outer row	29	23 (1); 24 (1); 25 (1); 26 (2); 27 (2); 28 (2); 29 (2); 30 (2); 31 (1); 32 (2); 33 (1)			17	-
Gill rakers (ceratobranchial)	9	7 (3); 8 (11); 9 (2)			17	8
Gill rakers (angle + epibranchial)	3	3 (17)			17	3

Vertebrae and caudal fin skeleton. (Fig. 3). A total of 30 vertebrae (excluding urostyle element), with 14 abdominal and 16 caudal vertebrae. The pterygiophore supporting last dorsal-fin spine is inserted between neural spines of 16th and 17th vertebra (counted from anterior to posterior). Pterygiophore supporting last anal-fin spine is inserted between haemal spines of 15th and 16th vertebra, rarely between ribs of 14th and haemal spine of 15th vertebra (N=2). Single predorsal bone (=supraneural bone) present. Hypurals 1 and 2 as well as hypurals 3 and 4 always fused into single seamless units.

Colouration in life (based on field photographs of adult specimens). (Fig. 3) Body ground colouration pale brown to light grey; anterior flank with yellow to golden reticulated pattern which becomes less prominent at level of anus and stops at level of caudal peduncle. Dark grey to brownish, interrupted midlateral band from operculum to just posterior caudal fin base, ending in mostly visible blotch; intensity midlateral band varies depending on mood often hardly visible. Midlateral band crossed by 13–15 vertical bars, which extend mainly ventrally, hardly recognizable except for more distinct first 4–5 anterior bars. In some specimens dorsum with irregular dark brown areas, which sometimes connect with midlateral band. Scales on, above and below midlateral band until level of anus with blackish-blue to greyish-blue centres. Dorsum and caudal peduncle pale brown to light grey; chest and belly light beige. Dorsal head surface pale brown to light grey; snout and cheek beige, ventrally brighter. Branchiostegal membrane light beige. Operculum beige to yellowish, sometimes with metallic turquoise speckles, a black opercular spot connecting with anterior extension of midlateral band (interrupted at level of preoperculum) ending in well-pigmented blotch slightly anterior of eye. Another dark grey to brownish element of variable form on ventral corner of operculum. Cheek with small, dark grey to brownish vertical stripe of variable shape and intensity, extending to slightly below eye (not reaching eye). Dark grey to brownish lachrymal stripe ending at posterior end upper lip. Very thin, dark grey to brownish nostril stripe (sometimes interrupted) *V*-shaped, extending between nostrils. Thin, dark grey to brownish interorbital stripe present; no distinct supraorbital stripe, but area just above eye somewhat darker than remaining dorsal head region. Upper and lower lip beige to pale brown, lower margin of upper lip greyish (darker coloured), lower lip lighter than upper. Dorsal-fin membrane transparent with orange maculae, sometimes arranged in inclined rows; maculae bordered with orange and outlined with black, especially in spinous part of fin. Anal fin transparent to yellow, towards margin becoming more intensively coloured, no maculae or eggspots present. Caudal fin yellowish to greyish with two or three rows of small yellow-orange maculae near fin base. Outer caudal-fin rays with black margin. Pectoral and pelvic fins transparent but rays yellowish to greyish.

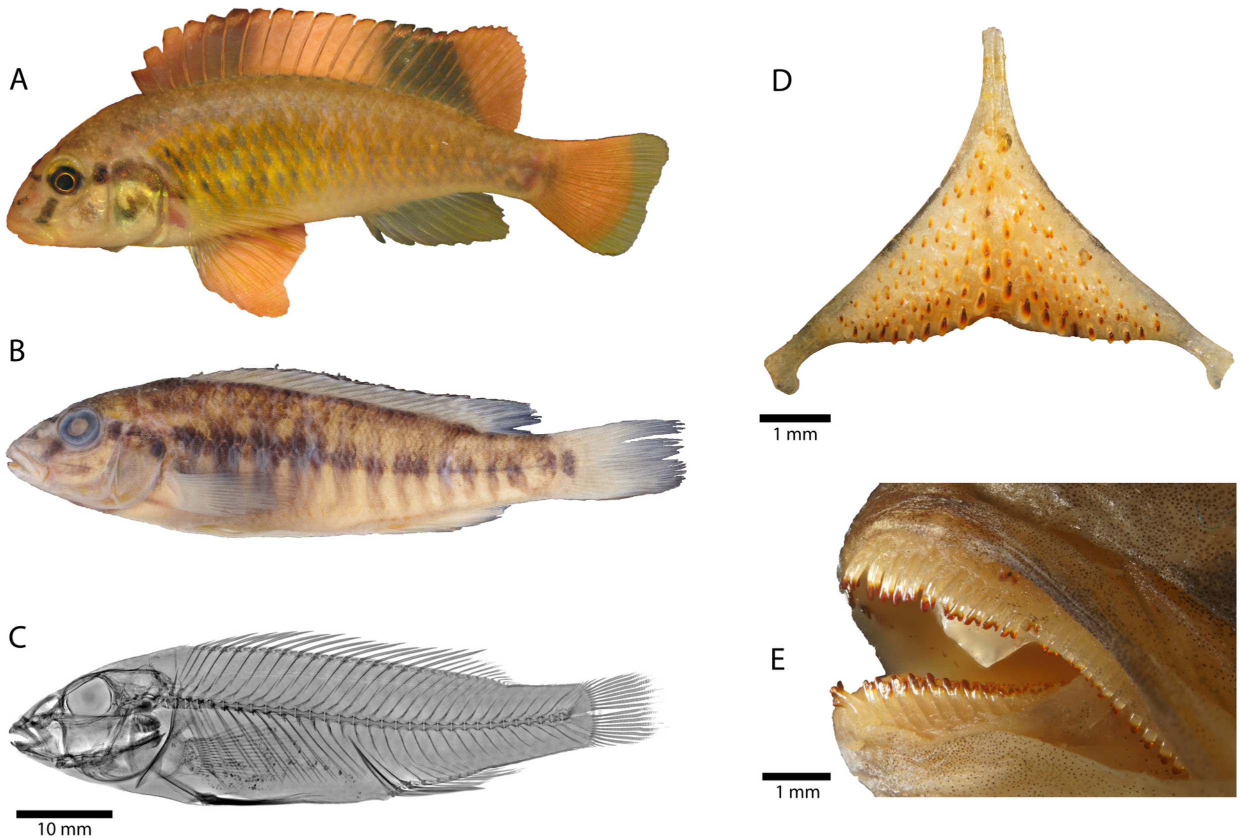

FIGURE 3. *Orthochromis mporokoso* **sp. nov. A.** probably the holotype, alive. Dorsal, anal and caudal fin background coloration is uniform semitransparent and might be lightly yellowish to greyish, i.e. not as in picture (human fingers holding the specimen in photo tank gave artificial beige color to semitransparent fins). **B.** Holotype (ZSM 46840), 59.0 mm SL; Zambia, Kasinsha stream **C.** radiograph of holotype **D.** lower pharyngeal bone (specimen with 59.8 mm SL; ZSM 41429) **E.** Overview of arrangement and morphology of oral jaw teeth (specimen with 74.5 mm SL; ZSM 41429).

Juvenile colouration in life. No information about juvenile colouration available.

Colouration in alcohol. Colouration and melanin patterns similar to live specimens, but due the preservation procedure of specimens, i.e., first formalin fixation, transfer to 75 % EtOH etc., specimens tend to lose original colouration (especially melanin patterns more intense than in live specimens). Overall body ground colouration light brownish; dorsum darker than flank below midlateral band. Chest and belly beige to yellowish-beige. Branchiostegal membrane beige, along operculum and ventrally becoming reddish brown. Dorsal head surface and dorsum brownish, ethmoidal region greyish-brown. Upper lip beige to light greyish anteriorly, lower lip beige. Cheek beige to pale brownish; vertical stripe on cheek faint. Operculum beige to pale brown greyish and with opercular spot as described above (brownish element on operculum less clearly defined than in live specimens and covering almost entire operculum). Head mask brownish. Midlateral band and vertical bars brownish and more intense (especially posterior bars). Dorsal fin whitish to light greyish and margins outlined in black; maculae visible but less intense and greyish. Anal fin whitish to beige; margins blackish outlined. Caudal fin light whitish to beige; margins blackish outlined, small greyish speckles visible on membrane. Pectoral fin and pelvic fin whitish to light grey.

Distribution and biology. *Orthochromis mporokoso* is known from two clear water streams in the vicinity of Mporokoso town. Kasinsha stream (holotype locality, Fig. 1) is about five meters wide with a rocky bottom and on average 50–100 cm deep (Fig. 8).

The water temperature at the type locality was 19.5 °C (15.07.2011, late afternoon) and had a pH of 6.7; at the second sampling locality (Mutoloshi River at Kapuma Falls) a temperature of 19.3 °C (15.07.2011) and a pH of 7.3 was recorded (pers. comm. H. van Heusden 2017). *Orthochromis mporokoso* is a benthic-rheophilic species.

Etymology. The species name *mporokoso* is derived from Mporokoso, a town in the Northern Province (Zambia) near the type locality of the species. A noun in apposition.

Orthochromis katumbii sp. nov.

Orthochromis sp. "Mambilima"—Schedel *et al.* 2014

Holotype. MRAC 2015-009-P-0006 (1, 85.9 mm SL), Democratic Republic of the Congo, Kiswishi River, near confluence with Matete stream, Luapula basin (-11.486528/ 27.650306)

Paratypes. MRAC 2015-009-P-0001 (1, 53.2 mm SL), Democratic Republic of the Congo, Kiswishi River, Futuka farm, Luapula basin (-11.488028/27.645833).—ZSM 46844 (1, ex MRAC 2015-009-P-0002, 81.8 mm SL), Democratic Republic of the Congo, Kiswishi River, Futuka farm, Luapula basin (-11.488028/ 27.645833).—MRAC 2015-009-P-0003 (1, 56.6 mm SL), Democratic Republic of the Congo, Kiswishi River, Futuka farm, Luapula basin (-11.488028/27.645833).—MRAC 2015-009-P-0007-0009 (3, 58.7–85.2 mm SL), collected with holotype.—ZSM 41450 (6, 27.2–57.4 mm SL), Zambia, Luapula River below Mambilima Falls (-10.5689/ 28.6783).

Additional material. ZSM 42322 (2, 71.3–88.9 mm SL), Zambia, Luapula River below Mambilima Falls; kept in aquarium (-10.5689/28.6783).

Differential diagnosis. *Orthochromis katumbii* is distinguished from all Malagarasi-*Orthochromis* species including *O.* sp. "Igamba" except *O. mazimeroensis* and *O. rubrolabialis* by having more scale rows on cheek (1–4 vs. 0). Further it is distinguished from *O. kasuluensis*, *O. mosoensis,* and *O. rugufuensis* by having more scales in lower lateral line (10–13 vs. 7–9) and furthermore from *O. kasuluensis* by having fewer dorsal-fin rays (7–9 vs. 10); from *O. mosoensis* by having more scales on operculum (2–3 vs. 0–1); from *O. uvinzae* by having fewer scales between upper lateral line and dorsal-fin origin (4–5 vs. 6-8), by having fewer dorsal-fin spines (16–18 vs. 19–20) and it is distinguished in position of pterygiophore supporting last dorsal-fin spine (vertebral count: 15–17 vs. 18-19). From *O. mazimeroensis* it is distinguished by having more horizontal line scales (30–31 vs. 26–28), more abdominal vertebrae (14–15 vs. 12–13) and more total vertebrae (30–31 vs. 26–28). It is distinguished from *O. rubrolabialis* by having more ceratobranchial gill rakers (7–9 vs. 5–6) and total gill raker (10–13 vs. 8-9); from *O. stormsi* by having more caudal vertebrae (16–17 vs. 14–15), more total vertebrae (30–31 vs. 28–29), more horizontal line scales (30–31 vs. 26–28) and fewer scales between upper lateral line and dorsal-fin origin (4–5 vs. 6–9); from *O. polyacanthus* by having more series of scales on cheek (1–4 vs. 0); from *O. torrenticola* by having fewer anal-fin spines (3 vs. 4). Meristic values of *O. katumbii* overlap with those of *O. kalungwishiensis* but is distinguished by differences in colour and melanin patterns (e.g. nostril stripe in *O. katumbii* not extending to interorbital stripe vs. extending in *O. kalungwishiensis*; operculum yellowish-grey in *O. katumbii* vs. reddish-brownish in *O. kalungwishiensis*; vertical bars crossing midlateral band more pronounced in *O. kalungwishiensis*). Meristic values of *O. katumbii* overlap with those of *O. luongoensis* but is distinguished by ratio length/depth of caudal peduncle (1.6–1.9 vs. 2.0–2.4); in addition *O. katumbii* tends to have fewer vertical bars on flank (7–9 vs. 9–12). Meristic values of *O. katumbii* overlap with those of *O. machadoi* but is distinguished by smaller body depth (22.4–27.7 vs. 30.0–32.2 % SL). It is distinguished from *S. neodon* by having more circumpeduncular scales (16 vs. 12), and fewer dorsal-fin rays (9–10 vs. 11–12). It differs from *H. snoeksi* by having more scales on lower lateral line (10–13 vs. 9), more abdominal vertebrae (14–15 vs. 13), fewer caudal vertebrae (16 vs. 17), more anal-fin rays (7–9 vs. 5–6) and more total gill rakers (10–13 vs. 9), in position pterygiophore supporting last anal-fin spine (vertebral count: 15–16 vs. 13) and by having hypurals 3 and 4 fused (vs. clearly separated or fused with distinctly visible seam); differs from *H. bakongo* and *H. moeruensis* by having more horizontal line scales (30–31 vs. 26–28), more caudal vertebrae (16–17 vs. 12–15) and more total vertebrae (30–31 vs. 26–29). Additionally, *O. katumbii* differs from *H. bakongo* by having more dorsal fin spines (16–18 vs. 14–15), by having hypurals 1 and 2 and hypurals 3 and 4 fused (vs. clearly separated or fused with distinctly visible seam) and by position of pterygiophore supporting last dorsal-fin spine (vertebral count: 15–17 vs. 13–14) and from *H. moeruensis* by having more scales on upper lateral line (21–24 vs. 19–20). It differs from *H. vanheusdeni* by having more horizontal line scales (30–31 vs. 26–29). It is distinguished from herein newly described species *O. kimpala* by having more horizontal line scales (30–31 vs. 27–29), fewer scales between upper lateral line and dorsal-fin origin (4–5 vs. 6–7); from *O. indermauri* by having more horizontal line scales (30–31 vs. 25–29), caudal vertebrae (16–17 vs. 14–15), total vertebrae (30–31 vs. 28–29) and by having hypurals 1 and 2 fused vs. clearly separated or fused with distinctly visible seam). Meristic values of *O. katumbii* overlap with those of *O. mporokoso* but is distinguished by having fewer vertical bars on flank (7–9 vs. 13–15) and in head mask pattern (i.e.: no cheek stripe present vs. present in *O. mporokoso*). Meristic values of *O. katumbii* overlap with those of *O. gecki* but is distinguished by having a wider interorbital (15.5–21.7 vs. 9.6–12.9 % HL), moreover *O. katumbii* lacks eggspots on anal fin (vs. present in *O. gecki*).

Description. Morphometric measurements and meristic characters are based on 13 type specimens. Values and their ranges are presented in Table 3. For general appearance see figure 4. Maximum length of wild caught specimens 85.9 mm SL. Moderately slender species with maximum body depth (28.1 % SL) at level of first dorsal-fin spine (smaller specimens) or slightly behind dorsal-fin origin (larger specimens), decreasing towards caudal peduncle. Caudal peduncle rather elongated and moderately deep (ratio of caudal peduncle length to depth: 1.6–1.9). Head length about one third of standard length. In adult specimens dorsal head profile gently curved and without prominent nuchal gibbosity. Dorsal head profile of subadult specimens more distinctly curved (Fig. 9). Eye diameter larger than interorbital width. Jaws isognathous or slightly retrognathous. Posterior tip of maxilla reaching vertical between nostril and anterior margin orbit. Lips not noticeably enlarged or thickened. Two separate lateral lines.

Squamation. Flank above and below lateral lines covered with comparatively large ctenoid scales. Anterior dorsal and ventral flank covered by cycloid scales. Belly with comparatively small cycloid scales. Chest covered with minute, deeply embedded cycloid scales; chest to flank transition with slightly larger cycloid scales. Snout scaleless. Interorbital scales cycloid and deeply embedded. Nape and occipital region with medium sized cycloid scales. Cheeks covered by small, partly embedded cycloid scales; 2–4 scale rows on cheek. Cycloid scales on operculum of variable size (small to medium) and shape (ovoid to circular); opercular blotch only partially covered by medium sized scales, but posterior margin always scaleless. Two to three scales on horizontal line starting from edge of postero-dorsal angle of operculum to anterior edge of operculum.

Upper lateral line scales 21–24, lower lateral line 10–13. Horizontal line scales 30–31. Caudal fin with 0–2 pored scales. Upper and lower lateral lines separated by two scales; 4–5 scales between upper lateral line and dorsal-fin origin. At level of last dorsal-fin spine one dorso-ventrally compressed cycloid scale and one normal sized ctenoid scale between origin of last dorsal-fin spine and upper lateral line. Anterior part of caudal fin covered with 3–4 vertical columns of small cycloid scales; with median scales being slightly larger; scaled area of caudal fin extended posteriorly, especially at upper and lower area, with minute, interradial scales (approximately up to two fifths of caudal fin). Sixteen scales around caudal peduncle.

TABLE 3. Measurements and counts of holotype and paratypes and of additional specimens of *Orthochromis katumbii* **sp. nov.**

Measurements	holotype	holotype + paratypes				ZSM 42322	
		min	Max	SD	n	Ind. 1	Ind. 2
Total length (mm)	103.6	33.3	103.6		13	84.8	106.5
Standard length SL (mm)	85.9	27.2	85.9		13	71.3	88.9
Head length HL (mm)	25.7	8.9	25.7		13	22.2	26.6
% HL							
Interorbital width	20.6	14.5	21.7	2.1	13	17.4	19.4
Preorbital width	35.1	26.2	35.1	2.7	13	32.6	36.0
Horizontal eye length	23.7	22.5	28.9	1.6	13	23.9	21.0
Snout length	40.7	28.5	40.7	3.5	13	37.4	39.0
Internostril distance	18.6	16.4	21.7	1.4	13	19.9	21.4
Cheek depth	25.1	18.5	28.4	2.7	13	32.8	26.0
Upper lip length	31.5	24.6	34.6	2.7	13	29.6	37.6
Lower lip length	30.2	18.9	31.2	3.9	13	28.4	33.1
Lower lip width	35.4	24.6	38.3	3.3	13	34.2	41.4
Lower jaw length	33.3	26.1	36.8	2.8	13	35.1	33.7
Lower pharyngeal jaw length	-	25.7		-	1		
Lower pharyngeal jaw width	-	30.1		-	1		
Width of dentigerous area of lower pharyngeal jaw	-	21.9		-	1		
% SL							
Predorsal distance	32.0	31.6	36.1	1.4	13	32.6	31.8
Dorsal-fin base length	55.1	54.1	58.1	1.2	13	55.9	57.0
Last dorsal-fin spine length	9.5	9.5	13.8	1.2	13	12.3	11.8
Anal-fin base length	18.9	14.7	20.2	1.5	13	15.5	17.8
Third anal-fin spine length	10.5	10.5	20.2	2.5	13	11.1	12.1
Pelvic fin length	21.0	19.6	25.7	1.8	13	18.1	18.1
Pectoral fin length	22.1	19.5	23.8	1.1	13	20.1	19.4
Caudal peduncle depth	11.0	10.3	12.2	0.6	13	11.0	11.0
Caudal peduncle length	19.1	17.9	20.9	0.7	13	18.6	16.9
Body depth (pelvic fin base)	27.6	22.4	27.7	1.9	13	27.5	28.5
Preanal length	58.5	54.9	62.1	1.6	13	63.2	62.2
Anus-anal fin base distance	3.8	1.4	4.0	0.9	13	3.1	3.4
Interpectoral width	15.5	10.6	15.5	1.4	13	16.0	15.4
Counts							
Dorsal-fin spines	17	16 (2); 17 (6); 18 (4)			12	18	17
Dorsal-fin rays	9	9 (7); 10 (5)			12	9	10
Anal-fin spines	3	3 (12)			12	3	3
Anal-fin rays	7	7 (6); 8 (5); 9 (1)			12	7	8
Pelvic-fin spines	1	1 (12)			12	1	1
Pelvic-fin rays	5	5 (12)			12	5	5
Pectoral-fin rays	15	15 (10); 16 (2)			12	15	15
Upper procurrent caudal-fin rays	7	6 (6); 7 (6)			12	7	7

......continued on the next page

TABLE 3. (Continued)

Measurements	holotype	holotype + paratypes			n	ZSM 42322	
		min	Max	SD	n	Ind. 1	Ind. 2
Lower procurrent caudal-fin rays	6	5 (1); 6 (11)			12	7	7
Caudal-fin rays	29	27 (1); 28 (5); 29 (6)			12	29	29
Scales (horizontal line)	30	30 (9); 31 (3)			12	30	30
Upper lateral line	21	21 (5); 22 (4); 23 (2); 24 (1)			12	24	22
Lower lateral line	13	10 (1); 11 (3); 12 (6); 13 (2)			12	11	11
Circumpeducular	16	16 (2)			12	16	16
Series of scales on cheek	2	1 (3); 2 (5); 3 (3); 4 (1)			12	3	3
Scales (horizontal line) on operculum	3	2 (6); 3 (6)			12	3	3
Scales between lateral line and dorsal fin origin	5	4 (2); 5 (10)			12	5	5
Scales between upper lateral line and last dorsal fin spine	2	2 (12)			12	2	2
Abdominal vertebrae	14	14 (10); 15 (2)			12	14	14
Caudal vertebrae	17	16 (6); 17 (6)			12	17	17
Total number of vertebrae	31	30 (4); 31 (8)			12	31	31
Teeth in upper outer row	52	29 (1); 30 (1); 32 (1); 36 (2); 38 (1); 39 (1); 41 (1); 45 (1); 48 (1); 49 (1); 52 (1)			12	46	54
Teeth in lower outer row	35	24 (1); 25 (1); 26 (2); 27 (1); 31 (1); 32 (1); 33 (2); 35 (1); 37 (1); 39 (1)			12	28	37
Gill rakers (ceratobranchial)	7	7 (8); 8 (2); 9 (2)			12	8	7
Gill rakers (angle + epibranchial)	3	3 (8); 4 (3); 5 (2)			12	4	4

Jaws and dentition. Anterior teeth of outer row of upper and lower jaw bicuspid to subequally bicuspid, large and closely set; more posterior teeth becoming subequally bicuspid, towards corner of mouth teeth smaller and less closely set and unicuspid. Individual bicuspid teeth with minimally expanded brownish crown, cusps slightly compressed and moderately widely set, neck moderately slender. Outer row of upper jaw with 29–52 teeth and outer row of lower jaw with 24–39 teeth (specimens: 37.2–85.6 mm SL). Larger specimens generally with more teeth. Two to three (rarely one or four) inner upper and lower jaw tooth rows with small tricuspid teeth. Generally larger individuals with more inner tooth rows. Lower pharyngeal bone (Fig. 4) of single dissected paratype (MRAC 2015-009-P-0007-0009, 77.2 mm SL) about 1.2 times wider than long with short anterior keel about 0.4 times length of dentigerous area. Dentigerous area of lower pharyngeal bone about 1.4 times wider than long, with 12+12 (empty tooth-sockets included) teeth along posterior margin and 6–8 (empty tooth-sockets included) teeth along midline. Anterior pharyngeal teeth (towards keel) bevelled and slender; those of posterior row larger than anterior ones, bevelled (bicuspid; well-developed major and minor cusp). Largest teeth medially situated in posterior row. Teeth along midline slightly larger than more lateral ones.

Gill rakers. Total gill raker count 10–13 with 2–4 epibranchial, one angle, and 7–9 ceratobranchial gill rakers. Most anterior ceratobranchial gill rakers smallest, increasing in size towards cartilaginous plug (angle). Anterior gill rakers on ceratobranchial unifid, towards cartilaginous plug sometimes bifid. Gill raker on cartilaginous plug shorter than longest ceratobranchial gill raker and epibranchial gill rakers further decreasing in size.

Fins. Dorsal fin with 16–18 spines and with 9–10 rays. First dorsal-fin spine always shortest. Dorsal-fin base length between 54.0–58.1 % SL. Posterior end of dorsal-fin rays almost reaching caudal-fin base; posterior tip of anal fin ending before caudal fin base. Caudal fin outline subtruncate and composed of 27–29 rays (16 principal caudal-fin rays and 11–13 procurrent caudal-fin rays). Anal fin with 3 spines (3^{rd} spine longest) and 7–9 rays. Anal-fin base length between 14.8–20.2 % SL. Pectoral fin with 15 or 16 rays. Pectoral-fin length between 19.5–23.8 % SL; longest pectoral ray not reaching level of anus. First upper and lower pectoral-fin rays very short to short.

Pelvic fin with 1st spine thickly covered with skin, and 5 rays. Pelvic fin base slightly further posterior pectoral fin base. Longest pelvic-fin ray almost reaching (especially in smaller specimens) or ending well before anus (ending approximately 2 flank scales width before).

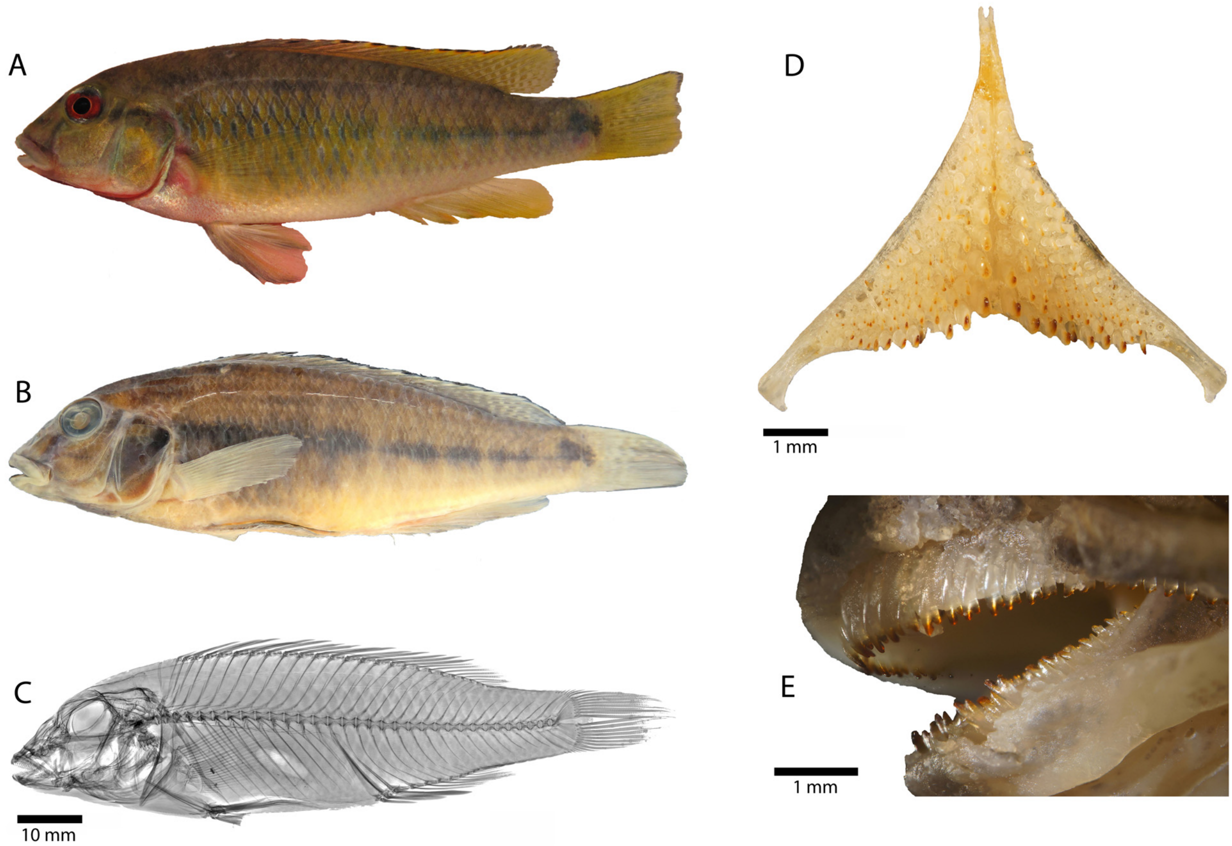

FIGURE 4. *Orthochromis katumbii* **sp. nov. A.** holotype, alive **B.** holotype (MRAC 2015-009-P-0006), 85.9 mm SL; Democratic Republic of the Congo, Kiswishi River **C.** radiograph of holotype **D.** lower pharyngeal bone (specimen: MRAC 2015-009-P-0007-0009, 77.2 mm SL) **E.** Overview of arrangement and morphology of oral jaw teeth (specimen: MRAC 2015-009-P-0007-0009, 77.2 mm SL).

Vertebrae and caudal fin skeleton. 30–31 total vertebrae (excluding urostyle element), with 14–15 abdominal and 16–17 caudal vertebrae. Pterygiophore supporting last dorsal-fin spine is inserted between neural spines of 15th and 16h, 16th and 17th, or 17th and 18th vertebra (counted from anterior to posterior). Pterygiophore supporting last anal-fin spine is inserted between haemal spines of 15th and 16 th vertebra or 16th and 17th vertebra. Single predorsal bone (=supraneural) present. Hypurals 1 and 2 as well as hypurals 3 and 4 always fused.

Colouration in life (based on field photographs of adult specimens). (Fig. 4) Body ground colouration pale brown to yellowish. Dark grey to brownish, interrupted midlateral band extending from operculum to just behind caudal fin base ending as a blotch (less distinct than in *O. luongoensis* and sometimes hardly visible at all); midlateral band intensity varies depending on mood, sometimes fainting to greyish band. Midlateral band crossed by 7–10 light brown to sooty black vertical bars; these bars are short (extending shortly above and below midlateral band) and rather faint in colouration and not always recognizable. However, it should be mentioned that intensity of body markings is strongly dependent on motivational state. Chest light beige with some reddish sparkles (especially in bigger specimens). Belly light beige. Dorsal head surface and snout pale brown to greyish; cheek beige to yellow-greyish. Iris reddish at level of interorbital stripe/anterior extension of midlateral band (red more prominent in bigger specimens). Lower jaw and mental area pale beige to reddish. Throat and branchiostegal membrane reddish (ventral side of branchiostegal membrane in *O. luongoensis* blackish). Operculum beige to yellow-greyish with a dark grey to blackish opercular spot connecting anterior extension of midlateral band that ends almost at posterior edge of eye. Another light brownish element of variable form and intensity on ventral corner of operculum; such element also present in *O. luongoensis* but less intense in *H. katumbii*. Dark grey to brownish lachrymal stripe ending at posterior end of upper lip. Thin, dark grey to brownish nostril stripe (sometimes interrupted) in form of flattened *U* extending between nostrils. Dark grey to brownish interorbital stripe more intense than nostril stripe. No supraorbital stripe present. Upper and lower lip beige to pale brown, lower margin of upper lip greyish, lower lip lighter then upper lip. Dorsal fin membrane light orange to pale brown with columns of light reddish-orange to brownish maculae between branched rays and to some degree between last dorsal-fin spine (membrane between maculae brighter, almost hyaline); spinous dorsal fin with black marginal band and reddish-orange lappets; marginal band extending to some degree onto rayed part of dorsal fin. Anal fin light orange to pale brown, more intensively coloured towards distal margin. Spinous anal fin with faint reddish-orange margin. No maculae or eggspots present. Caudal fin light orange to pale brown becoming more intensively coloured near margin; membrane between rays with three vertical columns of small greyish maculae (membrane between maculae brighter, almost hyaline, especially in central part of caudal fin). Outer caudal-fin rays with dark orange to blackish margin. Pectoral fin light orange, especially rays of this colour. Pelvic fin compared to pectoral fin less coloured, appearing almost transparent, membrane of pelvic fin spine greyish.

Juvenile colouration in life. (based on photos of tank-raised juveniles approximately 25 mm SL; Fig. 9) Ground colouration greyish, belly beige. Patterns and stripes of head as described for adults. Greyish vertical bars on flanks more prominent than in adults. Iris greyish. Dorsal fin hyaline with some blackish spots on membrane; all other fins hyaline.

Colouration in alcohol. Colouration and melanin patterns similar to live specimens, but due the preservation procedure of specimens, i.e., first formalin fixation, transfer to 75 % EtOH etc., specimens tend to lose original colouration (especially melanin patterns more intense than in live specimens). Overall body ground colouration brownish; dorsum, flank and caudal peduncle brownish becoming beige at ventral side (band of one to two scales ventrally of flanks and caudal peduncle). Chest beige to light brownish and belly beige. Branchiostegal membrane light greyish, ventral side of branchiostegal membrane dark brown, towards anterior tip becoming brighter. Dorsal head surface brownish as dorsum, ethmoidal area becoming greyish-brown. Upper lip light greyish to beige; lower margin of upper lip greyish; lower lip beige. Cheek beige to brownish; centrally below eye a brownish blotch of variable intensity visible (as in *O. luongoensis*, which is not the case in living specimens). Operculum brown to dark brownish with opercular spot as described above; light brownish element of living specimens hardly visible or indistinguishable from operculum ground colouration in conserved specimens. Markings of head mask dark brownish to dark grey. Midlateral band dark brownish and vertical bars light brownish (less distinct than midlateral band). Dorsal fin greyish with black margin, subsequently followed by beige lappets; greyish maculae mainly on rayed part still visible but less intense. Anal fin whitish to beige. Pectoral fin beige. Pelvic fin beige; membrane of spine light greyish. Caudal fin light, at base pale brownish, caudally becoming beige; greyish maculae still present but less intense; margins blackish.

Distribution and biology. *Orthochromis katumbii* is known from Kiswishi River, a western tributary of the Luapula and from the Mambilima Falls on the Luapula (Fig. 1). At the type, locality the Kiswishi River is about ten meters wide and on average about one meter deep and the bottom substrate consists of gravel and smaller rocks (Fig. 8). Water temperature varied between 19.3 and 23.8 °C (measured in August and September), pH between 7.73–7.95, electrical conductivity 377.7 and 380.1µS. *O. katumbii* is a benthic-rheophilic maternal mouthbrooder with clutch sizes, in captivity, of between 25 and 30 eggs (pers. comm. J. Geck). Recently a monogenean gill parasite *Cichlidogyrus consobrini* Jorissen, Pariselle and Vanhove 2017 was described from specimens obtained from *O. katumbii* and *Sargochromis mellandi* (Boulenger 1905).

Etymology. The species is named after Mr. Moïse Katumbi who supported part of the 2015 ichthyological research field expedition of the Mbisa Congo project in Katanga province of the DRC, who himself is a great fish enthusiast. Some specimens of the new species were collected on his farm "Ferme de Futuka".

***Orthochromis kimpala* sp. nov.**

Holotype. MRAC 2012-031-P-2096 (84.58 mm SL), Democratic Republic of the Congo, Kalule Nord River, right tributary of Lualaba River, near to the bridge on road Makulakulu-Lubudi (-9.6935/25.8479).

Paratypes. ZSM 46849 (2, ex MRAC uncat., 62.7–78.8 mm SL), collected with holotype.—ZSM 46850 (1, ex

MRAC uncat., 44.0 mm SL), collected with holotype.—MRAC 2015-005-P-0032-0033 (2, 56.9–62.6 mm SL), Democratic Republic of the Congo, Kalule Nord River, bridge Lubudi-Luena (-9.693472/25.847833).—MRAC 2015-005-P-0034-0035 (2, 56.3–60.5 mm SL), Democratic Republic of Congo, Kalule Nord River, Kyabule village, bridge Mukulakulu-Kolwezi (-9.66725/25.740056).—MRAC 2015-005-P-0036-0037 (2, 57.7–61.3 mm SL), Democratic Republic of the Congo, Kalule Nord River, Kyabule village, bridge Mukulakulu-Kolwezi (-9.66725/25.740056).

Differential diagnosis. *Orthochromis kimpala* can be readily distinguished from all species currently placed in *Orthochromis* (sensu de Vos & Seegers, 1998) except *O. torrenticola,* by presence of eggspot-like maculae on anal fin. Further, it is distinguished from Malagarasi-*Orthochromis* species, including *O.* sp. "Igamba", by having more scale rows on cheek (3–4 vs. 0 or 0–1 in case of *O. mazimeroensis* and *O. rubrolabialis*). Furthermore, *O. kimpala* differs from *O. luichensis*, *O. malagaraziensis*, *O. mazimeroensis*, *O. mosoensis,* and *O. rubrolabialis* by having more scales between upper lateral line and dorsal-fin origin (6–7 vs. 4–5). Additionally, it has fewer dorsal-fin spines than *O. luichensis*, *O. malagaraziensis,* and *O. rubrolabialis* (15–16 vs. 17–19). Moreover, it differs from *O. rubrolabialis* by having more total gill rakers (11–12 vs. 8–9) and by position of pterygiophore supporting last dorsal-fin spine (vertebral count: 14-16 vs. 17-19); from *O. mazimeroensis* by having more abdominal vertebrae (14–15 vs. 12–13); from *O. mosoensis* by having more scales (horizontal line) on operculum (3 vs. 0–1). *O. kimpala* is distinguished from *O. kasuluensis*, *O. rugufuensis* and *O. uvinzae* by having fewer dorsal-fin spines (15–16 vs. 17-20); from *O. kasuluensis* and *O. rugufuensis* by having more scales (horizontal line) on operculum (3 vs. 1–2); from *O. kasuluensis* and *O. uvinzae* by having fewer scales in upper lateral line (20–22 vs. 23–25) and fewer total vertebrae (28–30 vs. 31–33). Moreover,it differs from *O. uvinzae* by having fewer horizontal line scales (27–29 vs. 30–32) and by position of pterygiophore supporting last dorsal-fin spine (vertebral count: 14–16 vs. 18–19). It can be distinguished from *O. kalungwishiensis*, *O. luongoensis, O. polyacanthus,* and *O. torrenticola* by having fewer dorsal-fin spines (15–16 vs. 17–20); further from *O. kalungwishiensis*, *O. luongoensis,* and *O. torrenticola* by fewer horizontal line scales (27–29 vs. 30–32) and fewer total vertebrae (28–30 vs. 31–33); from *O. luongoensis* and *O. torrenticola* by fewer caudal vertebrae (13–16 vs. 17–18); from *O. torrenticola* by having fewer anal-fin spines (3 vs. 4). Moreover, it is distinguished from *O. torrenticola* and *O. polyacanthus* by position of pterygiophore supporting last anal-fin spine (vertebral count: 14–15 vs. 16–17). It is distinguished from *O. stormsi* by having fewer total gill rakers (11–12 vs. 13–15). It differs from *S. neodon* by having more scale rows on cheek (3–4 vs. 1–2), fewer horizontal line scales (27–29 vs. 30–31), more circumpeduncular scales (16 vs. 12), fewer inner series of teeth (2–3 vs. 4–6). It differs from *H. snoeksi* by having fewer horizontal line scales (27–29 vs. 30–31), fewer scales on upper lateral line (20–22 vs. 23), more abdominal vertebrae (14–15 vs. 13) and fewer caudal vertebrae (13–16 vs. 17), more anal-fin rays (8–10 vs. 5–6) and more total gill rakers (11–12 vs. 9); from *H. bakongo* by having more scales between upper lateral line and dorsal-fin origin (6–7 vs. 3–5); from *H. moeruensis* by having more upper procurrent caudal-fin rays (6–7 vs. 5) and more total caudal-fin rays (26–27 vs. 28–29); from *H. vanheusdeni* by having more scale rows on cheek (3–4 vs. 0–2). It is distinguished from herein newly described species *O. mporokoso* by more scales between upper lateral line and dorsal-fin origin (6–7 vs. 4–5); from *O. katumbii* by having fewer horizontal line scales (27–29 vs. 30–31), and by more scales between upper lateral line and dorsal-fin origin (6–7 vs. 4–5); from *O. gecki* by having more series of scales on cheek (3–4 vs. 0–2); from *O. indermauri* by having more series of scales on cheek (3–4 vs. 1–2) and by fewer dorsal-fin spines (15–16 vs. 17–18).

Description. Morphometric measurements and meristic characters are based on 10 type specimens. Values and their ranges are presented in Table 4. For general appearance see figure 5. Maximum length of wild caught specimens 84.6 mm SL. Moderately slender species with maximum body depth (24.8–30.5 % SL) at level of first dorsal-fin spine, decreasing rather quickly towards caudal peduncle. Caudal peduncle rather short and deep (ratio of caudal peduncle length to depth: 1.2–1.4). Head length almost one third of standard length. Dorsal-head profile rather strongly curved and without a prominent nuchal gibbosity. Eye diameter larger than interorbital width. Jaws isognathous. Posterior tip of maxilla reaching or almost reaching to anterior margin of orbit. Lips not noticeably enlarged or thickened, but upper lip becoming thicker posteriorly. Two separate lateral lines.

Squamation. Flank above and below lateral lines covered with comparatively large, well developed ctenoid scales. Anterior dorsal and ventral flank covered by cycloid scales. Margin of belly with deeply embedded medium sized scales; central belly region scaleless. Chest covered with minute, deeply embedded cycloid scales, giving impression of a scaleless chest; chest to flank transition with larger cycloid scales, however, still deeply embedded.

Snout scaleless. Interorbital scales minute to small, cycloid and deeply embedded. Nape region covered with small, deeply embedded cycloid scales becoming slightly larger towards occipital region. Occipital region with small to medium sized cycloid scales. Cheek covered by medium sized cycloid scales; 3–4 scale rows on cheek. Cycloid scales on operculum of medium size and variable shape (ovoid to circular); opercular blotch only on anterior margins covered by medium sized scales, main area of opercular blotch scaleless. Three scales on a horizontal line starting from edge of postero-dorsal angle of operculum to anterior edge of operculum.

TABLE 4. Measurements and counts of holotype and paratypes of *Orthochromis kimpala* **sp. nov.**

Measurements	holotype	holotype + paratypes			
		min	Max	SD	n
Total length (mm)	101.7	54.4	101.7		10
Standard length SL (mm)	84.6	44.0	84.6		10
Head length HL (mm)	26.7	14.2	26.7		10
% HL					
Interorbital width	18.1	13.0	18.1	1.7	10
Preorbital width	36.1	28.2	36.1	2.8	10
Horizontal eye length	23.4	20.6	28.4	2.3	10
Snout length	38.1	29.8	40.3	3.7	10
Internostril distance	22.7	17.2	22.7	1.6	10
Cheek depth	29.9	25.3	31.8	1.9	10
Upper lip length	36.9	29.0	36.9	2.9	10
Lower lip length	35.8	26.1	35.8	3.9	10
Lower lip width	44.6	27.1	44.6	4.7	10
Lower jaw length	37.8	33.4	40.4	2.3	10
Lower pharyngeal jaw length	-	29.3		-	1
Lower pharyngeal jaw width	-	34.0		-	1
Width of dentigerous area of lower pharyngeal jaw	-	25.8		-	1
% SL					
Predorsal distance	34.9	32.9	38.1	1.6	10
Dorsal-fin base length	56.7	51.4	56.9	1.9	10
Last dorsal-fin spine length	12.9	10.4	14.0	1.2	10
Anal-fin base length	20.0	17.4	20.6	1.1	10
Third anal-fin spine length	9.9	9.7	12.7	1.0	10
Pelvic fin length	20.8	20.6	25.2	1.4	10
Pectoral fin length	20.6	20.6	24.8	1.4	10
Caudal peduncle depth	11.9	10.5	11.9	0.5	10
Caudal peduncle length	15.5	12.7	16.1	1.0	10
Body depth (pelvic fin base)	29.7	24.8	30.5	2.0	10
Preanal length	67.8	60.3	67.8	2.3	10
Anus-anal fin base distance	3.1	2.0	4.7	0.8	10
Interpectoral width	16.4	12.9	16.9	1.2	10
Counts					
Dorsal-fin spines	16	15 (4); 16 (6)			10
Dorsal-fin rays	11	10 (4); 11 (6)			10
Anal-fin spines	3	3 (10)			10

......*continued on the next page*

TABLE 4. (Continued)

Measurements	holotype	holotype + paratypes			
		min	Max	SD	n
Anal-fin rays	9	8 (6); 9 (3); 10 (1)			10
Pelvic-fin spines	1	1 (10)			10
Pelvic-fin rays	5	5 (10)			10
Pectoral-fin rays	15	14 (1); 15 (6); 16 (3)			10
Upper procurrent caudal-fin rays	6	6 (5); 7 (5)			10
Lower procurrent caudal-fin rays	6	6 (10)			10
Caudal-fin rays	28	28 (5); 29 (5)			10
Scales (horizontal line)	29	27 (4); 28 (2); 29 (4)			10
Upper lateral line	22	20 (3); 21 (4); 22 (3)			10
Lower lateral line	11	8 (2); 9 (3); 10 (4); 11 (1)			10
Circumpeducular	16	16 (10)			10
Series of scales on cheek	4	3 (3); 4 (7)			10
Scales (horizontal line) on operculum	3	3 (10)			10
Scales between lateral line and dorsal fin origin	6	6 (7); 7 (3)			10
Scales between upper lateral line and last dorsal fin spine	2	2 (10)			10
Abdominal vertebrae	14	14 (9); 15 (1)			10
Caudal vertebrae	16	13 (1); 14 (1); 15 (7); 16 (1)			10
Total number of vertebrae	30	28 (2); 29 (7); 30 (1)			10
Teeth in upper outer row		30 (1); 33 (1); 37 (1); 38 (1); 43 (2); 44 (3); 47 (1)			10
Teeth in lower outer row		28 (1); 29 (2); 32 (1); 33 (2); 35 (1); 36 (1); 38 (2)			10
Gill rakers (ceratobranchial)		7 (1); 8 (8); 9 (1)			10
Gill rakers (angle + epibranchial)		3 (9); 4 (1)			10

Upper lateral line scales 20–22 and lower lateral line 8–11. Horizontal line scales 27–29. Caudal fin with 0–2 pored scales. Upper and lower lateral lines separated by two scales; 6–7 scales between upper lateral line and dorsal-fin origin. Anterior part of caudal fin covered with 2–3 vertical rows of small cycloid scales; with median scales slightly larger; scaled area of caudal fin extended posteriorly especially at upper and lower area with minute, interradial scales (approximately up to one half of caudal fin). Sixteen scales around caudal peduncle.

Jaws and dentition. Anterior teeth of outer row of upper and lower jaw bicuspid to subequal bicuspid, large and moderately closely set; towards corner of mouth, teeth smaller and more widely set and unicuspid. Individual bicuspid teeth with minimally expanded brownish crown, cusps uncompressed and moderately narrowly set, neck moderately stout. Outer row of upper jaw with 30–47 teeth and outer row of lower jaw with 28–38 teeth (specimens: 44.4–84.6 mm SL); larger specimens generally with more teeth. Two to three inner upper and lower jaw tooth rows with small tricuspid teeth (rarely bicuspid).

Lower pharyngeal bone (Fig. 5) of single dissected paratype (ZSM 46849, 62.7 mm SL) about 1.2 times wider than long with anterior keel about 0.5 times of length of dentigerous area. Dentigerous area of lower pharyngeal bone about 1.6 times wider than long, with 11+11 (empty tooth-sockets included) teeth along posterior margin and eight teeth along midline. Anterior pharyngeal teeth (towards keel) bevelled to pronounced and slender; those of posterior row larger than anterior ones, bevelled (minor cusp not well developed). Largest teeth medially situated in posterior tooth row. Teeth along midline slightly larger than more lateral ones.

Gill rakers. Total gill raker count 11, with 2–3 epibranchial, one in angle, and 7–8 ceratobranchial gill rakers. Most anterior ceratobranchial gill rakers smallest increasing quickly in size towards cartilaginous plug (angle). Gill raker in angle slightly shorter than longest ceratobranchial gill raker and epibranchial gill rakers further decreasing in size.

Fins. Dorsal fin with 15–16 spines and with 10–11 rays. First dorsal-fin spine always shortest. Dorsal-fin base length between 51.4–56.9 % SL. Posterior end of dorsal-fin rays reaching or slightly extending beyond caudal fin base; posterior tip of anal fin ending slightly before caudal fin base. Caudal fin outline subtruncate and fin composed of 28–29 rays (16 principal caudal-fin rays and 12–13 procurrent caudal-fin rays). Anal fin with 3 spines (3rd spine longest) and 8–10 rays. Anal-fin base length between 17.4–20.6 % SL. Pectoral fin with 14–16 rays. Pectoral-fin length between 20.6–24.8 % SL; longest pectoral ray not reaching level of anus. First upper and lower pectoral-fin rays very short to short. Pelvic fin with 1st spine thickly covered with skin and five rays. Pelvic-fin base slightly more posterior than pectoral fin base. Longest pelvic-fin ray not reaching anus (ending approximately 3 flank scale widths before).

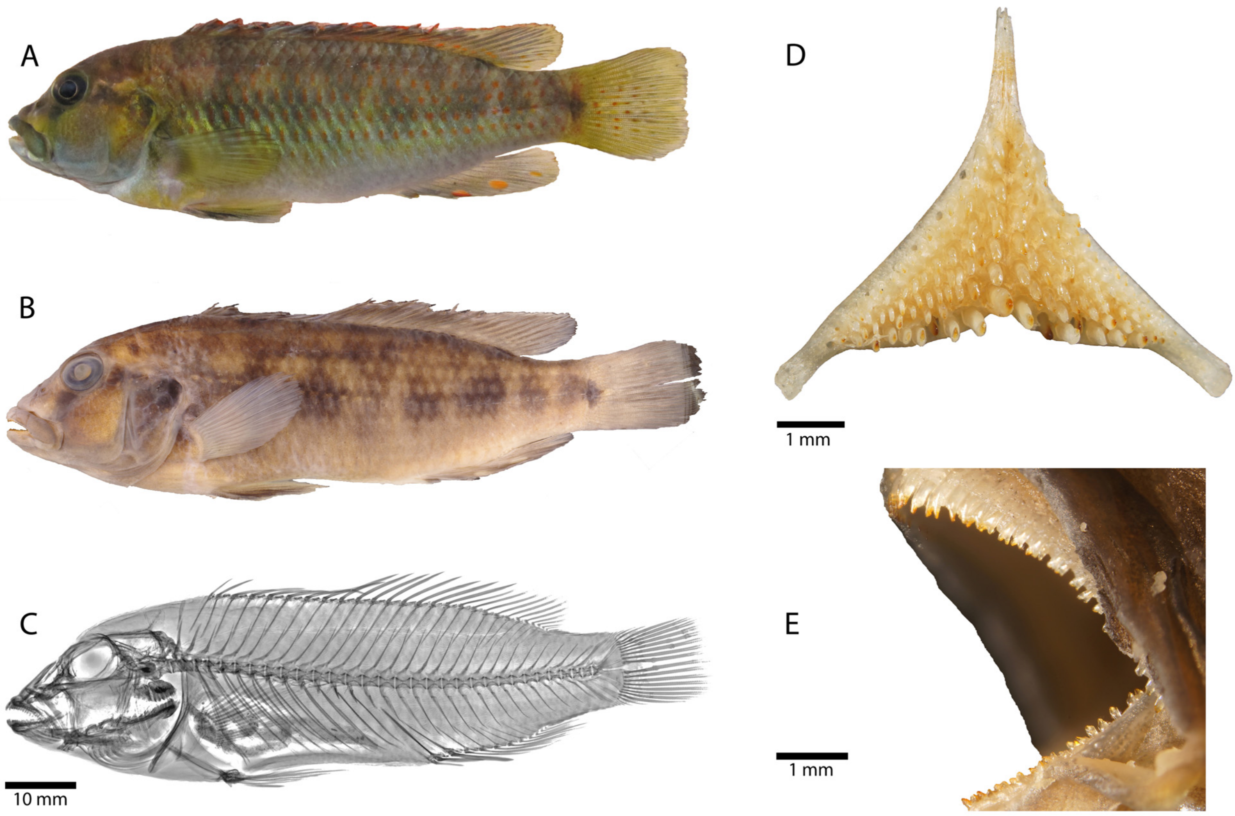

FIGURE 5. *Orthochromis kimpala* **sp. nov. A.** probably the holotype, alive **B.** Holotype, (MRAC 2012-031-P-2096), 84.6 mm SL; Democratic Republic of the Congo, Kalule Nord River stream **C.** radiograph of holotype **D.** lower pharyngeal bone (specimen: ZSM 46849, 62.7 mm SL) **E.** Overview of arrangement and morphology of oral jaw teeth (specimen: MRAC 2015-005-P-0036-0037, 61.3 mm SL).

Vertebrae and caudal fin skeleton. 28–30 total vertebrae (excluding urostyle element), with 14–15 abdominal and 13–16 caudal vertebrae. Pterygiophore supporting last dorsal-fin spine inserted between neural spines of 14th and 15th, 15th and 16th or 17th and 18th vertebra (counted from anterior to posterior). Pterygiophore supporting last anal-fin spine is inserted between rips of 14th (or 15th) and haemal spine of 15th (or 16th) vertebra or between haemal spine of 15th and 16th vertebra. Single predorsal bone (=supraneural bone) present. Hypurals 1 and 2 as well as hypurals 3 and 4 clearly separated (most common state) or fused while any other combination is possible (e.g. hypurals 1 and 2 fused and hypurals 3 and 4 separated or vice versa).

Colouration in life (based on field photographs of adult specimens). Body ground colouration pale brown to beige; dorsum, flank and caudal peduncle light brown; belly whitish; chest whitish to yellow. Dark grey to blackish, interrupted midlateral band from operculum to just behind caudal fin base, ending in dark blotch; midlateral band crossed by 7–9 light grey vertical bars (sometimes hardly visible) extending mainly dorsally; at level of upper lateral line most bars fuse forming dorso-lateral band which extends to posterior origin dorsal fin.

Scales on flank and dorsum with orange blotch on anterior surface and greenish metallic highlights, especially scales on or row above or below lower lateral line. Dorsal head surface brownish; anterior snout brownish, preorbital area and cheek yellowish to brownish; mental area and ventral parts of preoperculum and cheek light bluish. Operculum yellowish with brownish sprinkles; black opercular spot present. Greyish vertical preopercular stripe of variable intensity is always present, at least in the form of a faint blackish blotch at mid orbit level. Dark grey to brownish lachrymal stripe between orbit and posterior end upper lip. Greyish to brownish nostril stripe (less intense than lachrymal stripe) fused posteriorly with lachrymal stripe. Faint greyish interorbital stripe. Upper lip brownish to olive, beige to light bluish posteriorly and lower lip beige to light bluish. Dorsal fin membrane greyish with orange margins; soft rayed part of dorsal fin with orange maculae arranged in 2–3 rows. Anal-fin membrane greyish, margin of spinous part dark grey; 2–3 orange maculae on soft rayed part anal fin. First macula situated just posterior last anal-fin spine at outer margin of anal fin. Second macula almost in centre of rayed part anal fin. When present, third macula less prominent (smaller and less colourful). Maculae resembling eggspots but without white concentric ring. Caudal fin yellowish with grey margin and four columns of small orange maculae. Pectoral fin yellowish. Pelvic fin yellowish; skin around pelvic fin spine and adjacent membrane of first two rays blackish.

Juvenile colouration in live. No information about juvenile colouration available.

Colouration in alcohol. Colouration and melanin patterns similar to live specimens, but due the preservation procedure of specimens, i.e., first formalin fixation, transfer to 75 % EtOH etc., specimens tend to lose original colouration (especially melanin patterns more intense than in live specimens). Overall body ground colouration brownish; dorsum and flank brownish. Orange blotches on flank scales no longer visible. Chest and belly beige to light brown. Branchiostegal membrane greyish brown. Dorsal head surface brownish, ethmoidal region greyish brown. Upper lip greyish; lower lip greyish anteriorly becoming beige. Cheek light brown to brownish. Preoperculum greyish. Operculum dark brown to greyish with opercular spot as described above. Head mask dark brownish to grey. Midlateral band, vertical bars and dorso-lateral band brownish. Dorsal fin greyish, lappets with very fine black seam; maculae on soft-rayed part beige. Anal fin greyish; margin dark grey to black, eggspot-like maculae whitish. Caudal fin greyish with dark greyish margin; maculae dark grey. Pectoral fin light grey. Pelvic fin light grey, skin around pelvic fin spine and adjacent membrane of first two rays dark grey.

Distribution and biology. *Orthochromis kimpala* is known from the Kalule Nord River (Fig. 1), a right tributary of the Lualaba River in the Democratic Republic of the Congo. At the type locality the Kalule Nord River has a rocky bottom with some patches of sand and gravel, and is about 5–8 meters wide and on average about 50 cm deep (Fig. 8). Water temperature varied between 21.1 and 26.8 °C (measured over several years in August and September), pH between 7.95–8.71, electrical conductivity 333.5–359 µS. The species appears to be benthic-rheophilic.

Etymology. The species name *kimpala* refers to the local name for this species: "Kimpala" in the Sanga language. A noun in apposition.

Orthochromis gecki sp. nov.

Orthochromis sp. "Lubudi"

Holotype. MRAC 2012-031-P-2097 (73.8 mm SL), Democratic Republic of Congo, Lubudi River downstream of Kendo Rapids, near Tshifuntshi Village (-10.5635/24.6354).

Paratype. MRAC 2012-031-P-2098-2116 (19, 52.1–77.7 mm SL), collected with holotype.—ZSM 46851 (5, ex MRAC uncat., 46.3–62.9 mm SL), Democratic Republic of Congo, Lubudi River at Kendo Rapids, near Tshifuntshi Village (-10.5668/24.6373).—MRAC 2012-031-P-2117-2126 (10, 45.9–69.8 mm SL), Democratic Republic of Congo, Lubudi River at Kendo Rapids, near Tshifuntshi Village (-10.5670/24.6374). – ZSM 46852 (1, ex MRAC uncat., 67.1 mm SL), collected with holotype.

Differential diagnosis. *Orthochromis gecki* can be readily distinguished from all all species currently placed in *Orthochromis* (sensu de Vos & Seegers 1998) except *O. torrenticola* (which has eggspot-like maculae) by presence of eggspots on anal fin. It is further distinguished from *O. kasuluensis* by having fewer anal-fin rays (8–9 vs. 10); from *O. malagaraziensis* by having more scales between upper lateral line and dorsal-fin origin (5–8 vs. 3–4); from *O. mazimeroensis* by having more horizontal line scales (29–31 vs. 26–28); from *O. rubrolabialis*, *O.*

rugufuensis and *O. uvinzae* by having fewer anal-fin spines (16–17 vs. 18–20) and in position of pterygiophore supporting last dorsal-fin spine (vertebral count: 15–16 vs. 17–19). It is furthermore distinguished from *O. uvinzae* by having fewer abdominal vertebrae (13–14 vs. 15–16) and by position of pterygiophore supporting last anal-fin spine (vertebral count: 14–15 vs. 16–17). *O. gecki* is distinguished from *O. stormsi* by having more horizontal line scales (29–31 vs. 26–28) and fewer total gill rakers (9–12 vs. 13–15); from *O. polyacanthus* by having fewer dorsal-fin spines (16–17 vs. 18–20), more dorsal-fin rays (10–12 vs. 8–9) and it is distinguished by position of pterygiophore supporting last dorsal-fin spine (vertebral count: 15–16 vs. 17–18); from *O. torrenticola* by having fewer anal-fin spines (3 vs. 4). Meristic values of *O. gecki* overlap with those of *O. luongoensis*, *O. kalungwishiensis,* and *O. machadoi* but is distinguished by narrower interorbital width (9.62–12.86 vs. 13.18-21.27 % HL). It is distinguished from *S. neodon* by having more circumpeduncular scales (16 vs. 12); from *H. snoeksi* by having more anal-fin rays (8–9 vs. 5–6); from *H. bakongo* by more horizontal line scales (29–31 vs. 26–28), more dorsal-fin spines (16–17 vs. 15–15) and by position of pterygiophore supporting last dorsal-fin spine (vertebral count: 15–16 vs. 13–14); from *H. moeruensis* by having more horizontal line scales (29–31 vs. 27–28) and more scales in upper lateral line (21–25 vs. 19–20). Meristic values of *O. gecki* overlap with those of *H. vanheusdeni* but is distinguished by having a smaller interorbital width (9.62–12.86 vs. 14.20–20.30 % HL). It is distinguished from herein newly described species *O. kimpala* by having fewer series of scales on cheek (0–2 vs. 3–4). Meristic values of *O. gecki* overlap with those of *O. mporokoso*, *O. katumbii*, and *O. indermauri* but is distinguished by having smaller interorbital width (9.6–12.9 vs. 13.0–21.7 % HL).

Description. Morphometric measurements and meristic characters are based on 36 type specimens. Values and their ranges are presented in Table 5. For general appearance see figure 6. Maximum length of wild caught specimens 77.7 mm SL. Rather slender and elongated species with maximum body depth (20.2–27.4 % SL) slightly before or at level of first dorsal-fin spine, decreasing rather gradually towards caudal peduncle. Caudal peduncle moderately elongated and deep (ratio of caudal peduncle length to depth: 1.5–2.0). Head length about one third of standard length. Dorsal-head profile moderately curved, from anterior eye region to dorsal-fin origin only slightly curved. No prominent nuchal gibbosity present. Eye diameter larger than interorbital width. Jaws isognathous. Posterior tip of maxilla almost reaching to slightly beyond anterior orbit margin. Lips well developed. Two separate lateral lines.

Squamation. Flank above and below lateral lines covered with comparatively large ctenoid scales. Anterior dorsal and ventral flank covered by cycloid scales. Margin of belly with deeply embedded minute to small sized scales; central belly region scaleless. Chest completely scaleless, except for deeply embedded cycloid scales ventro-anteriorly of pectoral fin. Chest to flank transition relatively abrupt with small, embedded cycloid scales. Snout scaleless. Interorbital region scaleless or with minute, deeply embedded cycloid scales. Nape region covered with minute to small, embedded cycloid scales becoming slightly larger towards occipital region. Occipital region with small to medium sized cycloid scales. Cheek covered with small, partly deeply embedded cycloid scales sometimes almost appearing scaleless; 0-2 scale rows on cheek. Cycloid scales on operculum of variable size (small to medium) and variable shape (ovoid to circular); opercular blotch only on anterior margin covered with medium sized scales, main area of opercular blotch scaleless. 1–3 scales in column from edge of postero-dorsal angle of operculum to anterior edge of operculum.

Upper lateral line scales 21–25 and lower lateral line 8–12. Horizontal line scales 29–31. Caudal fin with 0–1 pored scale. Upper and lower lateral lines separated by two scales. 5–8 scales between upper lateral line and dorsal-fin origin. Anterior part of caudal fin covered with 2–3 columns of small cycloid scales; with median scales being slightly larger; scaled area of caudal fin extended posteriorly, especially at upper and lower end, with minute, interradial scales (approximately up to one half of caudal fin). Sixteen scales around caudal peduncle.

Jaws and dentition. Anterior teeth of outer row of upper and lower jaw bicuspid to subequally bicuspid, large and closely set; towards corner of mouth, teeth smaller and more widely set and becoming unicuspid (rarely tricuspid or subequally bicuspid teeth present in posterior upper jaw). Individual bicuspid teeth without or minimally expanded brownish crown, cusps (tips roundish) uncompressed and moderately narrowly set, neck moderately stout. Outer row of upper jaw with 33–49 teeth and outer row of lower jaw with 26–42 teeth (specimens: 46.3–77.7 mm SL); larger specimens generally with more teeth. Upper and lower jaw with 2–4 inner tooth rows with small tricuspid teeth (rarely 5 rows in upper jaw and 1 or 5 in lower jaw); larger specimens generally with more inner tooth rows. Lower pharyngeal bone (Fig. 6) of single dissected paratype (MRAC 2012-031-P-2098-2116, 69.1 mm SL) about 1.1 times wider than long with anterior keel about 0.6 times length of dentigerous area. Dentigerous area of lower pharyngeal bone about 1.4 times wider than long, with 10+9 teeth along posterior margin and 6 teeth along midline. Anterior pharyngeal teeth (towards keel) bevelled to pronounced and slender; those of posterior row larger than anterior ones, bevelled (minor cusp not well developed). Largest teeth medially in posterior tooth row. Teeth along midline slightly larger than more lateral ones.

Gill rakers. Total gill raker count 9–12, with 1–2 epibranchial, one angle, and 7–9 ceratobranchial gill rakers. Anteriormost ceratobranchial gill rakers smallest, increasing in size towards cartilaginous plug (angle). Anterior gill rakers on ceratobranchial unifid, towards cartilaginous plug sometimes bifid or trifid. Raker on cartilaginous plug largest in size and in most cases trifid, sometimes bifid. Epibranchial gill rakers then decreasing in size.

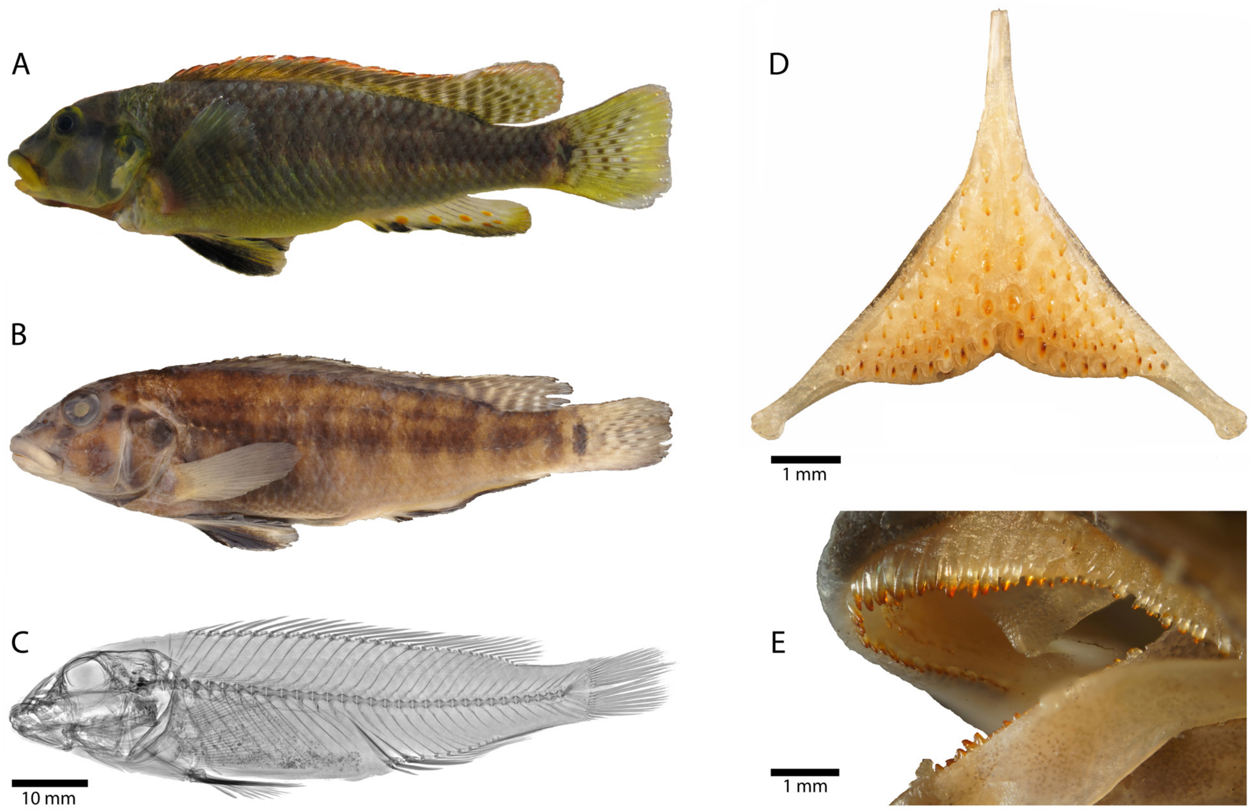

FIGURE 6. *Orthochromis gecki* **sp. nov. A.** probably the holotype, alive **B.** Holotype (MRAC 2012-031-P-2097), 73.8 mm SL; Democratic Republic of the Congo, Lubudi River **C.** radiograph of holotype **D.** lower pharyngeal bone (specimen with 69.1 mm SL; MRAC 2012-031-P-2098-2116) **E.** Overview of arrangement and morphology of oral jaw teeth (specimen with 75.0 mm SL; MRAC 2012-031-P-2098-2116).

Fins. Dorsal fin with 16–17 spines and with 10–12 rays. First dorsal-fin spine always shortest. Dorsal-fin base length between 52.1–61.0 % SL. Posterior tip of dorsal-fin rays reaching slightly beyond caudal fin base; posterior tip of anal fin reaching slightly before or at caudal-fin base. Caudal fin outline subtruncate and composed of 27–29 rays (16 principal caudal-fin rays and 11–13 procurrent caudal-fin rays). Anal fin with 3 spines (3rd spine longest) and 8–9 rays. Anal-fin base length between 15.6–20.7 % SL. Pectoral fin with 15–16 rays. Pectoral-fin length between 19.6–25.0 % SL; longest pectoral ray not reaching level of anus; first upper and lower pectoral-fin rays very short to short. Pelvic fin with 1st spine thickly covered with skin and 5 rays. Pelvic-fin base at level or slightly anterior of pectoral-fin base. Pelvic fin ending at same level as pectoral fin; longest pelvic-fin ray not reaching anus (ending approximately 2-3 flank scale widths before).

Vertebrae and caudal fin skeleton. 29–31 total vertebrae (excluding urostyle element), with 13–14 abdominal and 16–18 caudal vertebrae. Pterygiophore supporting last dorsal-fin spine inserted between neural spines of 15th and 16th or 16th and 17th vertebra (counted from anterior to posterior). Pterygiophore supporting last anal-fin spine is inserted between haemal spines of 15th and 16th vertebra or between rips of 14th and haemal spine of

15th vertebra. Single predorsal bone (=supraneural) present. Hypurals 1 and 2 in most types fused into either single, seamless unit or separated by clearly distinct seam. Hypurals 3 and 4 always fused into single seamless unit, except for one paratype which has clearly separated hypurals.

TABLE 5. Measurements and counts of holotype and paratypes of *Orthochromis gecki* **sp. nov.**

Measurements	holotype	holotype + paratypes			
		min	Max	SD	n
Total length (mm)	89.1	55.4	94.4		36
Standard length SL (mm)	73.8	46.3	77.7		36
Head length HL (mm)	22.5	14.1	25.2		36
% HL					
Interorbital width	12.9	9.6	12.9	0.7	36
Preorbital width	29.1	25.2	34.3	1.6	36
Horizontal eye length	21.2	18.1	26.8	3.0	36
Snout length	36.0	30.3	44.4	3.3	36
Internostril distance	17.9	12.7	20.2	1.6	36
Cheek depth	27.6	22.2	30.9	2.1	36
Upper lip length	34.3	27.9	36.9	2.7	36
Lower lip length	31.8	20.1	35.1	3.7	36
Lower lip width	32.6	25.0	37.0	3.4	36
Lower jaw length	32.0	28.6	38.4	2.5	36
Lower pharyngeal jaw length	-	28.1		-	1
Lower pharyngeal jaw width	-	32.3		-	1
Width of dentigerous area of lower pharyngeal jaw	-	21.8		-	1
% SL					
Predorsal distance	32.2	30.1	36.0	1.5	36
Dorsal-fin base length	57.1	52.1	61.0	2.2	36
Last dorsal-fin spine length	12.5	8.9	19.2	1.9	36
Anal-fin base length	19.2	15.6	21.7	1.4	36
Third anal-fin spine length	13.2	10.1	14.6	1.1	36
Pelvic fin length	21.4	20.4	24.7	1.1	36
Pectoral fin length	22.8	19.5	24.9	1.4	36
Caudal peduncle depth	10.3	9.3	11.5	0.6	36
Caudal peduncle length	17.4	15.9	19.8	0.9	36
Body depth (pelvic fin base)	25.3	20.2	27.4	1.6	36
Preanal length	60.3	56.8	63.8	1.5	36
Anus-anal fin base distance	3.2	2.2	5.4	0.7	36
Interpectoral width	13.6	9.0	16.0	1.4	36
Counts					
Dorsal-fin spines	16	16 (16); 17 (20)			36
Dorsal-fin rays	11	10 (17); 11 (18); 12 (1)			36
Anal-fin spines	3	3 (36)			36
Anal-fin rays	8	8 (11); 9 (25)			36
Pelvic-fin spines	1	1 (36)			36

......*continued on the next page*

TABLE 5. (Continued)

Measurements	holotype	holotype + paratypes			
		min	Max	SD	n
Pelvic-fin rays	5	5 (36)			36
Pectoral-fin rays	16	15 (8); 16 (28)			36
Lower procurrent caudal-fin rays	7	6 (6); 7(24)			36
Lpper procurrent caudal-fin rays	6	5 (7); 6 (29)			36
Caudal-fin rays	29	27 (2); 28 (15); 29 (19)			36
Scales (horizontal line)	30	29 (9); 30 (26); 31 (1)			36
Upper lateral line	22	21 (3); 22 (13); 23 (15); 24 (4); 25 (1)			36
Lower lateral line	12	8 (2); 9 (13); 10 (15); 11 (5); 12 (1)			36
Circumpeducular	16	16 (36)			36
Series of scales on cheek	1	0 (10); 1 (15); 2 (11)			36
Scales (horizontal line) on operculum	2	1 (3); 2 (16); 3 (17)			36
Scales between lateral line and dorsal fin origin	6	5 (9); 6 (15); 7 (6); 8 (2)			32
Scales between upper lateral line and last dorsal fin spine	2	2 (36)			36
Abdominal vertebrae	14	13 (8); 14 (28)			36
Caudal vertebrae	16	15 (1); 16 (13); 17 (19); 18 (3)			36
Total number of vertebrae	30	29 (2); 30 (16); 31 (18)			36
Teeth in upper outer row	44	33 (1); 34 (2); 36 (2); 37 (4); 38 (1); 39 (6); 40 (1); 41 (2); 42 (3); 44 (2); 45 (3); 46 (1); 47 (1); 48 (2); 49 (1)			36
Teeth in lower outer row	42	25 (1); 26 (1); 27 (3); 28 (5); 29 (1); 30 (2); 31 (6); 32 (1); 33 (2); 34 (3); 35 (1); 36 (2); 37 (1); 38 (3); 39 (2); 40 (1); 42 (1)			36
Gill rakers (ceratobranchial)	7	7 (17); 8 (16); 9 (3)			36
Gill rakers (angle + epibranchial)	2	2 (7); 3 (29)			36

Colouration in life (based on field photographs of adult specimens). Body ground colouration brownish to greyish; dorsum, flanks and caudal peduncle greyish, beneath lower lateral line becoming yellowish; belly yellow; chest anteriorly whitish and remaining area yellow. Dark grey interrupted midlateral band from eye (anteriorly extended midlateral band) to just behind caudal-fin base ending in well pigmented vertically elongated blotch. Midlateral band crossed by 7–9 greyish vertical bars; at level of upper lateral line they sometimes fuse with each other forming dorso-lateral band sometimes interrupted and ending at posterior end of dorsal fin. On ventral flank at level of pectoral fin vertical bars sometimes fuse to ventro-lateral band (less intensive then previous mentioned ones) that ends well before level of anus. Iris dorsally yellow remaining greyish. Dorsal head surface, ethmoidal area, preorbital area greyish; cheek greyish near eyes, yellowish below and with vertical stripe-like pattern centrally (less distinct than other stripes of face mask). Preoperculum light greyish-yellow; operculum greyish, black opercular spot outlined with yellow. Branchiostegal membrane brownish to orange. Dark grey lachrymal stripe ending slightly anterior of caudal end upper lip. Greyish nostril stripe caudally fused with lachrymal stripe (beneath eye); interorbital stripe greyish. No clearly defined supraorbital stripe or nape band but recognizable to some extent by darker (grey) colouration than remaining dorsal head surface. Upper lip and lower lip yellow-orange; upper and lower margin of upper lip greyish. Dorsal-fin membrane brownish (especially spinous part) to yellowish (soft rayed part); margin orange; brownish to dark greyish maculae from about posterior half of spiny part to end soft-rayed part arranged in several almost vertical columns. Anal-fin membrane transparent proximally becoming yellowish distally (soft rayed part), margin of spiny and soft-rayed part black becoming yellow to brownish towards posterior tip; 3–6 orange eggspots (large orange centre surrounded by yellow concentring ring and outlined by more or less ill-defined transparent margin) on anal fin in both sexes. Eggspots arranged into 1–2 rows, first eggspot located centrally on fin just behind last anal spine. Caudal fin yellowish, orangey distally, margin outlined in grey-black; caudal with brownish maculae arranged into 3–4 vertical columns. Pectoral fin transparent, rays greyish. Pelvic fin deep black (especially skin around spine) except for small yellow central portion of rayed area.

Juvenile colouration in live. (based on wild caught juveniles of approximately 25 mm SL; Fig. 9)**.** Ground colouration beige, belly whitish. Patterns and head mask as described for adults but less prominent. Brown to greyish vertical bars on flank appear wider than in adults, dorso-lateral band and ventro-lateral band not visible. Last vertical bar on caudal fin base roundish blotch extending onto caudal fin (not a vertical bar as in adults). Dorsal fin brownish with several hyaline patches, margin not orange. Anal fin light brownish-orange; no eggspots on anal fin present. Caudal fin brownish-orange, no maculae present. Pectoral fin hyaline. Pelvic fin white to yellowish.

Colouration in alcohol. Colouration and melanin patterns similar to live specimens, due the preservation procedure of specimens, i.e., first formalin fixation, transfer to 75 % EtOH etc., specimens tend to lose original colouration (especially melanin patterns more intense than in live specimens). Overall body ground colouration brownish; dorsum and flank brownish becoming brighter ventrally. Chest and belly light brown to beige. Branchiostegal membrane dark greyish. Dorsal head surface brownish; ethmoidal area greyish brown. Upper and lower lip beige; upper and lower margin of upper lip greyish brown. Cheek light brown to brownish; cheek stripe dark brown. Operculum dark brown becoming somewhat darker ventrally; with opercular spot as described above. Head mask dark grey. Midlateral band, vertical bars, dorso-lateral band and ventro-lateral band dark brown. Dorsal fin greyish brown becoming greyish beige caudally, margin blackish with very fine black seam; maculae on spiny and soft-rayed part dark grey. Anal fin beige with blackish distal margin and dark grey at posterior margin; eggspots on anal fin faded and not visible in preserved specimens. Caudal fin beige to light greyish with dark greyish margin; maculae dark grey. Pectoral fin beige to light grey. Pelvic fin deep black except small central portion of rayed part greyish.

Distribution and biology. *Orthochromis gecki* is known from the Lubudi River a left-hand tributary of the Lualaba River in the Katanga region, Democratic Republic of the Congo (Fig. 1). It was also found to be present in the Mukuleshi River. At the type locality the Lubudi River has a rocky bottom with patches of gravel and sand, and is about 15 meters wide and about 50 cm deep; upstream the river is much deeper with 3 meters or more (Fig. 9). *O. gecki* seems to be a maternal mouthbrooder. One of the female paratypes (MRAC 2012-031-P-2117-2126; 57.0 mm SL), was found mouthbrooding when preserved and carried around 12 comparatively large eggs. Fixed eggs are brownish and oval and ca. 3.8 mm long and 2.5 mm wide.

Etymology. The species is named in honour of Mr. Jakob Geck who is a passionate, German fish naturalist, thanking him for his dedicated volunteer work and untiring support for the ichthyology section of the ZSM. His great experience in keeping rheophilic cichlids contributed to the knowledge of behaviour and ecology of many cichlid taxa, including *O. katumbii* and *O. indermauri*.

Orthochromis indermauri sp. nov.

Orthochromis sp. "Chomba" Indermaur 2014

Holotype. ZSM 46853 (1, ex ZSM 43080, 54.0 mm SL), Zambia, Lufubu River, below last series of rapids near Chomba village, ~ 25.5 km (air distance) from confluence with Lake Tanganyika and 20 km (air distance) south of Sumbu (-8.687010/30.556273)

Paratypes. ZSM 46855 (13, 35.8–68.9 mm SL), Zambia, Lufubu River, Lower Lufubu at Chomba Village, ~30 km from confluence with Lake Tanganyika, Northern Province (-8.686376/30.563983).—ZSM 46854 (1, 61.2 mm SL), Zambia, Lufubu River, Lower Lufubu at Chomba Village, ~30 km from confluence with Lake Tanganyika, Northern Province (-8.686376/30.563983).—ZSM 43083 (4, 45.6–59.4 mm SL), collected with holotype.—ZSM 43080 (2, 42.0–43.1 mm SL), collected with holotype.—ZSM 44283 (3, 50.8-63.5 mm SL), Zambia, Lufubu River, Lower Lufubu at Chomba Village, ~30 km from confluence with Lake Tanganyika, Northern Province (-8.686376/30.563983).—MRAC 2018-006-P-0001-0002 (2, ex ZSM 44283, 56.8–51.9 mm SL) Zambia, Lufubu River, Lower Lufubu at Chomba village, ~30 km from confluence with Lake Tanganyika, Northern Province (-8.686376/30.563983).—MRAC 2018-006-P-0003-0008 (6, 43.3–64.1 mm SL), Zambia, Lufubu River, Lower Lufubu at Chomba village, ~30 km from confluence with Lake Tanganyika, Northern Province (-8.686376/30.563983).

Diagnosis. *Orthochromis indermauri* is distinguished from all all species currently placed in *Orthochromis* (sensu de Vos & Seegers, 1998) except O. *torrenticola,* by having hypurals 1 and 2 clearly separated or separated by distinct seam (vs. always fused). It is further distinguished from Malagarasi-*Orthochromis* species, except *O. mazimeroensis, O. malagaraziensis,* and *O. rubrolabialis,* by having fewer caudal vertebrae (14–15 vs. 16–18) and total vertebrae (28–29 vs. 30–32). It is also distinguished from *O. luichensis, O. malagaraziensis*, *O. mazimeroensis*, *O. mosoensis* by having more inner series of teeth in upper jaw (3–5 vs. 1–2). Moreover, it differs from *O. kasuluensis* by having fewer anal-fin rays (7–9 vs. 10); from *O. malagarazienisis* by having more scales between upper lateral line and dorsal-fin origin (5–7 vs. 3–4) and by having more ceratobranchial gill rakers (8–11 vs. 6–7); from *O. mazimeroensis* by having more abdominal vertebrae (14–15 vs. 12–13); from *O. mosoensis* and *O. rubrolabialis* by having more ceratobranchial gill rakers (8–11 vs. 5–7) and total gill rakers (11–15 vs. 8–10); from *O. uvinzae* by having fewer horizontal line scales (25–29 vs. 30–32), fewer dorsal-fin spines (17–18 vs. 19–20) and by position of pterygiophore supporting last dorsal-fin spine (vertebral count: 16–17 vs. 18–19). It is distinguished from *O. kalungwishiensis*, *O. luongoensis*, and *O. torrenticola* by having fewer horizontal line scales (28–29 vs. 30–32) and by having fewer caudal vertebrae (14–15 vs. 17–18). Further, it differs from *O. luongoensis* and *O. machadoi* by having fewer series of scales on cheek (0–1 vs. 2–5); from *O. kalungwishiensis* by having fewer total vertebrae (28–29 vs. 31–33). It is distinguished from *S. neodon* by having fewer horizontal line scales (28–29 vs. 30–31), more circumpeduncular scales (16 vs. 12), fewer caudal vertebrae (14–15 vs. 16–17), fewer total vertebrae (28–29 vs. 30–32), fewer dorsal-fin rays (8–10 vs. 11–12) and by having hypurals 1 and 2 clearly separated or separated by distinct seam (vs. fused). It differs from *H. snoeksi* by having fewer scales on cheek (0–1 vs. 2–3), fewer horizontal line scales (25–29 vs. 30–31), more abdominal vertebrae (14–15 vs. 13), fewer caudal vertebrae (14–15 vs. 17), fewer total vertebrae (28–29 vs. 30), more anal-fin rays (7–9 vs. 5–6), more dorsal-fin spines (17–18 vs. 16), more ceratobranchial gill rakers (8–11 vs. 6) and total gill rakers (11–15 vs. 9); from *H. bakongo* by having more inner series of teeth (3–5 vs. 1–2), more dorsal-fin spines (17–18 vs. 14–15) and in position of pterygiophore supporting last dorsal-fin spine (vertebral count: 16–18 vs. 13–14); from *H. moeruensis* by having hypurals 1 and 2 clearly separated or separated by distinct seam (vs. always fused). Meristic values of *O. indermauri* overlap with those of *H. vanheusdeni* but is distinguished by differences in head mask (e.g. nostril stripe present vs. absent; caudal corner of cheek with blackish element vs. no such element present) and by size and colouration of eggspot-like maculae on anal fin (e.g. deep red centre vs. orange centre in *H. vanheusdeni*). It is distinguished from *O. mporokoso* and *O. katumbii* by having fewer caudal vertebrae (14–15 vs. 16–17), fewer total vertebrae (28–29 vs. 30–31) and by having hypurals 1 and 2 and hypurals 3 and 4 clearly separated or separated by distinct seam (vs. always fused). Further from *O. mporokoso* by having fewer series of scales on cheek (0–1 vs. 2–4); from *O. katumbii* by having fewer horizontal line scales (25–29 vs. 30–31). It is distinguished from *O. kimpala* by having fewer series of scales on cheek (0–1 vs. 3–4) and by having more dorsal-fin spines (17–18 vs. 15–16). Meristic values of *O. indermauri* overlap with those of *O. gecki* but is distinguished by having a wider interorbital width (13.5–18.2 vs. 9.6–12.9 %HL).

Description. Morphometric measurements and meristic characters are based on 21 out 32 type specimens. Values and their ranges are presented in Table 6. For general appearance see figure 7. Maximum length of wild caught specimens 68.9 mm SL. Moderately slender species with maximum body depth (24.5–29.9 % SL) slightly posterior or at level of first dorsal-fin spine, decreasing rather gradually towards caudal peduncle (but decreasing relatively quick just before caudal peduncle). Caudal peduncle rather short and deep (ratio of caudal peduncle length to depth: 1.2–1.4). Head length almost one third of standard length. Dorsal-head profile moderately curved without prominent nuchal gibbosity. Eye diameter always larger than interorbital width. Jaws slightly retrognathouswith lower jaw shorter than upper jaw. Posterior tip of maxilla not reaching anterior margin of orbit but slightly before. Lips not noticeably enlarged or thickened. Two separate lateral lines.

Squamation. Flank above and below lateral lines covered with cycloid scales, even in smaller specimens. Belly and chest covered by deeply embedded minute scales giving appearance of being scaleless. Ventro-anterior area of pectoral fin with small, deeply embedded cycloid scales. Chest to flank transition with small, embedded cycloid scales.

Snout scaleless. Interorbital region with minute, deeply embedded cycloid scales. Nape and occipital region covered with minute to small, embedded cycloid scales becoming slightly larger towards occipital region. Cheek appears scaleless, but rarely small deeply embedded cycloid scales present just below eye; 0–1 scale rows on cheek. Cycloid scales on operculum of variable size (small to medium) and mainly of circular shape; opercular blotch only on anterior margin covered by medium sized scales, main area of opercular blotch scaleless. 5–7 scales on horizontal line from edge of postero-dorsal angle of operculum to anterior edge of operculum.

Upper lateral line scales 20–23 and lower lateral line 7–11. Horizontal line scales 27–29. Caudal fin with 0–2 pored scales. Upper and lower lateral lines separated by two scales. 3–5 scales between upper lateral line and dorsal-fin origin. Anterior part of caudal fin covered with 2–3 vertical rows of small cycloid scales with median scales being slightly larger; scaled area of caudal fin extended posteriorly with interradial scales (approximately up to two thirds of caudal fin). Sixteen scales around caudal peduncle.

Jaws and dentition. Anterior teeth of outer row of upper and lower jaw bicuspid to subequally bicuspid, large and very densely set; teeth smaller towards corner of mouth, more widely set and becoming unicuspid (rarely tricuspid or subequally bicuspid teeth present on upper jaw near corner mouth). Individual bicuspid teeth with not expanded brownish crown, cusps (tips pointed) slightly compressed and narrowly set, and neck slender. Outer row of upper jaw with 42–59 teeth and outer row of lower jaw with 26–45 teeth (specimens: 35.8–68.9 mm SL); larger specimens generally with more teeth. Inner upper jaw with 3–5 tooth rows and 3–4 rows (rarely 2) in lower jaw, all with small tricuspid teeth.

Lower pharyngeal bone (Fig. 7) of single dissected paratype (ZSM 46854, 61.2 mm SL) about as wide as long with anterior keel about 0.6 times length of dentigerous area. Dentigerous area of lower pharyngeal bone about 1.5 times wider than long, with 11+11 teeth (empty tooth-sockets included) along posterior margin and eight teeth along midline. Anterior pharyngeal teeth (towards keel) bevelled and slender; teeth posterior row larger than anterior ones, bevelled (bicuspid; well-developed major and minor cusp). Largest teeth medially in posterior row. Teeth along midline slightly larger than more lateral ones.

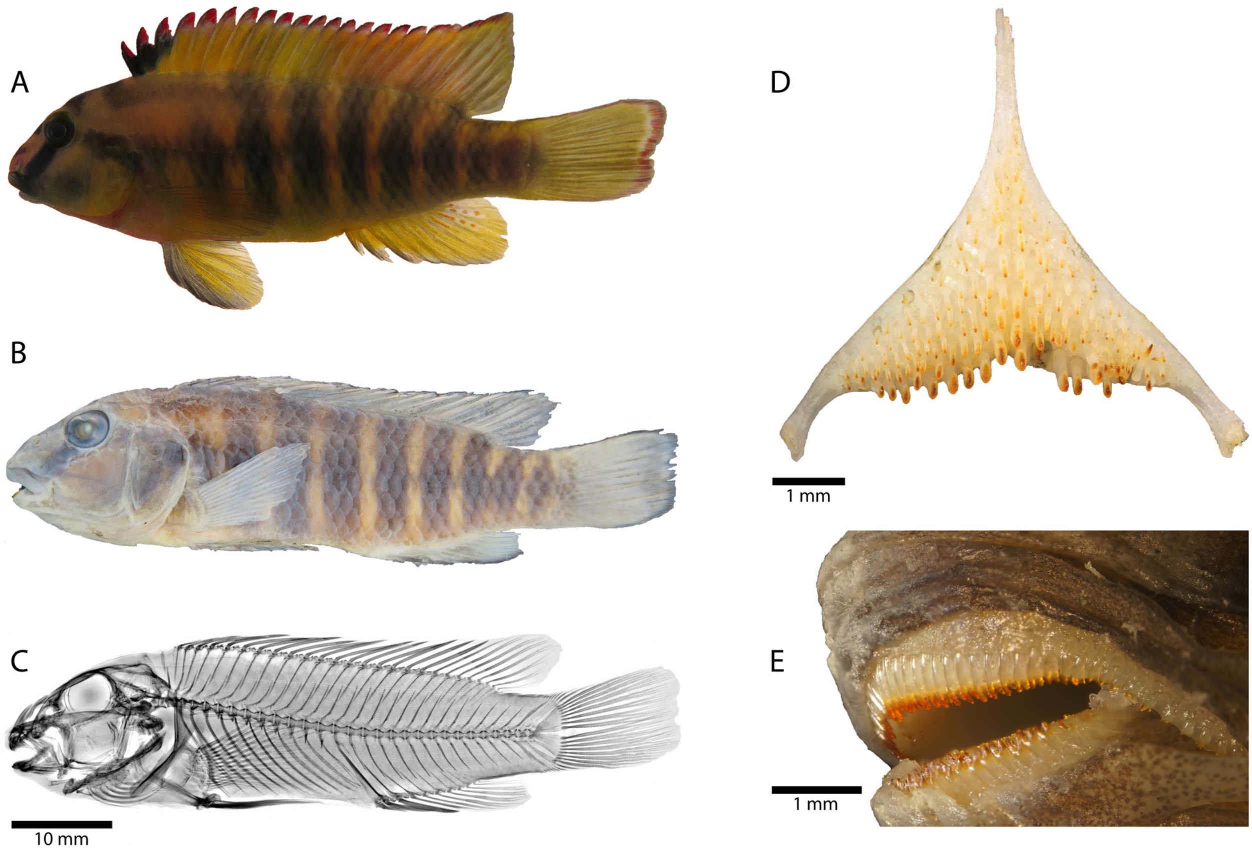

FIGURE 7. *Orthochromis indermauri* **sp. nov. A.** paratype (ZSM 44283), 63.5 mm SL, alive **B.** Holotype (ZSM 46853, 54.0 mm SL), 54.0 mm SL; Zambia, Lufubu River **C.** radiograph of holotype **D.** lower pharyngeal bone (ZSM 46854, 61.2 mm SL) **E.** Overview of arrangement and morphology of oral jaw teeth (specimen: ZSM 43083, 59.4 mm SL).

TABLE 6. Measurements and counts of holotype and paratypes of *Orthochromis indermauri* **sp. nov.**

Measurements	holotype	holotype + paratypes			
		min	Max	SD	n
Total length (mm)	66.2	44.6	86.0		32
Standard length SL (mm)	54.0	35.8	68.9		32
Head length HL (mm)	18.0	11.7	21.4		32
% HL					
Interorbital width	15.1	13.5	18.2	1.4	21
Preorbital width	32.8	30.2	39.7	2.3	21
Horizontal eye length	21.4	20.1	25.0	1.4	21
Snout length	37.9	36.3	43.3	2.1	21
Internostril distance	17.5	15.7	32.8	3.6	21
Cheek depth	28.9	24.2	34.1	2.7	21
Upper lip length	30.4	23.8	32.5	2.5	21
Lower lip length	26.2	20.0	29.2	2.5	21
Lower lip width	35.0	26.2	43.3	3.7	21
Lower jaw length	23.4	23.4	37.5	3.6	21
Lower pharyngeal jaw length	-	31.9		-	1
Lower pharyngeal jaw width	-	33.2		-	1
Width of dentigerous area of lower pharyngeal jaw	-	24.5		-	1
% SL					
Predorsal distance	31.9	31.4	35.9	1.0	21
Dorsal-fin base length	60.3	56.9	65.4	2.6	21
Last dorsal-fin spine length	13.5	12.5	16.0	0.9	21
Anal-fin base length	17.4	16.7	21.9	1.3	21
Third anal-fin spine length	13.3	11.0	15.5	1.1	21
Pelvic fin length	22.1	20.5	26.04	1.5	21
Pectoral fin length	22.7	19.7	25.6	1.3	21
Caudal peduncle depth	12.9	11.8	14.22	0.6	21
Caudal peduncle length	17.5	14.7	18.5	1.0	21
Body depth (pelvic fin base)	28.1	24.45	30.54	1.7	21
Preanal length	61.4	54.9	63.6	2.3	21
Anus-anal fin base distance	2.2	2.1	4.9	0.8	21
Interpectoral width	14.9	12.2	16.9	1.1	21
Counts					
Dorsal-fin spines	18	17 (7); 18 (14)			21
Dorsal-fin rays	9	8 (3); 9 (15); 10 (3)			21
Anal-fin spines	3	3 (21)			21
Anal-fin rays	8	7 (1); 8 (18); 9 (2)			21
Pelvic-fin spines	1	1 (21)			21
Pelvic-fin rays	5	5 (21)			21
Pectoral-fin rays	15	14 (5); 15 (16)			21
Upper procurrent caudal-fin rays	7	6 (5); 7 (16)			21
Lower procurrent caudal-fin rays	6	5 (1); 6 (20)			21

......continued on the next page

TABLE 6. (Continued)

Measurements	holotype	holotype + paratypes			
		min	Max	SD	n
Caudal-fin rays	29	27 (1); 28 (4); 29 (16)			21
Scales (horizontal line)	28	27 (6); 28 (14); 29 (1)			21
Upper lateral line	21	20 (2); 21 (8); 22 (10); 23 (1)			21
Lower lateral line	10	7 (2); 8(3); 9 (10); 10 (5); 11 (1)			21
Circumpeducular	16	16 (21)			21
Series of scales on cheek	0	0 (16); 1 (5)			21
Scales (horizontal line) on operculum	2	2 (10); 3 (11)			21
Scales between lateral line and dorsal fin origin	6	5 (2); 6 (9); 7 (10)			21
Scales between upper lateral line and last dorsal fin spine	1	1 (12); 2 (9)			21
Abdominal vertebrae	14	14 (19); 15 (2)			21
Caudal vertebrae	15	14 (7); 15 (14)			21
Total number of vertebrae	29	28 (5); 29 (16)			21
Teeth in upper outer row	54	42 (1); 45 (2); 47 (2); 48 (2); 49 (1); 50 (3); 51(1); 53 (2); 54 (1); 56 (1); 57 (1); 58 (2); 59 (1); 66 (1)			21
Teeth in lower outer row	41	26 (1); 30 (2); 31 (1); 32 (2); 31 (1); 35 (3); 36 (1); 37 (2); 38 (3); 39 (1); 40 (1); 41 (2); 45 (1)			21
Gill rakers (ceratobranchial)	9	8 (6); 9 (13); 10 (2)			21
Gill rakers (angle + epibranchial)	5	3 (2); 4 (11); 5 (8)			21

Gill rakers. Total gill raker count 11–15, with 2–4 epibranchial, one angle, and 8–10 ceratobranchial gill rakers. Anteriormost ceratobranchial gill rakers smallest increasing in size towards cartilaginous plug (angle). Anterior gill rakers on ceratobranchial generally unifid, sometimes bifid towards cartilaginous plug. Gill raker on cartilaginous plug shorter than longest ceratobranchial gill raker and epibranchial gill rakers further decreasing in size.

Fins. Dorsal fin with 17–18 spines and with 8–10 rays. First dorsal-fin spine always shortest. Dorsal-fin base length between 56.9–65.4 % SL. Posterior end of dorsal-fin rays extending slightly beyond caudal fin base; posterior tip of anal fin reaching slightly before or at caudal fin base. Caudal fin outline subtruncate and composed of 27–29 rays (16 principal caudal-fin rays and 11–13 procurrent caudal-fin rays). Anal fin with 3 spines (3rd spine longest) and 7–9 rays. Anal-fin base length between 16.7–21.9 % SL. Pectoral fin with 14 to 15 rays and length between 19.7–25.6 % SL; longest pectoral ray not reaching or in rare cases almost reaching level of anus (ending approximately 1-2 flank scale widths in front of it). First upper and lower pectoral-fin rays very short to short. Pelvic fin with 1st spine thickly covered with skin and 5 rays. Pelvic fin base at same level pectoral fin base. Longest pelvic-fin ray not reaching or in rare cases almost reaching anus (ending approximately 1-2 flank scale widths in front of it).

Vertebrae and caudal fin skeleton. 28–29 total vertebrae (excluding urostyle element), with 14–15 abdominal and 14–15 caudal vertebrae. Pterygiophore supporting last dorsal-fin spine inserted between neural spines of 16th and 17th or 17th and 18th vertebra (counted from anterior to posterior). Pterygiophore supporting last anal-fin spine inserted between haemal spines of 15th and 16th or 16th and 17th vertebra, rarely between rips of 14th and haemal spine of 15th vertebra (N=1). Single predorsal bone (=Supraneural bone) present. Hypurals 1 and 2 either clearly separated or separated by distinct seam but never fused into single seamless unit. Hypurals 3 and 4 either fused into single seamless unit or separated by distinct seam.

Colouration in life (based on field photographs of adult specimens). Body ground colouration brownish yellow, towards belly more yellowish; dorsum brownish yellow to pale brown; chest below pectoral fins yellow becoming reddish ventrally; belly yellow. Dorsal head surface pale brown dorsally with reddish speckles; ethmoidal area pale brown and densely speckled with reddish spots, especially in dominant males (Indermaur

2014). Iris reddish posteriorly, yellow dorsally, remaining greyish. Upper lip dark grey anteriorly sometimes with reddish speckles; lower lip light greyish, yellowish posteriorly. Cheek pale brown becoming yellowish towards corner mouth and mental area; blackish pear-shaped blotch at caudal-ventral corner, expanding to anterior extension of midlateral band. Branchiostegal membrane along operculum yellow becoming whitish to pale pinkish ventrally. Operculum yellow with black opercular spot, which is fused with anterior extension of midlateral band which is ending just anterior of the eye. Broad blackish lachrymal stripe between orbit and caudal corner of upper lip. A relatively faint greyish nostril stripe, sometimes covered by many reddish speckles. Relatively wide blackish interorbital stripe. Blackish supraorbital stripe connected with nape band. Nape band ending slightly anterior of dorsal-fin origin and fused with dorso-lateral band. Dorso-lateral band slightly below dorsal fin base and visible up to third or fourth anterior vertical bar. Relatively thin midlateral band ending with dark blotch just posterior base caudal fin. 7–9 blackish vertical bars crossing midlateral band and extending onto dorsal fin almost to fin margin; anterior-most vertical bar (just behind operculum) less intensive than remaining bars. Vertical bars wider than space between them. Dorsal-fin membrane yellow without maculae, skin/membrane of first three dorsal-fin spines black creating the appearance of a broad black oblique band between 1st and 4th spine. Margin of spiny part dorsal fin with fine black outline and red (distally) and transparent submarginal band; rayed part of dorsal fin lacks transparent submarginal band. Anal fin yellow; margin greyish outlined. Posterior half of anal fin with deep-red maculae on membrane (between last four anal-fin rays); maculae elongated proximally becoming more rounded distally (maculae not to fin margin but ending slightly before). In general, these maculae resemble egg-spots: large deep red centre surrounded by faint greyish ring then by ill-defined transparent ring. Caudal fin yellow with deep red maculae as described for anal fin but only with roundish maculae. Caudal fin with reddish marginal band with narrower bluish submarginal band; another submarginal band of red maculae (intensity varies). Outer caudal-fin rays outlined in black. Pectoral fin yellow to orange. Pelvic fin yellowish with dark greyish anterior margin spanning spine and first two rays.

Juvenile colouration in life. (based on tank-raised juveniles of approximately 20 to 30 mm SL; Fig. 9). Ground colouration greyish to beige. Patterns and head mask as described for adults. No reddish speckles present. Dorsal and midlateral band, greyish vertical bars on flank as described for adults. Dorsal fin hyaline to beige with vertical flank bars extending onto fin. Anal, caudal, pectoral and pelvic fin hyaline.

Colouration in alcohol. Colouration and melanin patterns similar to live specimens, but due the preservation procedure of specimens, i.e., first formalin fixation, transfer to 75 % EtOH etc., specimens tend to lose original colouration (especially melanin patterns more intense than in live specimens). Overall body ground colouration pale brownish to pale yellowish; chest and belly beige to yellowish. Branchiostegal membrane greyish-beige to greyish-brown. Dorsal head surface pale brownish; ethmoidal region greyish-brown. Upper lip brownish and lower lip beige. Cheeks beige to brownish; pear-shaped blotch on lower caudal corner of cheek greyish-brownish and less prominent than in living specimens. Operculum greyish and with opercular spot as described above. Head mask and mid- and dorso-lateral band and vertical bars brownish to greyish. Dorsal fin light greyish except dark grey skin/membrane of first three anterior spines, remaining fin with black margin; extensions of vertical bars on dorsal fin dark grey. Anal fin light greyish; margin outlined in dark grey; no maculae visible. Caudal fin light greyish and margins outlined in black; some thin blackish streaks on membrane between rays may be present. Pectoral fin light grey. Pelvic fin light grey, skin/membrane of pectoral spine and first two rays greyish.

Distribution and biology. *Orthochromis indermauri* is only known from the lower reaches of the Lufubu River (Zambia), the third largest tributary of Lake Tanganyika (Fig. 1). Several cascades and waterfalls seem to represent insurmountable barriers to the upstream movement of the lake ichthyofauna hence the fish communities of the upper and lower reaches are clearly distinct. The Upper Lufubu has faunistic similarities to the Congo and Zambezi systems while the Lower Lufubu shows faunistic influences of Lake Tanganyika (Koblmüller *et al.* 2012). At the type locality the Lufubu River is rocky with some patches of sand and gravel, about 20 meters wide and on average 50 cm deep (Fig. 8). The water temperature varies throughout the year, 23 °C was measured in July and 28.1 °C in November, the pH ranged between 8.0–8.55, and electrical conductivity around 29 µS (Indermaur 2014, pers. com. Bernd Egger). *O. indermauri* is benthic-rheophilic and prefers stretches of fast flowing water where it is found between and among large rocks or patches of gravel. No stomach contents were examined, however, underwater observations indicate it scrapes aufwuchs from the substrate and forages between rocks and patches of sand and gravel (Indermaur 2014, pers. obs. FS). *Orthochromis indermauri* is a maternal mouthbrooder. Females in captivity have comparatively small clutches of between 17 and 21 fry (two spawns, pers. com. Adrian Indermaur).

FIGURE 8. Type localities of the five newly described species A. Type locality of *Orthochromis mporokoso,* Kasinsha stream (July 2011, Hans van Heusden) B. Type locality of *Orthochromis katumbii,* Kiswishi River (2015, VLIR expedition) C. Type locality of *Orthochromis gecki*, Lubudi River (July 2017, Katanga 2016 Expedition) D. Type locality of *Orthochromis kimpala*, Kalule North River near bridge on the road Makulakulu-Lubudi (2012, PRODEPAAK expedition) E. Type locality of *Orthochromis indermauri*, Lufubu River at Chomba village (August 2015, photo F. Schedel).

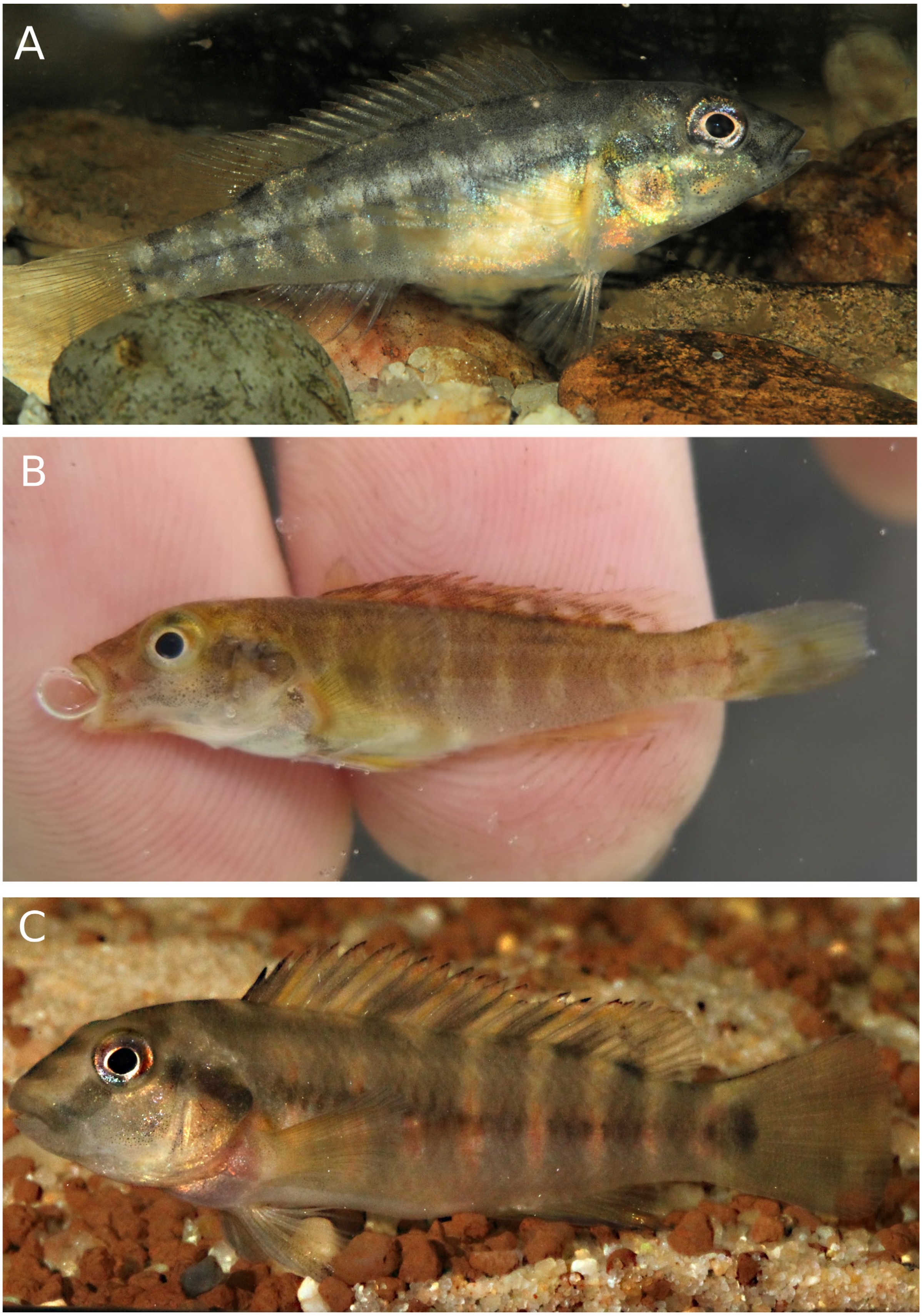

FIGURE 9. Live Pictures of juveniles. A. captive raised F1 juvenile of *Orthochromis katumbii* about 25 mm SL (Photo J. Geck). B. wild caught juvenile of *Orthochromis gecki* C. captive raised F1 juvenile of *Orthochromis indermauri.*

Etymology. The species name *indermauri* honours the Swiss ichthyologist Dr. Adrian Indermaur, who was the first to document this new species with underwater photographs, videos, and with aquarium observations, thereby contributing to a large extent to our knowledge of behavior and ecology of this species.

Discussion

Generic placement and affinities. Overall, the five new species superficially resemble species of *Orthochromis,* but their characters are only partially compatible with the morphological diagnosis of that genus as of the latest generic diagnosis of *Orthochromis* by De Vos & Seegers (1998), and they differ in most diagnostic characteristics from *Schwetzochromis* sensu De Vos & Seegers (see Tables 7 and 8). Nevertheless, we chose to place them in the genus *Orthochromis* instead of placing them in the catch-all genus *Haplochromis* Hilgendorf 1888, as had been done for *Haplochromis vanheusdeni,* another rheophilic species which shares superficial similarities with *Orthochromis* (Schedel *et al.* 2014). The reasons for this overall placement are as follows: (1) phylogenetic reconstructions based on nuclear and mitochondrial DNA sequence data strongly indicate that rheophilic haplochromines superficially similar to *Orthochromis* as currently defined are polyphyletic (e.g. Salzburger *et al.* 2002, Koblmüller *et al.* 2008, Schwarzer *et al.* 2012, Dunz & Schliewen 2013, Weiss *et al.* 2015, Matschiner *et al.* 2016). Therefore, placement of the new species within the anyway polyphyletic genus *Orthochromis* does not compromise current taxonomic (in)stability; (2) although all new species described herein appear distinct from all *Orthochromis* s.s., the latter are equally rheophilic haplochromine-like cichlids of the Malagarasi and Luiche drainages, an haplochromine subgroup which appears to be comparatively uniform with regard to meristic values, other morphological and colouration characters, and which has been inferred to be monophyletic by molecular analyses with an almost complete taxon sampling of that group (Matschiner *et al.* 2016), and that, most importantly, hosts *O. malagaraziensis*, the type species of the genus *Orthochromis*. All five new species described herein are overall phenotypically similar to *Orthochromis* s.s. as they exhibit several morphological similarities; (3) haplochromine cichlid phylogenetic intra-relationships have not been investigated with a fully comprehensive taxon sampling, neither on the morphological nor on the molecular level; nevertheless, all results of partial analyses suggest strongly that many haplochromine genera are paraphyletic, and that rheophilic haplochromine taxa are widely dispersed in available haplochromine phylogenetic hypotheses (e.g., Schwarzer *et al.* 2012, Weiss *et al.* 2015). Until a fully representative phylogenetic evaluation of haplochromine cichlids incorporating morphological and genetic data will be available, a stable taxonomic appraisal of the generic placement of the new species most likely remains drastically fragmentary. Therefore, placing the new species in *Orthochromis* will be a temporal solution but creating at least a temporal nomenclatural stability highlighting phenotypic dissimilarity with members of the other haplochromine catch-all genus *Haplochromis*.

Furthermore, apart from the new species described herein, at least two new species of the Malagarasi-*Orthochromis* lineage (*Orthochromis* sp. "Igamba" and *Orthochromis* sp. "red"; only the first species was available for this study) await formal description; and, moreover, preliminary data suggest that *O.* cf. *torrenticola* specimens collected from the Lufira River below Kiubo Falls represent an as yet undescribed species which is the sister taxon to *O. torrenticola*, which was described from specimens collected above the falls. These species will be described in forthcoming papers once more data become available.

The five new species described herein appear to belong to at least three different evolutionary lineages based on published and not yet published preliminary molecular phylogenetic analyses, a result which is partially reflected by distinctive morphological and colouration characters, as well as patterns of geographic distribution: the four species *O. luongoensis*, *O. kalungwishiensis, O. katumbii* and *O. mporokoso* are distributed in the Luapula-Lake Mweru drainage, and, according to preliminary molecular phylogenetic data they form a monophyletic group (Schedel *et al.* unpublished), and, to some extent, show meristic similarities (see Fig. 2). However, inter- and intrarelationships of this clade need further examination as *O. kalungwishiensis* was shown to be either related to *Pseudocrenilabrus*-like cichlids (mtDNA-data) or to *O. stormsi* and *O. polyacanthus* (nuclear DNA data) (Schwarzer *et al.* 2012, Weiss *et al.* 2015). The two new species *O. gecki* and *O. kimpala* both feature eggspots or eggspot-like maculae on their anal fin, and their pelvic fin shows a characteristic colouration with the spines and adjacent membranes being blackish, suggesting a closer relationship of these two species. In addition, unpublished molecular data suggest that they potentially represent a distinct haplochromine lineage. Based on preliminary

TABLE 7. Overview of morphological characters associated with *Orthochromis* in comparison with the new species described herein.

Morphological characters associated with *Orthochromis* (as in De Vos & Seegers 1998)	*Orthochromis mporokoso*	*Orthochromis katumbii*	*Orthochromis kimpala*	*Orthochromis gecki*	*Orthochromis indermauri*
Rather slender body	Yes	Yes	Yes	Yes	Yes
Eyes generally superolateral in position, giving the fish a goby-like appearance	Yes	Yes	Yes	Yes	yes
Scales on the sides mainly ctenoid and if present, cycloid and minute on chest and belly, often deeply imbedded in the skin. Chest and belly scaleless in some species.	Yes	Yes	Yes (central belly region scaleless)	Yes (central belly region scaleless, chest scaleless)	Yes
Absence or extensive reduction of cheek squamation	No (2-4 scale rows on cheek)	No (2-4 scale rows on cheek)	No (3-4 scale rows on cheek)	Yes	Yes
Increased number of spinous rays in the dorsal fin (without a corresponding reduction in the number of branched rays)	Yes	Yes	Yes	Yes	Yes
elongated second or second and third branched rays in the pelvic fin	Yes	Yes	Yes	Yes	Yes
Outer row of both jaws with unequally bicuspid teeth. Often a few teeth in the corners are unicuspid but there is no tendency for a conical or spatulate shape of the cusps in the larger specimens, as is often the case in other haplochromines. Inner teeth of upper and lower jaws tricuspid or partly unicuspid and arranged into 2-4 rows.	Yes	Yes	Yes	Yes (2-4 inner upper and lower jaw tooth rows with small tricuspid teeth, rarely five tooth rows in upper jaw and one or five rows in lower jaw)	Yes (3-5 inner upper jaw tooth rows and 3-4 lower jaw tooth rows (rarely two) with small tricuspid teeth)
Dorsal head profile is decurved with a strongly sloping preorbital skull profile	Dorsal-head profile slightly curved	Dorsal head profile gently curved	Dorsal-head profile rather strongly curved	Dorsal-head profile moderately curved	Dorsal-head profile moderately curved
Hypurals 1 and 2, and 3 and 4 of the caudal fin skeleton are fused	Yes	Yes	No (Hypurals 1 and 2 as well as hypurals 3 and 4 always clearly separated)	No (Hypurals 1 and 2 fused into a single seamless unit or separated by a clearly visible seam. Hypurals 3 and 4 fused into a single seamless unit or with clearly separated hypurals.)	No (Hypurals 1 and 2 either clearly separated or separated by a clearly visible seam but never fused into a single seamless unit. Hypurals 3 and 4 either fused into a single seamless unit or separated by a clearly visible seam.)
Without true egg-dummies as shown in the genus *Haplochromis* sensu lato.	Yes	Yes	No (2-3 orange eggspot-like maculae on soft-rayed part of anal fin)	No (3-6 orange eggspots)	No (deep red maculae on anal fin membrane; resembling eggspots)

TABLE 8. Overview of morphological characters associated with *Schwetzochromis* in comparison with the new species described herein.

Morphological characters associated with *Schwetzochromis* (as in De Vos & Seegers, 1998)	*Orthochromis mporokoso*	*Orthochromis katumbii*	*Orthochromis kimpala*	*Orthochromis gecki*	*Orthochromis indermauri*
Highly sexually dichromatic: mature males brilliantly coloured with a series of sharply contrasting longitudinal stripes; females relatively drab with six to eight vertical bars	No	No	No	No	No
Large *Haplochromis*-like eggspots in both sexes	No (eggspots missing)	No (eggspots missing)	Eggspot-like maculae present (not large)	Eggspots present (not large)	Red maculae resembling eggspot-like maculae (not large)
No lachrymal stripes and/or dark bars across the snout and the orbit	No (lachrymal stripe present)	No (lachrymal stripe present)	No (lachrymal stripe present)	No (lachrymal stripe present)	No (lachrymal stripe present)
Pelvic fin long, elongate in males, shorter in females	No	No	No	No	No
Upper jaw with 4-6 inner tooth rows, not well separated from the outer row	No (two to three)	No (two to three)	No (two to three)	No (two to four)	No (three to five)
Development of unicuspid, slender or broad-tipped spatulate teeth in the jaws of large specimens	No (bicuspid teeth)	No (bicuspid to subequally bicuspid teeth)	No (bicuspid to subequally bicuspid teeth)	No (bicuspid to subequally bicuspid teeth)	No (bicuspid to subequally bicuspid teeth)

molecular analyses of mitochondrial data *O. indermauri* appears to represent a lineage of its own, too (Schedel *et al.* submitted). It is worth mentioning that the overall appearance of *O. indermauri* reminds of Eretmodini (e.g. *Eretmodus),* which are endemic to Lake Tanganyika and its outlet Lukuga (Kullander & Roberts 2011), because as in *Eretmodus, O. indermauri* has a comparatively short, laterally compressed body, superolaterally positioned eyes and broad vertical bars on flanks. On the other hand, *O. indermauri* differs in several morphological characters from Eretmodini species as its dorsal fin is composed of 17 or 18 spines whereas Eretmodini species have comparatively high dorsal-fin spine counts of between 21 and 25, which are among the highest among cichlids (Poll 1986). Although each of the three Eretmodini genera is characterized by a distinctive oral tooth shape (e.g. spatulate, cylindrical or conical) all have in common unicuspid oral teeth (Huysseune *et al.* 1999, Vandervennet *et al.* 2006); this contrasts with the bicuspid to subequally bicuspid teeth in the outer row of upper and lower jaw of *O. indermauri*. Further, *O. indermauri* exhibits maculae which are vaguely similar to egg-spots, which contrasts with the lack of egg-spots or eggspot-like maculae on the anal fin of Eretomodini. Several molecular phylogenetic studies established alternative hypotheses for the placement of Eretmodini when comparing nuclear and mitochondrial phylogenies (e.g. Clabaut *et al.* 2005, Meyer *et al.* 2015, Weiss *et al.* 2015), and Weiss *et al.* (2015) found support for a mosaic genomic composition of Eretmodini with phylogenetic signal of both Lamprologini and Malagarasi-*Orthochromis* and/or Haplochromini. *Orthochromis indermauri* might represent an additional lineage with a mosaic genomic composition but so far no nuclear data for this taxon are available.

Conservation. The five new species appear to be endemics of the Katanga-Chambeshi region (sensu Cotterill 2005), a landscape mosaic of savannah grasslands and wetlands, centred within the Zambezian phytochorion (sensu White 1983). The Katanga-Chambeshi region is characterised by high physiographic diversity encompassing several high plateaux (e.g. Bia, Kibara, and Kundelungu plateaux), deep ravines and wide depressions providing a wide variety of habitats which is also reflected by the diversity of vegetation types in this area (Broadley & Cotterill 2004). The Katanga-Chambeshi region is only loosely defined but includes parts of three freshwater ecoregions sensu Thieme *et al.* (2005): Bangwelu-Mweru (*O. mporokoso*, *O. katumbii*), Upper Lualaba (*O. kimpala, O. gecki*) and Lake Tanganyika (*O. indermauri*). These ecoregions have been reported to harbour a rich aquatic fauna with a high degree of endemism, e.g., one third of the Bangwelu-Mweru ecoregion fish species appear to be endemic to it (Balon & Stewart 1983, Thieme *et al.* 2005). A very rich aquatic herpetofauna is documented from the Upper Lualaba ecoregion but the ichthyological fauna appears to be only incompletely known even though many endemic fish species are reported from this ecoregion (Poll 1976, Thieme *et al.* 2005).

The different drainage systems of the Katanga-Chambeshi region are prone to different environmental threats. Major threats for aquatic fauna of the poorly studied Upper Lualaba ecoregion are the extensive mining activities due to the rich mineral deposits such as copper, zinc, and cobalt, and this especially along the Copperbelt with the associated negative impacts on the environment such as erosion, contaminations, and pollution of the soil and waterbodies (Thieme *et al.* 2005, Katemo Manda *et al.* 2010). Generally, the five new species described herein might be threatened by the common hazards for aquatic wildlife in the region (e.g. unsustainable fishing methods, deforestation, damming, pollution, and mining), which might be aggravated by the fact that most of their known distribution ranges are located outside of protected areas. Moreover, it appears that the ichthyological fauna of the Bangwelu-Mweru ecoregion and Upper Lualaba ecoregion is understudied as several species caught along with the new species still were new and await formal description. Future conservation plans and prioritisations should therefore consider that the number of endemic taxa in these regions might not only be higher than previously assumed but potentially also locally restricted to individual river drainages or stretches due to biogeographical barriers such as waterfalls (e.g. Lufubu River). An updated assessment of the ichthyodiversity of National Parks (e.g. Parc National de Kundelungu and Parc National de Upemba) in DRC is in preparation (Mbisa Congo Project), but areas outside these parks still need more attention.

Acknowledgements

We thank James MacLaine (BMNH), Miguel Parrent (MRAC), Willy Baudouin (MRAC), John Friel (formerly CU), Fabrizia Ronco (Universtiy of Basel, Tanganjikasee-Buntbarsch-Sammlung), O. Seehausen (EAWAG) for their efforts with loan arrangements for comparative specimens. Dirk Neumann (ZSM) is kindly acknowledged for collection management at ZSM. Moreover, we thank Hans van Heusden and Adrian Indermaur for countless fruitful discussions and their inspiring enthusiasm. We further thank Berd Egger for sharing his data on water parameters of the Lufubu River. In addition, we acknowledge Fenton P. D. Cotterill (Univ. Stellenbosch), for his support during the 2015 Zambian field trip, and Alex D. Chilala (Provincial Agricultural Coordinator, Western Province, Republic of Zambia) for help with collection and export permits (issued on 05.10.2015 in Kasama by the Ministry of Agriculture and Livestock; Department of Fisheries Provincial Fisheries Office).

Last but not least we would like to thank our donors: UKS and FS are funded by the Volkswagen-Stiftungs project "Exploiting the genomic record of living biota to reconstruct the landscape evolution of South Central Africa." Further financial support for the various field collections came from Mbisa Congo Project (2013-2018), a framework agreement project of the RMCA and the Belgian Development Cooperation, and PRODEPAAK (NN/3000769) CTB/BTC project (2008-2013) for financial and logistical support to the 2012 Katanga Expedition. The manuscript benefitted substantially from constructive reviews prepared by Jay Stauffer and Ad Konings, and by the smooth review process by J. Armbruster - thank you very much!

References

Barel, C.D.N., van Oijen, M.J.P., Witte, F. & Witte-Maas, E.L.M. (1977) An introduction to the taxonomy and morphology of the haplochromine Cichlidae from Lake Victoria. *Netherlands Journal of Zoology,* 27 (4), 333–389. https://doi.org/10.1163/002829677X00199

Balon, E.K. & Stewart, D.J. (1983) Fish assemblage in a river with unusual gradient (Luongo, Africa Zaire system), reflections on river zonation, and description of another new species. *Environmental Biology of Fishes,* 9, 225–252. https://doi.org/10.1007/BF00692373

Boulenger, G.A. (1899) Matériaux pour la faune du Congo. Poissons nouveaux du Congo. Cinquième Partie. Cyprins, Silures, Cyprinodontes, Acanthoptérygiens. *Annales du Musée du Congo*, Series Zoology, 1 (5), 97–128.

Boulenger, G.A. (1902) Contributions to the ichthyology of the Congo.—II. On a collection of fishes from the Lindi River. *Proceedings of the Zoological Society of London*, 1 (4), 265–271.

Boulenger, G.A. (1905) On a collection of fishes from Lake Bangwelo. *Annals and Magazine of Natural History*, Series 7, 16 (96 Art. 72), 642–647. https://doi.org/10.1080/03745480509443309

Broadley, D.G. & Cotterill, F.P.D. (2004) The reptiles of south-east Katanga, an overlooked 'hot spot'. *African Journal of Herpetology,* 53, 35–61. https://doi.org/10.1080/21564574.2004.9635497

Clabaut, C., Salzburger, W. & Meyer, A. (2005) Comparative phylogenetic analyses of the adaptive radiation of Lake Tanganyika cichlid fish: Nuclear sequences are less homoplasious but also less informative than mitochondrial DNA. *Journal of Molecular Evolution*, 61, 666–681. https://doi.org/10.1007/s00239-004-0217-2

Cotterill, F.P.D. (2005) The Upemba lechwe, *Kobus anselli*: an antelope new to science emphasizes the conservation importance of Katanga, Democratic Republic of Congo. *Journal of Zoology,* 265, 113–132. https://doi.org/10.1017/S0952836904006193

David, L. (1937) Poissons de l'Urundi. *Revue de Zoologie et de Botanique Africaines*, 29 (4), 413–420.

De Vos, L. & Seegers, L. (1998) Seven new *Orthochromis* species (Teleostei: Cichlidae) from the Malagarasi, Luiche and Rugufu basins (Lake Tanganyika drainage), with notes on their reproductive biology. *Ichthyological Exploration of Freshwaters,* 9 (4), 371–420.

De Zeeuw, M.P., Westbroek, I., van Oijen, M.J.P. & Witte, F. (2013) Two new species of zooplanktivorous haplochromine cichlids from Lake Victoria, Tanzania. *ZooKeys,* 256, 1–34. https://doi.org/10.3897/zookeys.256.3871

Dunz, A. & Schliewen, U.K. (2010) Description of a new species of *"Tilapia"* Smith, 1840 (Teleostei: Cichlidae) from Ghana. *Zootaxa*, 2548, 1–21.

Dunz, A.R. & Schliewen, U.K. (2013) Molecular phylogeny and revised classification of the haplotilapiine cichlid fishes formerly referred to as "*Tilapia*". *Molecular Phylogenetics and Evolution*, 68, 64–80. https://doi.org/10.1016/j.ympev.2013.03.015

Free Spatial Data DIVA-GIS (2018) Available from: http://www.diva-gis.org/Data (accessed 29 January 2018)

Greenwood, H.P. & Kullander, S.O. (1994) A taxonomic review and redescription of *Tilapia polyacanthus* and *T. stormsi* (Teleostei: Cichlidae), with descriptions of two new *Schwetzochromis* species from the Upper Zaire River drainage. *Ichthyological Exploration of Freshwaters,* 5 (1), 161–180.

Greenwood, P.H. (1954) On two species of cichlid fishes from the Malagarazi River (Tanganyika), with notes on the pharyngeal apophysis in species of the *Haplochromis* group. *Annals and Magazine of Natural History,* Series 12, 7 (78),

401–414.
https://doi.org/10.1080/00222935408656059
Greenwood, P.H. (1979) Towards a phyletic classification of the 'genus' *Haplochromis* (Pisces, Cichlidae) and related taxa, part I. *Bulletin of the British Museum (Natural History) Zoology,* 35, 265–322.
https://doi.org/10.5962/bhl.part.20455
Hammer, Ø., Harper, D.A.T. & Ryan, P.D. (2001) PAST: Paleontological statistics software package for education and data analysis. *Palaeontologia Electronica*, 4 (1), 9.
Hilgendorf, F.M. (1888) Fische aus dem Victoria-Nyanza (Ukerewe-See), gesammelt von dem verstorbenen Dr. G. A. Fischer. S*itzungsberichte der Gesellschaft Naturforschender Freunde zu Berlin,* 1888, 75–79.
Huysseune, A. Rüber, L. & Verheyen, E. (1999) A single tooth replacement pattern generates diversity in the dentition in cichlids of the tribe Eretmodini, endemic to Lake Tanganyika (Teleostei: Cichlidae). *Belgian Journal of Zoology*, 129, 157–174.
Indermaur, A. (2014) Über den Tellerrand geschaut - Buntbarsche aus dem Lufubu. *Die Aquarien- und Terrarien-Zeitschrift,* 10, 16–23.
Jorissen, M.W.P, Pariselle, A., Huyse, T., Vreven, E.J., Snoeks, J., Volckaert, F.A.M., Chocha Manda, A., Kapepula Kasembele, G., Artois, T. & Vanhove, M.P.M. (2017) Diversity and host specificity of monogenean gill parasites (Platyhelminthes) of cichlid fishes in the Bangweulu-Mweru ecoregion. *Journal of Helminthology*, 92 (4), 417–437.
https://doi.org/10.1017/S0022149X17000712
Katemo Manda, B., Colinet, G., Manda, A.C., Marquet, J.P. & Micha, J.C. (2010) Evaluation de la contamination de la chaîne trophique par les éléments traces (Cu, Co, Zn, Pb, Cd, U, V et As) dans le bassin de la Lufira supérieure (Katanga/RD Congo). *Tropicultura*, 28 (4), 246–252.
Koblmüller, S., Schliewen, U.K., Duftner, N., Sefc, K.M., Katongo, C. & Sturmbauer, C. (2008) Age and spread of the haplochromine cichlid fishes in Africa. *Molecular Phylogenetics and Evolution,* 49, 153–169.
https://doi.org/10.1016/j.ympev.2008.05.045
Koblmüller, S., Katongo, C., Phiri, H. & Sturmbauer, C. (2012) Past Connection of the Upper Reaches of a Lake Tanganyika Tributary with the Upper Congo Drainage Suggested by Genetic Data of Riverine Cichlid Fishes. *African Zoology*, 47 (1), 182–186.
https://doi.org/10.3377/004.047.0115
Kullander, S.O. & Roberts, T.R. (2011) Out of Lake Tanganyika: endemic lake fishes inhabit rapids of the Lukuga River. *Ichthyological Exploration of Freshwaters,* 22, 355–376.
Matschiner, M., Musilová, Z., Barth, J.M.I., Starostova, Z., Salzburger, W., Steel, M. & Bouckaert, R. (2016) Bayesian Phylogenetic Estimation of Clade Ages Supports Trans-Atlantic Dispersal of Cichlid Fishes. *Systematic Biology,* 66, 3–22.
https://doi.org/10.1093/sysbio/syw076
Meyer, B.S., Matschiner, M. & Salzburger, W.A. (2015) A tribal level phylogeny of Lake Tanganyika cichlid fishes based on a genomic multi-marker approach. *Molecular Phylogenetics Evolution*, 83, 56–71.
https://doi.org/10.1016/j.ympev.2014.10.009
Poll, M. (1948) Descriptions de Cichlidae nouveaux recueillis par le Dr. J. Schwetz dans la rivière Fwa (Congo belge). *Revue de Zoologie et de Botanique Africaines*, 41 (1), 91–104.
Poll, M. (1967) Contribution à la faune ichthyologique de l'Angola. *Publicações Culturais, Companhia de Diamantes de Angola (DIAMANG), Lisboa,* 75, 1–381, Pls. 1–20.
Poll, M. (1976) Poissons. Exploration du Parc National de l'Upemba, Mission G. F. de Witte, Bruxelles. *Reports of the Swedish Deep-Sea Expedition 1947-1948*, 73, 1–127.
Poll, M. (1986) *Classification des Cichlidae du lac Tanganika. Tribus, genres et espèces*., Collection in 8 - 2ème série; Bruxelles, 45 (2), 1–163.
Roberts & Stewart, D.J. (1976) An ecological and systematic survey of fishes in the rapids of the lower Zaire or Congo River. *Bulletin of the Museum of Comparative Zoology,* 147 (6), 239–317.
Salzburger, W., Meyer, A., Baric, S., Verheyen, E. & Sturmbauer, C. (2002) Phylogeny of the Lake Tanganyika cichlid species flock and its relationship to the Central and East African haplochromine cichlid fish faunas. *Systematic Biology,* 51 (1), 113–135.
https://doi.org/10.1080/106351502753475907
Schedel, F.D.B., Friel, J.P. & Schliewen, U.K. (2014) *Haplochromis vanheusdeni*, a new haplochromine cichlid species from the Great Ruaha River drainage, Rufiji basin, Tanzania (Teleostei, Perciformes, Cichlidae). *Spixiana*, 37 (1), 135–149.
Schedel, F.D.B. & Schliewen, U.K. (2017) *Hemibates koningsi* spec. nov: a new deep-water cichlid (Teleostei: Cichlidae) from Lake Tanganyika. *Zootaxa*, 4321 (1), 92–112.
https://doi.org/10.11646/zootaxa.4312.1.4
Schwarzer, J., Swartz, E.R., Vreven, E., Snoeks, J., Cotterill, F.P.D., Misof, B. & Schliewen, U.K. (2012) Repeated trans-watershed hybridization among haplochromine cichlids (Cichlidae) was triggered by Neogene landscape evolution. *Proceedings of the Royal Society B*, 279 (1746), 4389–4398.
https://doi.org/10.1098/rspb.2012.1667
Thieme, M.L., Abell, R., Stiassny, M.L.J., Skelton, P., Lehner, B., Teugels, G.G., Dinerstein, E., Kamdem-Toham, A., Burgess, N. & Olson, D. (2005) *Freshwater Ecoregions of Africa and Madagascar: A Conservation Assessment*. Island Press,

Washington, D.C., 483 pp.
Thys van den Audenaerde, D.F.E. (1963) Description d'une espèce nouvelle d'*Haplochromis* (Pisces, Cichlidae) avec observations sur les *Haplochromis* rhéophiles du Congo oriental. *Revue de Zoologie et de Botanique Africaines*, 68, 140–152.
Thys van den Audenaerde, D.F.E. (1964) Les *Haplochromis* du Bas-Congo. *Revue de Zoologie et de Botanique Africaines*, 70, 154–173.
Van Oijen, M.J.P., Snoeks, J., Skelton, P.H., Maréchal, C. & Teugels, G.G. (1991) *Haplochromis*. *In*: Daget, J., Gosse, J.P., Teugels, G.G. & Thys van den Audenaerde, D.F.E. (Eds.), *Check-list of the freshwater fishes of Africa (CLOFFA). Vol. 4*. ISNB, Bruxelles, MRAC, Tervuren and ORSTOM, Paris, pp. 100–184.
Van Oijen, M.J.P. (1996) The generic classification of the haplochromine cichlids of Lake Victoria, East Africa. *Zoologische Verhandelingen, Leiden*, 302, 57–110.
Vandervennet, E., Wautier, K., Verheyen, E. & Huysseune, A. (2006) From conical to spatulate: Intra- and interspecific changes in tooth shape in closely related cichlids (Teleostei; Cichlidae: Eretmodini). *Journal of Morphology*, 267, 516–525. https://doi.org/10.1002/jmor.10418
Wamuini Lunkayilakio, S. & Vreven, E.J. (2010) '*Haplochromis*' *snoeksi*, a new species from the Inkisi River basin, Lower Congo (Perciformes: Cichlidae). *Ichthyological Exploration of Freshwaters*, 21 (3), 279–3287.
Weiss, J.D., Cotterill, F.PD. & Schliewen, U.K. (2015) Lake Tanganyika—A 'Melting Pot' of ancient and young cichlid lineages (Teleostei: Cichlidae)? *PLOS ONE*, 10, e0125043. https://doi.org/10.1371/journal.pone.0125043
White, F. (1983) *The vegetation of Africa. A descriptive memoir to accompany the UNESCO/AETFAT/UNSO vegetation map of Africa. Natural Resources Research No. 20*. UNESCO, Paris, 352 pp.

Appendix. Comparative material examined

Haplochromis bakongo Thys van den Audenaerde 1964: MRAC 142002, 1, holotype, 74.7 mm SL; Democratic Republic of Congo, Ngombe River at Banza Mfinda, Lower Congo (-5.38/15).—MRAC 142003-009, 7, paratypes, 63.5–87.8 mm SL; Ngombe River at Banza Mfinda, Lower Congo, (-5.38/15).—MRAC 142010-011, 2, paratypes, 75.3–87.8 mm SL; Moerbeke, Lower Congo, (-5.5/14.7).—ZSM 37741, 2, 41.9–46.1 mm SL; Democratic Republic of Congo, drainage Kwilu, small stream, north of Yabi station on Jules van Lancker farm (-5.5901/14.7514).

Haplochromis moeruensis (Boulenger 1899): MRAC 216-222, 4, syntypes, 49.4–75.7 mm SL; Democratic Republic of Congo, Pweto, Lake Mweru (-8.46/28.7).

'Haplochromis' snoeksi Wamuini Lunkayilakio & Vreven 2010: MRAC A7-009-P-0001, 1, holotype, 82.5 mm SL; Democratic Republic of the Congo, River Ngeba/Ngufu, village Ngeba, affluent of River Inkisi, Lower Congo (-5.1838/15.2064).—MRAC A7-009-P-0004, 1, paratype, 93.8 mm SL; Democratic Republic of the Congo, River Ngeba/Ngufu, village Ngeba, affluent of River Inkisi, Lower Congo (-5.1838/15.2064).—MRAC A9-014-P-0001, 1, paratype, 81.2 mm SL; Democratic Republic of the Congo, River Ngeba, village Ngeba, affluent of River Inkisi, at Kimasi Bridge, Lower Congo (-5.1838/15.2064).

Haplochromis vanheusdeni Schedel, Friel & Schliewen 2014: CUMV 97639, 1, Holotype, 70.7 mm SL, Tanzania, Morogoro State, drainage Rufiji, Sonjo River at bridge in Man'gula on road from Mikumi to Ifakara, altitude 302 m (-7.808231/36.896561).—CUMV 93835, (1)13, paratypes 31.5–78.7 mm SL, Tanzania, Morogoro state, drainage Rufiji, Sonjo River at bridge in Man'gula on road from Mikumi to Ifakara, altitude 302 m (-7.808231/36.896561).—ZSM 40703, 2, paratypes 50.3–58.7 mm SL), Tanzania, Morogoro state, drainage Rufiji, Sonjo River at bridge in Man'gula on road from Mikumi to Ifakara, altitude 302 m (-7.808231/36.896561).—MRAC 34-09-P-001-003, 3, paratypes, 54.0–58.3 mm SL, Tanzania, Morogoro state, drainage Rufiji, Sonjo stream at bridge on road Ifakara- Kidodi (-7.808339/36.896189).—ZSM 41440, 3, paratypes, 56.2–63.6 mm SL, Tanzania, Morogoro state, drainage Rufiji, Sonjo stream at bridge on road Ifakara-Kidodi (-7.808339/36.896189.—ZSM 41559, 7, paratypes, 47.2–67.8 mm SL, Tanzania, Morogoro state, drainage Rufiji, Sonjo stream at bridge on road Ifakara- Kidodi (-7.808339/36.896189).—ZSM 42308, 1, paratype, 83.9 mm SL Tanzania, Morogoro state, drainage Rufiji, Sonjo River at bridge in Man'gula on road from Mikumi to Ifakara, altitude 302 m (-7.808231/36.896561).—CUMV 93833, 2(3), 31.5–60.4 mm SL; drainage Rufiji, Great Ruaha River at bridge in Kidatu on road from Mikumi to Ifakara (-7.66174/36.9773).—CUMV 93834, 2, 36.6–56.2 mm SL; drainage Rufiji, Idete River at bridge in Idete on road from Ifakara to Taveta (-8.10391/36.4881).

Orthochromis kalungwishiensis (Greenwood & Kullander 1994): MRAC 99-035-P-0031-0032, 2, 69.3–78.3 mm SL; Keso village, Pambashe River, local name Luena River, (possibly:-9.6000/29.4833).—MRAC 99-035-P-0033-0035, (2)3, 66.4–69.2 mm SL, Luena River (=Pambashe River), tributary of Kalungwishi River (possibly: -9.6000/29.4833).—ZSM 41427, 1, 79.2 mm SL; Zambia, Kalungwishi stream above Lumanmgwe Falls on road Mukunsa-Kawambwa (-9.5431/29.3878).—ZSM 41431, 6, 44.4–75.8 mm SL; Zambia, Kalungwishi stream above Lumanmgwe Falls on road Mukunsa-Kawambwa (-9.5431/

29.3878).—ZSM 44369, (8)13, 48.5–70.7 mm SL; Zambia, Kalungwishi River, above Kundabwika and below Kabwelume Falls, near to road Mporokoso—Mununga (-9.217887/ 29.304202)

Orthochromis kasuluensis De Vos & Seegers 1998: MRAC 93-152-P-0725-0740, 4(15), paratypes, 63.5–68.4 mm SL; Mgandazi River, Ruchugi drainage, Malagarasi basin, around 80 km north of Kigoma on road to Kasulu, few km before Kasulu (-4,56/30.1).—ZSM 41455, 5, 48.2–67.0 mm SL; Tanzania, Ruchugi River east of Kasulu on road to Kasulu-Kibondo (-4.5347/30.1483).

Orthochromis luichensis De Vos & Seegers 1998: MRAC 93-152-P-0122-0135, 7(13), paratypes, Mkuti River, affluent Luiche, about 40 km on the road Kigoma-Kasulu (-4.86/29.86).—ZSM 41445, 7, 38.0–72.7 mm SL; Tanzania, Mkuti River, road bridge east of Kandihwa village (-4.8867/29.8703).

Orthochromis luongoensis (Greenwood & Kullander 1994): CU 91747, 1, 69.9 mm SL; Zambia, Lufubu River Falls below bridge at Chipili on Mansa-Munuga road, (-10.7286/29.0936).—ZSM 41437, (5)6, 46.3–68.4 mm SL; Zambia, Luongo stream at bridge on road Mwenga-Kashiba, affluent to Lake Mweru / Upper Congo basin (-10.4708/29.0261).—ZSM 44345, 6, 61.5–106.9 mm SL; Zambia, Kalungwishi River, immediately above Kabwelume Falls (below Lumangwe Falls), ~ 20 km downstream bridge on road Mporokoso-Kawambwa, Northern Province, (-9.527083/29.353102).—ZSM 44432, 7, 53.8–98.0 mm SL; Zambia, Luongo River, at bridge on road Kawambwa-Mansa about 40 km (driving distance) S of Kawambwa (-10.144359/ 29.167193).—ZSM 44467, (5)7, 42.6-59.0 mm SL; Zambia, Luongo River, below Mumbuluma Falls, ~ 40 km (air distance) NW of Luwingu Luapula Province (-10.106146/ 29.571487).—ZSM 44569, 1, 69.9 mm SL; Zambia, Kalungwishi River, above Kundabwika and below Kabwelume Falls, near to road Mporokoso—Mununga (-9.217887/ 29.304202).

Orthochromis machadoi (Poll 1967): BMNH 1984.2.6.104-108, 5, 42.31–52.1 mm SL; Angola, Cunene River (-17.267/ 14.50).—BMNH 1984.2.6.109, 1, 44.7 mm SL; Angola, Cunene River (-17.05/13.5).—BMNH 1984.2.6.113, 1, 52.2 mm SL; Angola, Cunene River (-17/13.25).—BMNH 1984.2.6.116-131, (1) 22, 50.5–60.1 mm SL; Angola, Cunene River (-16.983333/ 13.366667).—BMNH 1984.2.6.132-141, 3, 43.4–55.4 mm SL, Angola, Cunene River (-14.383333/15.300000).—BMNH 1984.2.6.142-145, 4, 50.3–65.7 mm SL; Angola, Cunene River (-14.916667/15.100000).

Orthochromis malagaraziensis David 1937: MRAC 47077-47079, 3, 74.5-83.3 mm SL; paralectotypes, Malagarasi River and its affluents, near Bururi (-4.43/29.76).—ZSM 41469, 2, 66.5-68.8 mm SL; Tanzania, Malagarasi River close to Uvinza (-5.1183/30.3825).

Orthochromis mazimeroensis De Vos & Seegers 1998: MRAC 91-062-P-1620-1651, (4)31, paratypes, 44.3-55.8 mm SL; Kabingo, Mazimero River, road Rutana-Kinyinya, Malagarasi basin (-3.9/30.21).—MRAC 93-150-P-0432-0476, (4)44, 52.1-58.3 mm SL; paratypes, Mazimero River, affluent Malagarasi, on the Road Prov. 85 after ”Faille des Allemands“ direction Giharo (-3.9/30.21).—University Basel Uncat, 1, 45.5 mm SL; Burundi, Mazimero River, affluent of Upper Malagarasi River, upstream of bridge (-3.884722/ 30.197750).—University Basel KDD3, 1, 39.9 mm SL; Burundi, Mazimero River, affluent of Upper Malagarasi River, upstream of bridge (-3.884722/ 30.197750).—University Basel KDD4, 1, 44.2 mm SL; Burundi, Mazimero River, affluent of Upper Malagarasi River, upstream of bridge (-3.884722/ 30.197750).—University Basel KDD6, 1, 40.4 mm SL; Burundi, Mazimero River, affluent of Upper Malagarasi River, upstream of bridge (-3.884722/ 30.197750).—University Basel KDC8, 1, 59.7 mm SL; Burundi, Mazimero River, affluent of Upper Malagarasi River, upstream of bridge (-3.884722/ 30.197750).—University Basel KDC9, 1, 43.0 mm SL; Burundi, Mazimero River, affluent of Upper Malagarasi River, upstream of bridge (-3.884722/ 30.197750).

Orthochromis mosoensis De Vos & Seegers 1998: MRAC 93-150-P0478-0481, 4, 47.1-60.3 mm SL; River Rurur, 9 km from Muyaga near Cenda Juru, Malagarasi basin (-3.3/30.55).

Orthochromis polyacanthus (Boulenger 1899): Personal collection of O. Seehausen (Field number MKB18), 5, 60.1-66.4 mm SL; drainage Lake Mweru, no further information available.—MKL 11, 2, 51.1-65.1 mm SL; no further information available.—Personal collection of O. Seehausen (Field number MKL 12), 1, 63.5 mm SL; no further information available.

Orthochromis rubrolabialis De Vos & Seegers 1998: MRAC 96-022-P-0002-004, 3, paratypes, 43.4-48.7 mm SL; Majamazi River, Malagarasi drainage, Ugalla subdrainage, 58 km north of Mpanda on road to Uvinza; (-5.93/30.95).—ZSM 41463, (7)8, 44.5-86.7 mm SL; Tanzania, Malagarasi River close to Uvinza (-5.1183/30.38)

Orthochromis rugufuensis De Vos & Seegers 1998: MRAC 96-022-P-0006, 1, paratype, 47.1 mm SL; Tanzania, Upper Rugufu River: on road from Uvinza to Mpanda, about 83 km south of Uvinza (-5.7000/ 30.6666.

Orthochromis stormsi (Boulenger 1902): MRAC 96-031-P-1303-1307, (3)5, 38.5-64.5 mm SL; Democratic Republic of the Congo, Lualaba River chutes 47 km on road of Kisangani-Lubutu near of the Concasserie, no GPS data available.—ZSM 32393, (5)6, 40.0-65.6 mm SL; Republic of Congo, Congo main channel near Djoue River confluence at “Les Rapides” (-

4.31306/15.2289).—ZSM 37603, 1, 44.8 mm SL; Democratic Republic of the Congo, Lubuya stream below bridge on Lubutu road, close to Wanie Rukula (0.1928/25.5319).—ZSM 37541, 3, 63.5-80.3 mm SL; Democratic Republic of the Congo, Kisangani market, bought from woman who sells fishes from Wagenia rapids or fishes bought directly at Wagenia village (0.4939/25.2072).—ZSM 38129, 3, 52.5- 88.0 mm SL; Democratic Republic of the Congo, Congo River, obtained from local fishermen at Kinsuka rapids, exact collecting location unclear (-4.3278/15.2306).—ZSM 38337, 1, 52.8 mm SL; Democratic Republic of the Congo, Congo River "Chutes Kipokosso" at Wanie Rukula, (0.1856/25.5218).—ZSM 38382, 1, 69.1 mm SL; Democratic Republic of the Congo, Congo River obtained from local fishermen at Kinsuka rapids, exact collecting location unclear (-4.3278/15.2306).

Orthochromis torrenticola (Thys van den Audenaerde 1963): MRAC 140100, 1, holotype, 67.3 mm SL; Democratic Republic of the Congo, Lufira River rapids, just above the main falls at Kiubo, Congo, no GPS data available.—MRAC 140101, 1, paratype, 67.3 mm SL; Democratic Republic of the Congo, Lufira River rapids, just above the main falls at Kiubo, Congo, no GPS data available.—MRAC 182787-182804, (4)17, 66.0-85.5 mm SL; Lufira River, between Koni and Mwashia (-10.71/ 27.35).—ZSM 38201, (4)5, 37.2-52.3 mm SL; Democratic Republic of the Congo, drainage Congo, Lufira River near Mwashia village near small rapids (-10.7008/27.3403).

Orthochromis uvinzae De Vos & Seegers 1998: ZSM 41430, (6)7, 57.2-80.8 mm SL; Tanzania, Malagarasi River close to Uvinza (-5.1183/30.38).—ZSM 41562, (4)5, 63.7- 83.9 mm SL; Tanzania, Malagarasi River, riffles/rapids upstream of Uvinza (-5.1889/30.0517).—ZSM 41564, 5, 56.6-73.3 mm SL; Tanzania, Malagarasi River, riffles/ rapids upstream of Uvinza (- 5.1889/30.0517).

***Orthochromis* sp. "Igamba"**: ZSM 41561, 5, 49.9-73.1 mm SL; Tanzania, Malagarasi River, Igamba cataracts approximately 56 km downriver of Uvinza (-5.1803/30.0531).—ZSM 41563, 3, 57.0-79.3 mm SL; Tanzania, Malagarasi River, Igamba cataracts approximately 56 km downriver of Uvinza (-5.1803/30.0531).

Schwetzochromis neodon Poll 1948: MRAC 79591-79644, (14)53, 69.5-92.2 mm SL; Democratic Republic of the Congo, River Fwa, no GPS data available.

Appendix.

Individual species-specific principal component analyses (with a reduced taxon sets). Pictures of different species and specimens depicted in the plots were obtained on different field trips and form private photo collections: *O. katumbii* sp. nov. *(holotype), O. kimpala sp*. nov. (probably the holotype), *O. mporokoso* sp. nov. (probably the holotype), *O. gecki* sp. nov. (photo: probably the holotype and a second specimen from the Katanga 2016 Expedition), *O. indermauri* sp. nov. (paratype), *H. bakongo* (preserved specimen: MRAC 142003-142009; paratype), *H. snoeksi* (preserved specimen; holotpye), *H. vanheusdeni* (photo: H. van Heusden), *S. neodon* (preserved specimen, MRAC 79591-79644), *O. kalungwishiensis* (Zambia 2015 Expedition), *O. luongoensis* (photo: Zambia 2015 Expedition), *O. uvinzae* (representing the Malagarasi-*Orthochromis*; photo: J. Geck), *O. machadoi* (photo: E. Schraml), *O. cf. polyacanthus* (Aquarium specimen, F. Schedel),*O. stormsi* (Aquarium specimen, photo: J. Geck), *O. torrenticola* (Katanga 2016 Expedition).

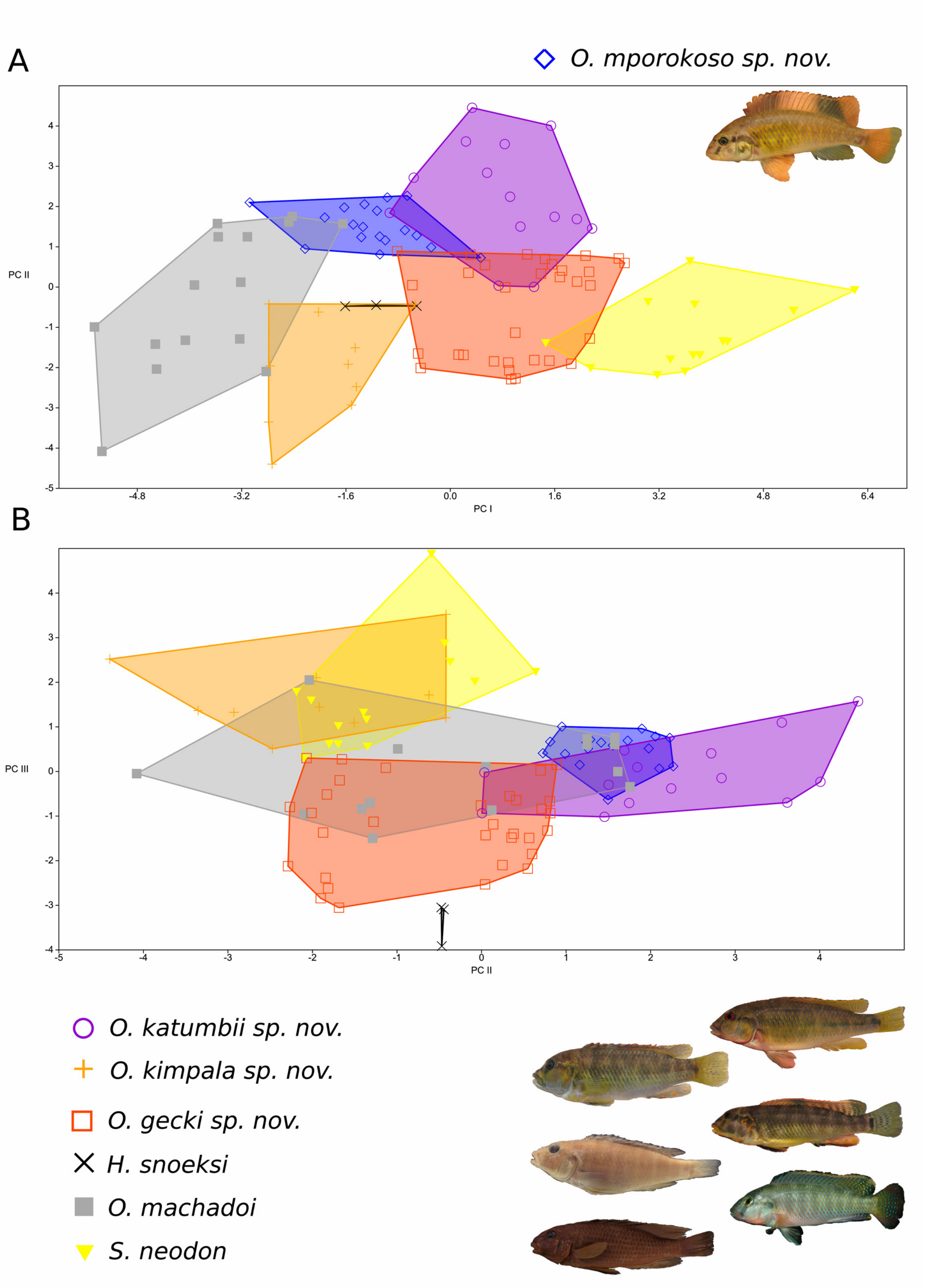

FIGURE S1: Species-specific PCA scatter plots focusing on *O. mporokoso* **sp. nov.** based on 20 meristics; species score limits visualized as convex hulls. PC I vs PC II (A)and PC vs PC III (B) for a 106 examined specimens. PC I explain 27.87 %, PC II explains 15.43 % and PC III explains 10.77 % of the variance. Species depicted from top to bottom: *O. mporokoso* **sp. nov.** , *O. katumbii* **sp. nov**., *O. kimpala* **sp. nov.**, *O. gecki* **sp. nov.**, *H. snoeksi, O. machadoi, S. neodon*.

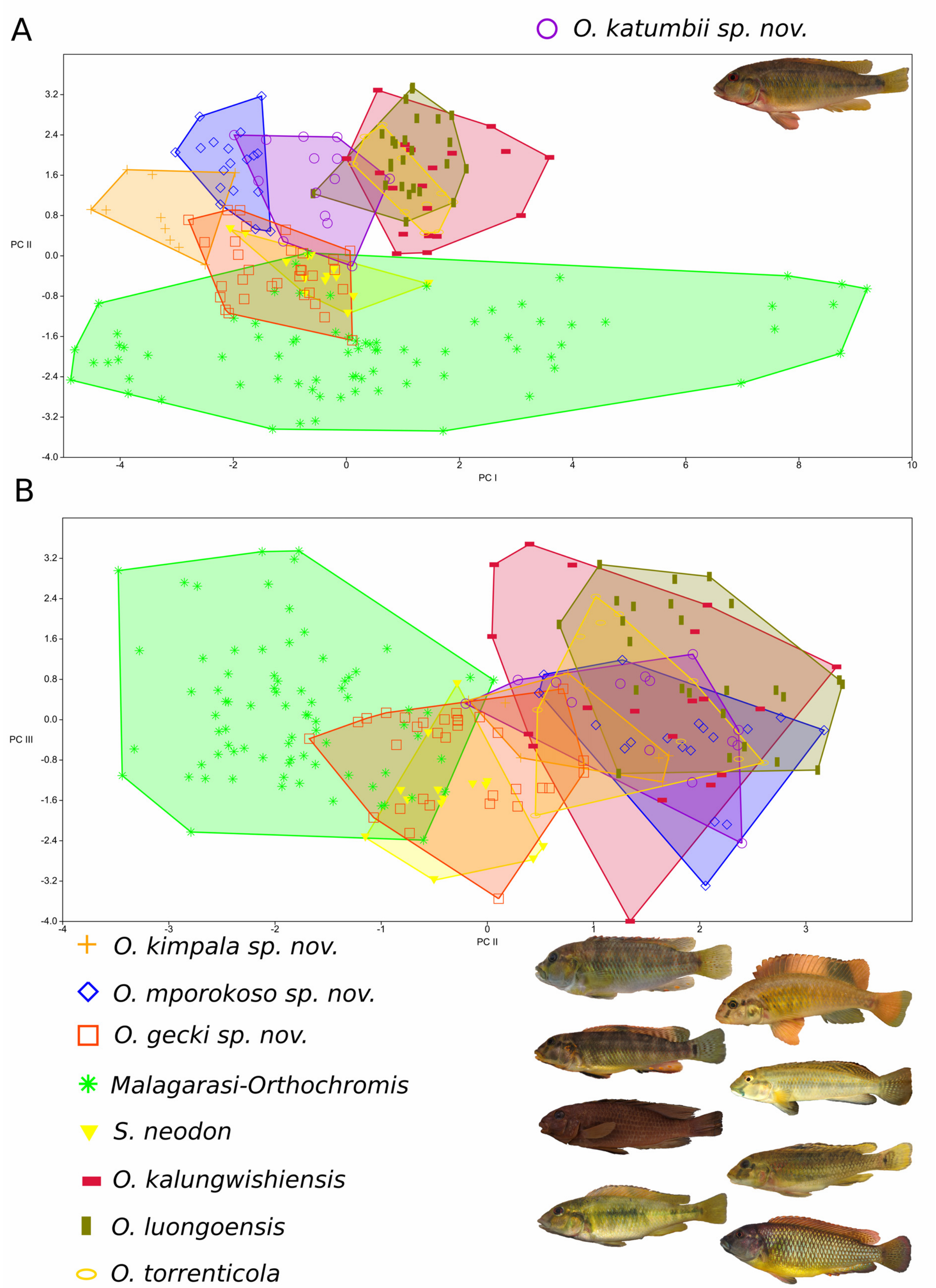

FIGURE S2: Species-specific PCA scatter plots focusing on *O. katumbii* **sp. nov.** based on 20 meristics; species score limits visualized as convex hulls. PC I vs PC II (A) and PC vs PC III (B) for a 225 examined specimens. PC I explain 30.76 %, PC II explains 14.68 % and PC III explains 9.89 % of the variance. Species depicted from top to bottom: *O. katumbii* **sp. nov.**, *O. kimpala* **sp. nov.**, *O. mporokoso* **sp. nov.**, *O. gecki* **sp. nov.**, *O. uvinzae, S. neodon, O. kalungwishiensis, O. luongoensis, O. torrenticola*.

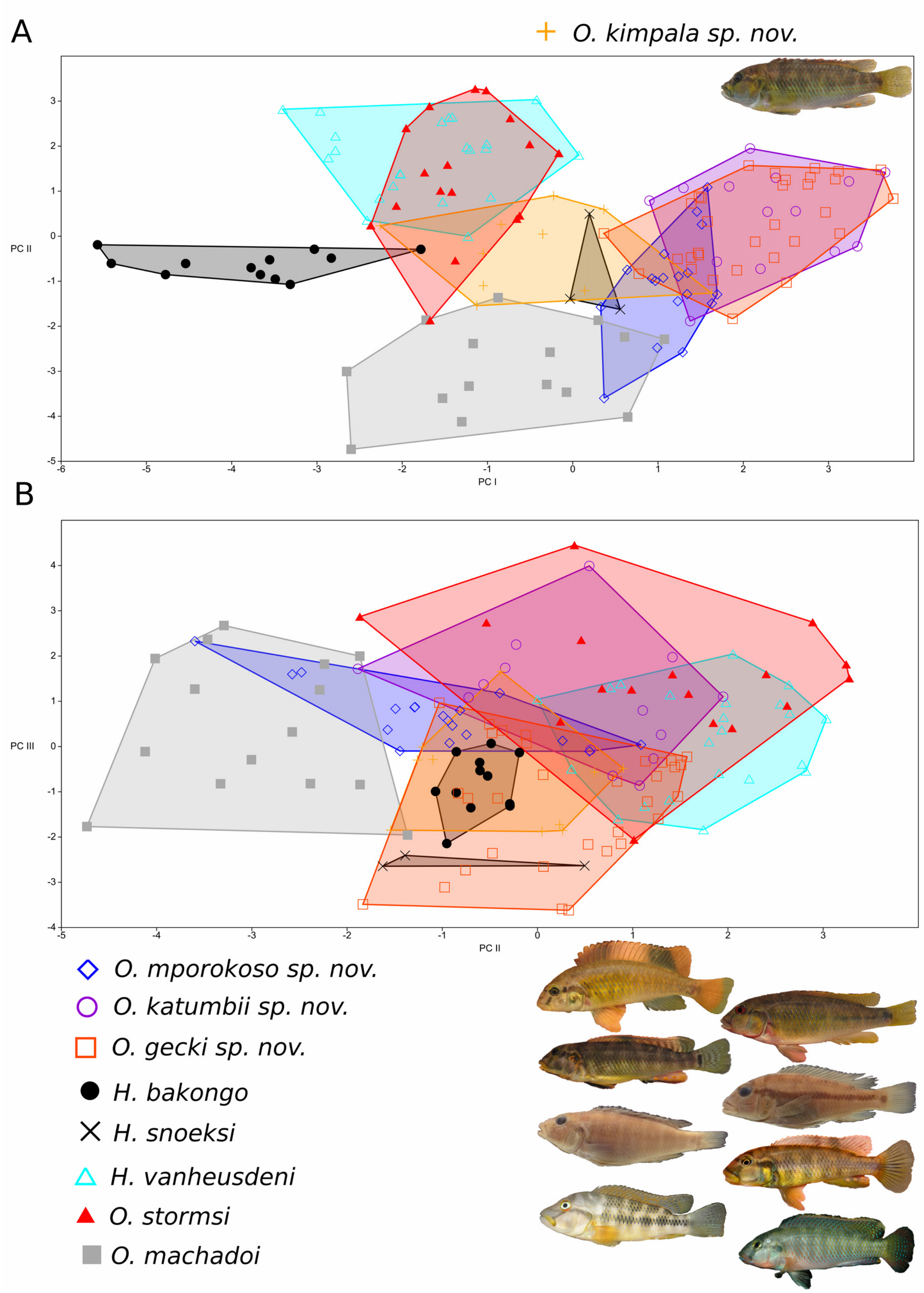

FIGURE S3: Species-specific PCA scatter plots focusing on *O. kimpala* **sp. nov.** based on 19 meristics; species score limits visualized as convex hulls. PC I vs PC II (A) and PC vs PC III (B) for a 143 examined specimens. PC I explain 23.09 %, PC II explains 14.63 % and PC III explains 12.34 % of the variance. Species depicted from top to bottom: *O. kimpala* **sp. nov.**, *O. mporokoso* **sp. nov.**, *O. katumbii* **sp. nov.**, *O. gecki* **sp. nov.**, *H. bakongo, H. snoeksi, H. vanheusdeni, O. stormsi, O. machadoi*.

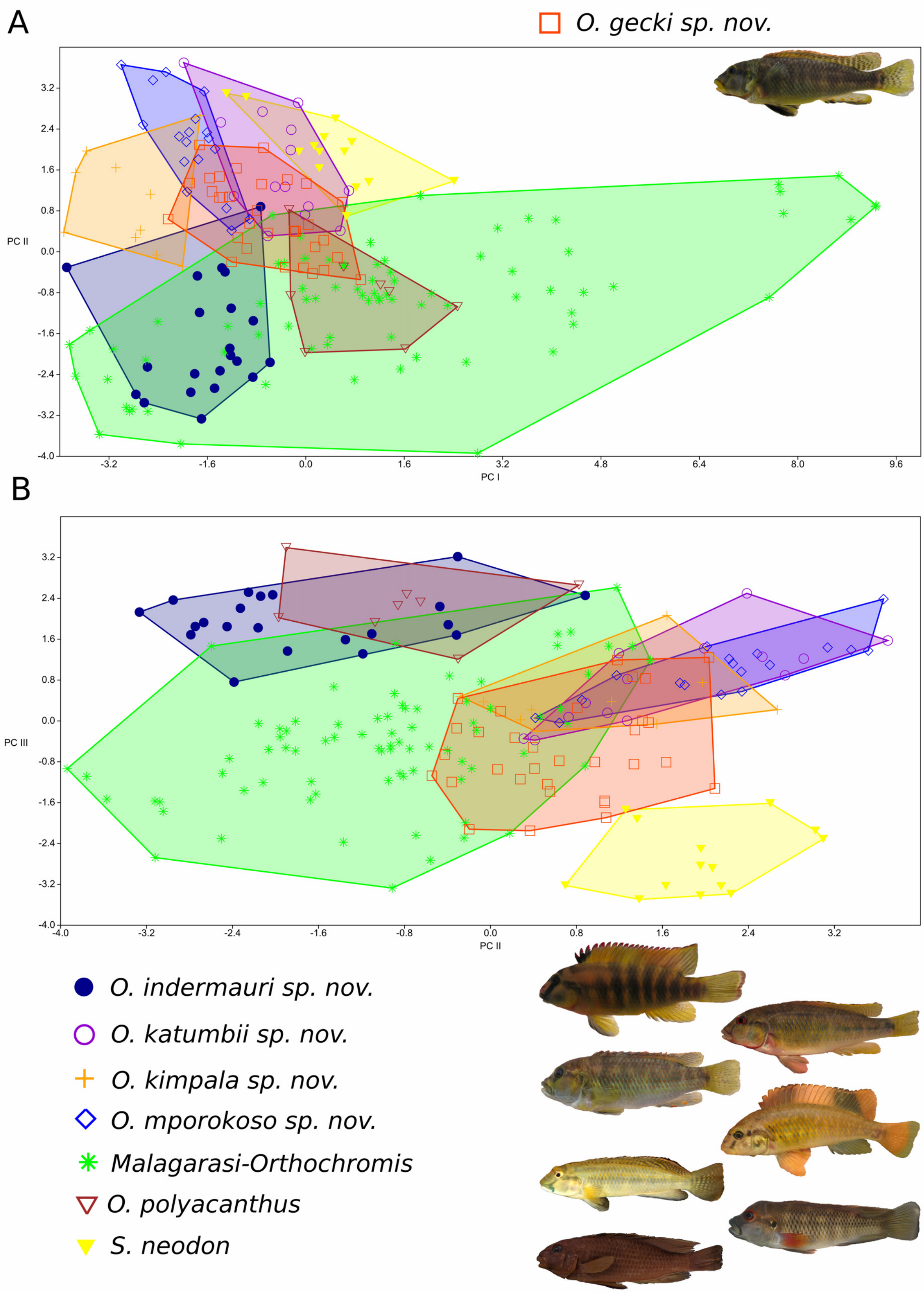

FIGURE S4: Species-specific PCA scatter plots focusing on *O. gecki* **sp. nov.** based on 19 meristics; species score limits visualized as convex hulls. PC I vs PC II (A) and PC vs PC III (B) for a 196 examined specimens. PC I explain 33.42 %, PC II explains 14.91 % and PC III explains 11.95 % of the variance. Species depicted from top to bottom: *O. gecki* **sp. nov.**, *O. indermauri* **sp. nov.**, *O. katumbii* **sp. nov.**, *O. kimpala* **sp. nov.**, *O. mporokoso* **sp. nov.**. *O. uvinzae, O. cf. polyacanthus, S. neodon.*

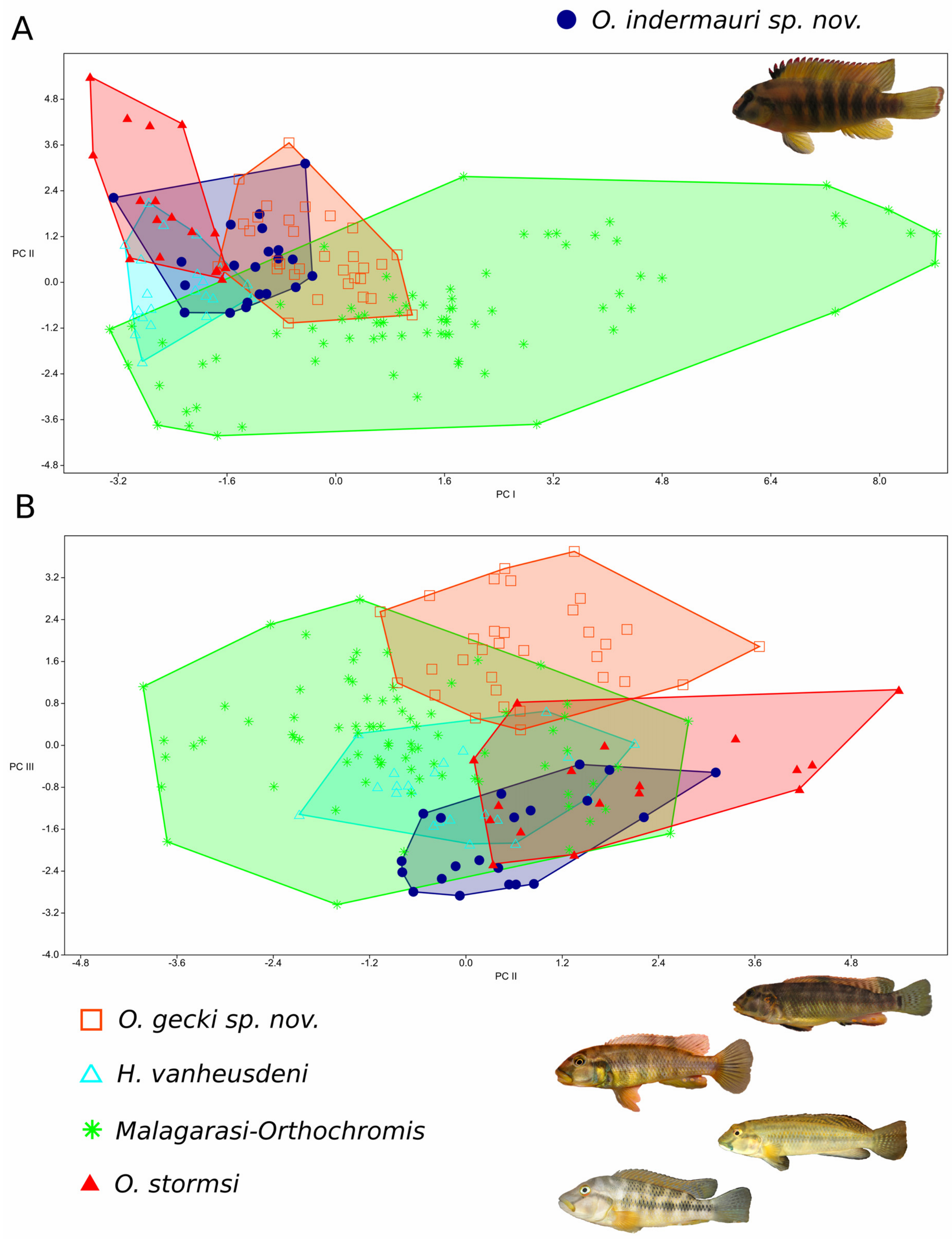

FIGURE S5: Species-specific PCA scatter plots focusing on *O. indermauri* **sp. nov.** based on 19 meristics; species score limits visualized as convex hulls. PC I vs PC II (A) and PC vs PC III (B) for a 171 examined specimens. PC I explain 36.45 %, PC II explains 13.84 % and PC III explains 10.65 % of the variance. Species depicted from top to bottom: *O. gecki* **sp. nov.** *H. vanheusdeni*, *O. uvinzae, O. stormsi.*